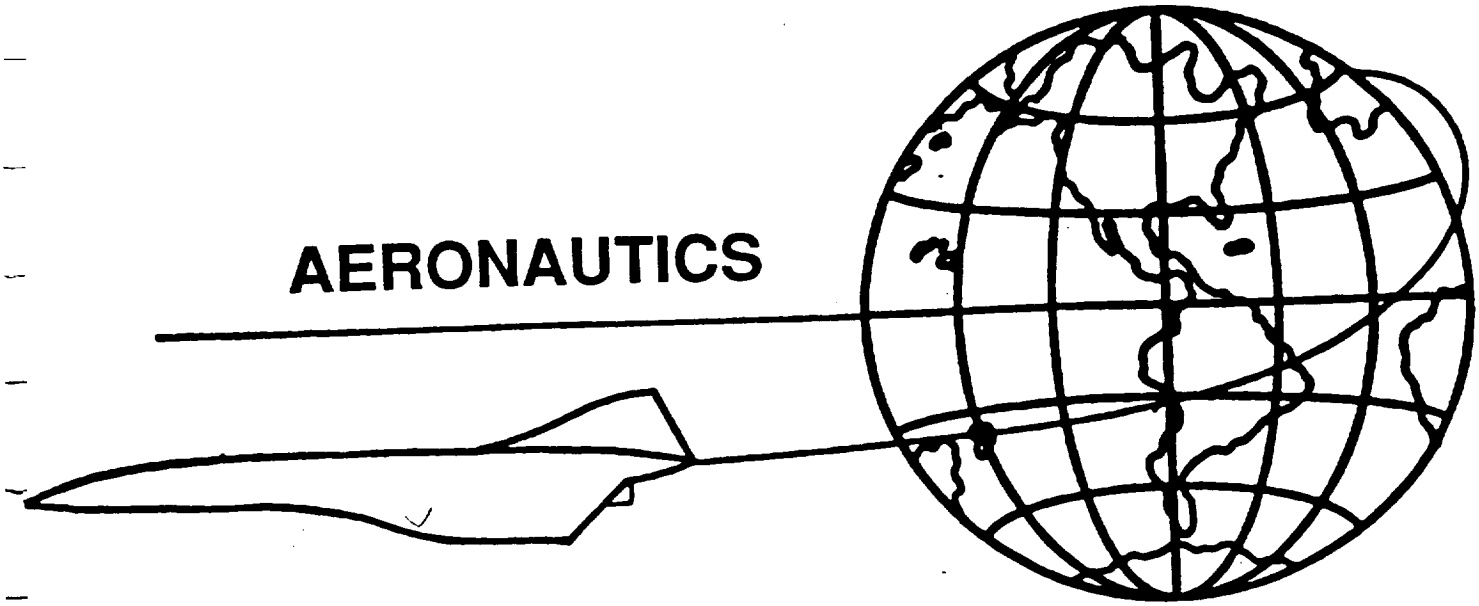

CALIFORNIA STATE POLYTECHNIC UNIVERSITY, POMONA

NASA / USRA ADVANCED DESIGN PROGRAM

JUNE 11, 1988

VOLUME 5

CONDOR:

Long Endurance
High Altitude Aircraft

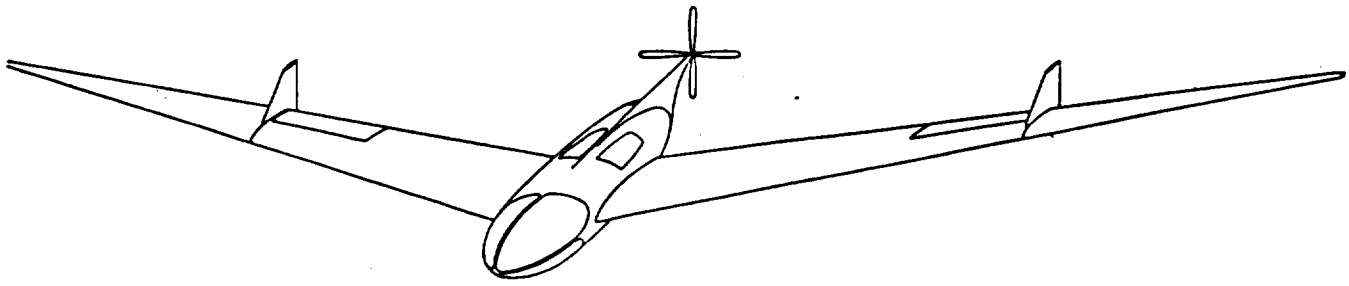

NASA/USRA Advanced Design Project

California State Polytechnic University, Pomona
Aerospace Engineering Department

Final Report 1987-88

CONDOR

Long Endurance High Altitude Vehicle

Design Team Members:
L. Cullen Andrews: Project Leader
Bill Augsburger
Thomas Cote
Mihael Ghitea
Il Sik Lee
Susik Lee
Gary Leong

11 June 1988

TABLE OF CONTENTS

LIST OF FIGURES

LIST OF TABLES

LIST OF SYMBOLS

Symbol	Definition	Dimension
A	aspect ratio	---
b	wing span	ft
BSFC	brake specific fuel consumption	$\frac{\text{bhp-hr}}{\text{lbf}}$
c	wing mean geometric chord	ft
c.g.	center of gravity	in
C_D	airplane drag coefficient	---
C_{D_α}	variation of drag coefficient with angle of attack	rad^{-1}
$C_{D_{\dot{\alpha}}}$	variation of drag coefficient with rate of change of angle of attack	---
$C_{D_{\alpha_E}}$	variation of drag coefficient with elevator angle	---
C_{D_q}	variation of drag coefficient with pitch rate	---
C_{D_u}	variation of drag coefficient with speed (speed damping)	---
C_L	airplane lift coefficient	---
C_{L_α}	variation of lift coefficient with angle of attack	rad^{-1}
$C_{L_{\dot{\alpha}}}$	variation of lift coefficient with rate of change of angle of attack	---
$C_{L_{\alpha_E}}$	variation of lift coefficient with elevator angle	rad^{-1}
C_{L_q}	variation of lift coefficient with pitch rate	---
C_{L_u}	variation of lift coefficient with speed	---
C_{l_β}	variation of rolling moment coefficient with sideslip angle (dihedral effect)	rad^{-1}
$C_{l_{\delta_A}}$	variation of rolling moment coefficient with aileron angle (lateral control power)	rad^{-1}
$C_{l_{\delta_R}}$	variation of rolling moment coefficient with rudder angle	rad^{-1}
C_{l_p}	variation of rolling moment coefficient with roll rate	---

C_{l_r}	variation of rolling moment coefficient with yaw rate	---
C_m	airplane pitching moment	---
C_{m_α}	variation of pitching moment coefficient with angle of attack	rad^{-1}
$C_{m_{\dot{\alpha}}}$	variation of pitching moment coefficientwith rate of change of angle of attack	---
$C_{m_{\delta_E}}$	variation of pitching moment coefficient with elevator angle	rad^{-1}
C_{mf}	pitching moment due to flaps	---
C_{mo}	zero lift pitching moment coefficient	---
C_{mq}	variation of pitching moment coefficient with pitch rate	---
C_{mT}	pitching moment due to flaps	---
C_{mu}	variation of pitching moment coefficient with speed	---
C_{n_β}	variation of yawing moment coefficient with sideslip angle	rad^{-1}
$C_{n_{\delta_A}}$	variation of yawing moment coefficient with aileron angle	rad^{-1}
$C_{n_{\delta_R}}$	variation of yawing moment coefficient with rudder angle	rad^{-1}
C_{np}	variation of yawing moment coefficient with roll rate	rad^{-1}
C_{nr}	variation of yawing moment coefficient with yaw rate	rad^{-1}
C_p	specific fuel consumption	$\frac{\text{bhp-hr}}{\text{lbf}}$
C_{y_β}	variation of side-force coefficient with sideslip angle	rad^{-1}
$C_{y_{\delta_A}}$	variation of side-force coefficient with aileron angle	rad^{-1}
$C_{y_{\delta_R}}$	variation of side-force coefficient with rudder angle	rad^{-1}
C_{yp}	variation of side-force coefficient with roll rate	rad^{-1}
C_{yr}	variation of side-force coefficient with yaw rate	rad^{-1}
D	total drag force	lbf
e	Oswalds efficiency factor	---
E	endurance	hr

FAR	federal aviation Regulation	---
g	acceleration of gravity	$\frac{ft}{sec}$
I_{xx}	rolling moment of inertia	slug-ft^2
I_{yy}	pitching moment of inertia	slug-ft^2
I_{zz}	yawing moment of inertia	slug-ft^2
I_{xy}	xy product of inertia	slug-ft^2
I_{xz}	xz product of inertia	slug-ft^2
I_{yz}	yz product of inertia	slug-ft^2
L	total lift force	Lbf
L/D	lift to drag ratio	---
L.E.	leading edge	---
MGC	mean geometric chord	ft
n	load factor	---
q	dynamic pressure	$\frac{Lbf}{ft^2}$
R	range	n.m.
R	propeller radius	ft
RFP	request for proposal	---
S_w	wing area	ft^2
SSL	standard sea level conditions	---
T	total thrust	lbf
t/c	thickness ratio	---
V	speed	$\frac{ft}{sec}$, kts
W	weight	lbf
W/P	power loading	lbf/hp
W/S	wing loading	$\frac{Lbf}{ft^2}$
X	fuselage station	in

Greek Symbols

α	angle of attack	deg
β	sideslip angle	deg
δ_f	flap deflection	deg
η_p	propeller efficiency	---
λ	wing taper ratio	---
μ	coefficient of friction	---
ρ	air density	$\frac{slug}{ft^3}$
$\Lambda_{L.E.}$	wing leading edge sweep angle	deg
$\Lambda_{c/4}$	wing quarter-chord sweep angle	deg

Subscripts

ac	aerodynamic center
C	cruise
lim	limit load
Max	maximum
Min	minimum
neg	negative
TO	take-off
wb	wing-body

1.0 INTRODUCTION

With the technological advances in materials and propulsion in the past few years it has become possible to make a manned aircraft capable of flying continuously for long periods of time. Such an aircraft can be very useful in military, scientific, and civil applications. Possible military applications include command and control, communications relay, surveillance, and intelligence. Scientific applications include atmospheric, oceanographic, and astronautical research. There are many possible civil applications, such as, emergency communication relay, border patrol surveillance, monitoring natural and man-made disasters.

This report covers the "CONDOR", a response to the request for proposal (RFP) in the 1988 AIAA/GENERAL DYNAMICS CORPORATION Team Aircraft Design Competition. This RFP requires an aircraft that can stay in the air for 72 hours and carry two crew members. In the design close attention was paid to crew comfort, reliability, and ease of use of the payload.

The complete RFP is discussed in Chapter 2. The reasons for the CONDOR's final configuration is discussed in Chapter 3. The different design disciplines (eg. mass properties, aerodynamics, ...) are broken down in Chapters 4,5,7,8 where they are explored in depth. Chapter 6 details the performance of the CONDOR. The stability and control of the aircraft is discused in Chapter 9. The crew comforts and payload are talked about in Chapter 10. Chapter 11 shows the manufacturing and certification plan for the aircraft. The economic analysis is studied in Chapter 12, and Chapter 13 discussed exactly how the CONDOR matches all of the points mentioned by the RFP. Finally the conclusions are presented in Chapter 14

2.0 REQUEST FOR PROPOSAL (RFP)

2.1 Specifications

This report is a response to the Request For Proposal (RFP) for the AIAA/GENERAL DYNAMICS CORPORATION Team Aircraft Design Competition. A copy of the complete RFP is shown in Appendix A. The RFP states that the aircraft must maintain continuous altitude at or above 45,000 feet for at least a 3-day mission, be able to comfortably support a two-man crew during this period with their field of vision not obstructed to a significant degree, carry a payload of 200 Lbf with minimum dimensions of 4 ft^3 and provide a power supply to the payload of 2000 watts. The take-off and landing distances must be below 5000 feet, time to reach cruise altitude must not exceed 3 hours (which does not count in the time of the cruise). The nominal cruise speed must be $\geq$ 150 Knots (154 ft/sec) true air speed. The aircraft must be designed for a ultimate load factor of at least 3.8. The aircraft must be able to be disassembled and fit into a C-130 transport aircraft or on the bed of a tractor trailer which will allow for transportation of the aircraft to desirable airports.

2.2 Mission Profile

From the specifications of the RFP a mission profile was completed as shown in Figure 2.1. During the design of the CONDOR the mission profile was carefully followed to make sure the aircraft met all specifications.

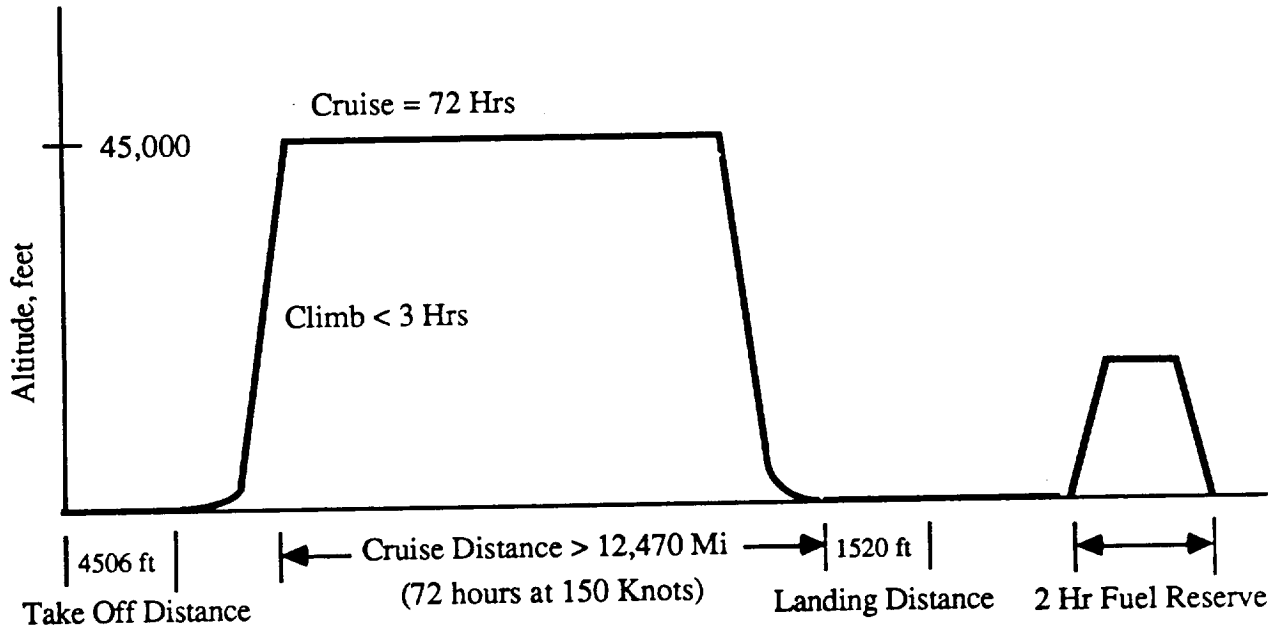

Figure 2.1 : Mission Profile

3.0 CONFIGURATION SELECTION

Configuration selection for the CONDOR was a study of compromises leading to the design most suited to the Request For Proposal (RFP). The design specially addressed problems of pilot fatigue, crew comfort, aircraft disassembly, reliability, visibility, and maintainability.

3.1 Possible Configurations

Four major configurations were looked at in depth. Many other configurations were discussed, but they were discarded because they could not meet the RFP as well as the four chosen. The four major configurations are shown in Figure 3.1: Joined wing, Dual-Wing, Twin Boom, and Flying Wing. This chapter will discuss positive and negative points of each configuration and show why the Flying Wing configuration is the best .

3.1.1 Joined Wing Configuration

The joined wing configuration offers a relatively short wing span as compared to the flying wing and twin boom aircraft and uses two lifting surfaces to trim the aircraft, eliminating the need for a tail. Problems with this configuration include the structure, aerodynamics, and pilot visibility. This configuration will require six major disassembly points with the points at the wing intersection being very complex. The space required between the two wings will add to the length of the fuselage which will add to the structural weight. This configuration will also have added drag due to the interference between the two wings. A tractor propeller will probably be used in this configuration to allow for propeller ground clearance. This will increase the cabin noise which can lead to pilot fatigue. The tractor propeller will also lower pilot visibility.

3.1.2 Dual-Wing Configuration

The dual-wing configuration is very similar to the joined wing, with the same benefits of reduced wing span as compared to a single wing configuration, and the possible removal of the tail (Figure 3.1 shows the configuration with a tail). It also has the same disadvantages: six complex disassembly points, aerodynamic interference between the two wings, and the probable use of a tractor propeller

3.1.3 Twin Boom Configuration

The twin boom configuration was also studied. The major benefits of this configuration are its stability and control characteristics and its low drag as compared to the above configurations.

Correct placement of its wing and tail will make the aircraft both statically and dynamically stable (Reference 21) (stability is one of the problems with the other 3 configurations). The twin boom will only have one wing, reducing the drag over the two winged aircraft. The configuration will also allow the use of a pusher propeller which will enhance pilot visibility and lower cabin noise. Problems with the twin boom configuration include aeroelastic effects on the booms, and higher drag as compared to the flying wing

configuration. The two booms will have aeroelastic problems during the cruise due to the propeller wash and the airplane vibration. To counteract this, the booms weight will have to be increased. The booms will also add to the drag of the aircraft.

3.1.4 Flying Wing Configuration

The flying wing was the configuration chosen for the CONDOR because of its low drag, pusher propeller, ease of disassembly, and high pilot visibility.

The flying wing configuration has the lowest drag of all the configurations because of its clean body. With only a small fuselage and two small vertical tails the flying wing will have approximately 15% less drag than the twin boom and 20% less drag than the joined and dual wing configurations. A pusher propeller can be used on the flying wing configuration which will reduce the cabin noise. This configuration only needs five disassembly points, one less than the other configurations. The flying wing, with a pusher propeller, will also allow for high pilot visibility. The only disadvantage to the flying wing is its stability. It was believed in the beginning design phases that the flight control problems could lessened during the design phase and then, if necessary, controlled by a stability augmentation system.

For the above reasons the Flying Wing configuration was selected for the CONDOR.

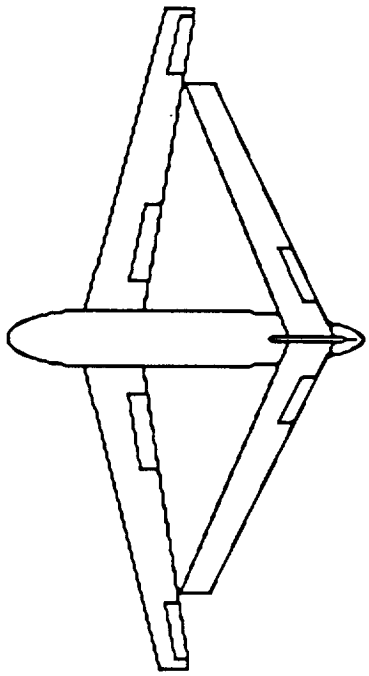

Joined Wing Design

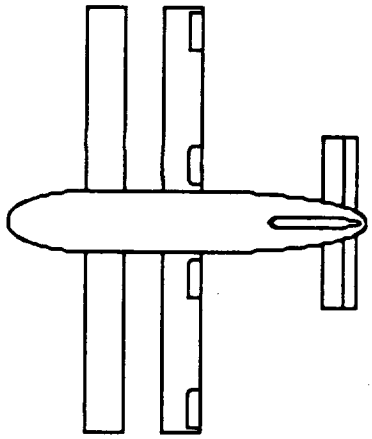

Dual Wing Design

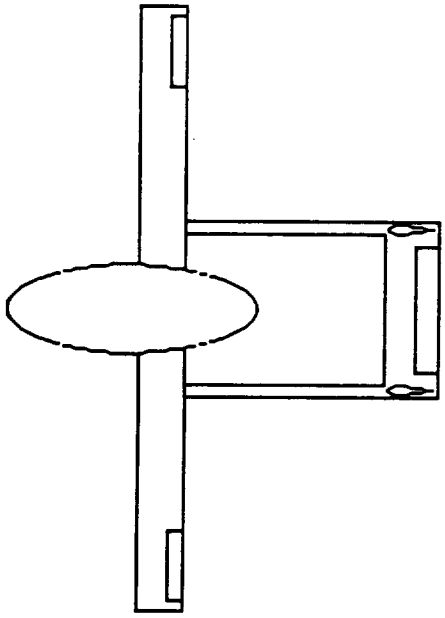

Twin Boom Design

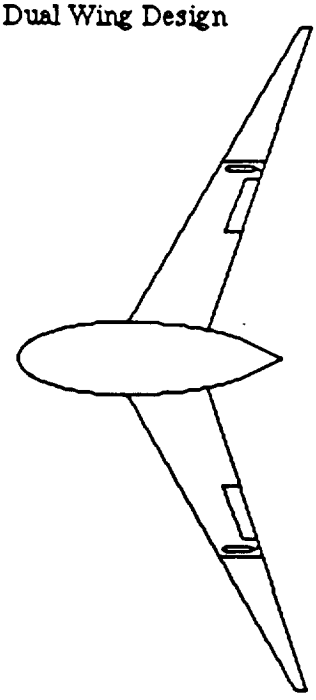

Flying Wing Design

Figure 3.1 : Possible Configurations

3.2 Final Configuration

The final configuration for the CONDOR is shown in the Figure 3.2. The specific numbers in the 3-view will be discussed in further detail in later chapters. Table 3.1 shows the CONDOR specifications in detail.

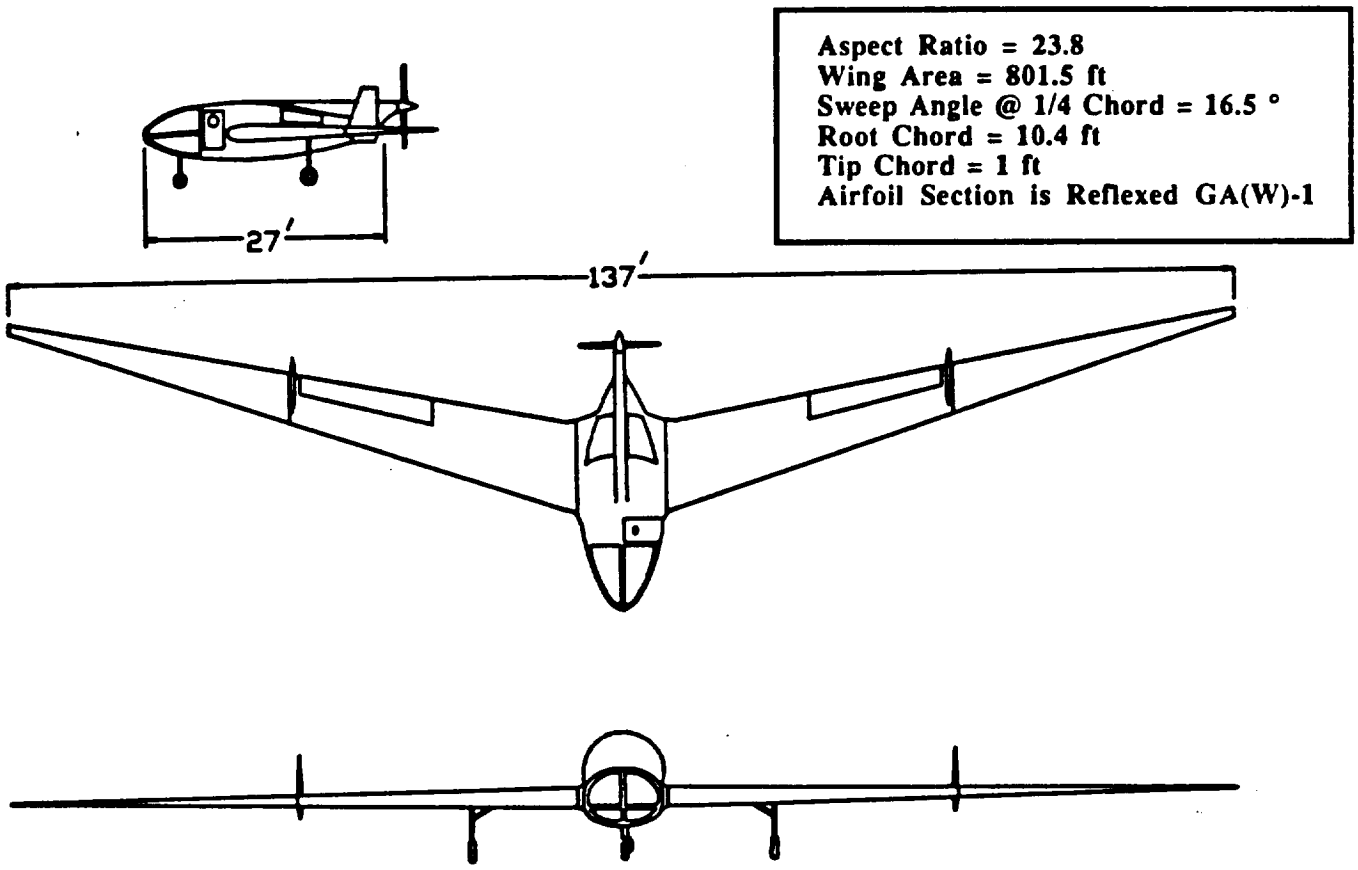

Figure 3.2 : CONDOR 3-View

Wing:	Fuselage:
$S = 801\ ft^2$	$l = 27$ ft
$b = 137$ ft	$h_{max} = 6.6$ ft
$AR = 23.7$	$W_{max} = 9.5$
$c = 6.89$ ft	
$c_t = 1.0$ ft	
$c_r = 10.5$ ft	Miscellaneous:
$\lambda_{LE} = 18°$	$W_{TO} = 11408$ Lbf
$\lambda_{1/4} = 16.5°$	$W_{fuel} = 3700$ Lbf
Airfoil = Reflexed GA(W)-1	$V_{cruise} = 150$ Knot
	$Alt_{cruise} = 45{,}000$ ft
	$Time_{climb} = 2.75$ hrs

Table 3.1 : CONDOR Specifications

4.0 Mass Properties

The initial design characteristics of the CONDOR were developed in this chapter. This chapter also deals with the methods used for all the weight, center of gravity, and inertia calculations done on the CONDOR. Because of the RFP requirements of high altitude and long endurance, comparisons to specific aircraft are limited. Therefore, comparisons were made to trends developed from past general aircraft. The analysis began with estimates of the aircraft take-off weight and design point. The initial estimate was elaborated on to develop the detailed weight, center of gravity, and inertia values. This was done with a component breakdown, and mass properties estimations. The CONDOR was broken into sixty components for this purpose. In addition, a comprehensive in-flight analysis was done for all the mass properties, and a center of gravity envelop was developed for manned and un-manned mission.

4.1 Initial Weight Sizing

The first step taken in the initial weight estimate was to estimate mission phase fuel fractions. A reserve fuel allowance of 2 hours was added to the CONDOR, but it was not a factor in the initial weight sizing. Table 4.1 lists The fuel fraction used on CONDOR.

Engine start and warm-up : .999
Aircraft Taxi : .999
Take-Off : .999
Climb : .9838
Cruise : .6718
Descent : .992
Landing, Taxi, Shutdown : .999
Mission Fuel Fraction : .65

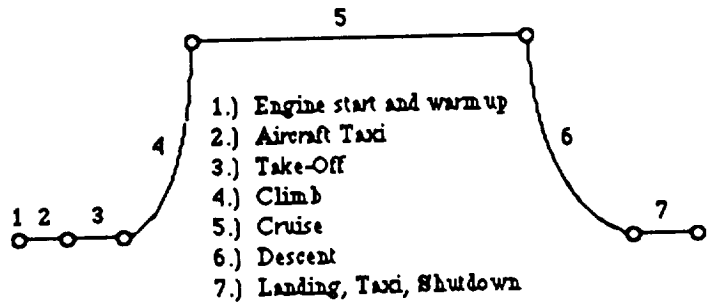

Table 4.1 : CONDOR Mission Phase Fuel Fractions

These fuel fractions were developed from average aircraft values (Reference 44) that were modified due to the CONDOR mission range and endurance. Using methods presented in Reference 39, equations were developed for empty weight versus take-off weight curves, at given mission fuel fractions. A fixed weight of 600 lbs. was used in these equations, which linearly equated the take-off weight to the empty weight through the mission fuel fraction. These curves were then compared to similar curves from a summation of past aircraft, also given in Reference 39. This is shown graphically in figure 4.2 . The sensitivity of the fuel fraction equations for cruise and loiter are also shown in this figure. These values show the potential change in take-off weight if any of these variables are changed. Note that the loiter is assumed to take place on the reserve fuel.

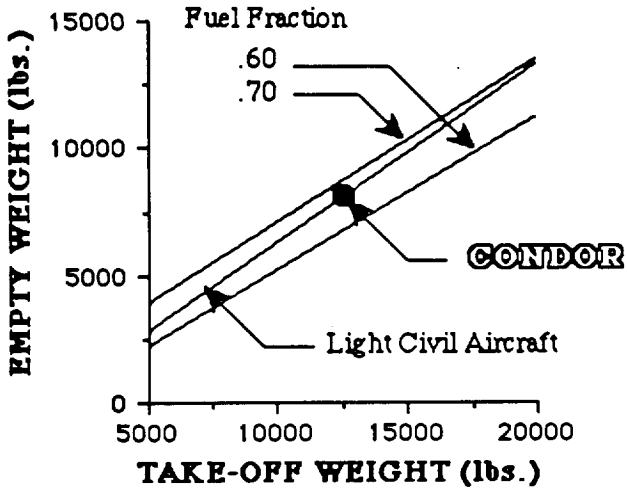

Take-Off Weight Sensitivities

	Cruise	Loiter
$\delta W_{to} / \delta C_p$ (lb/lb/hp/hr)	9361	661.9
$\delta W_{to} / \delta \eta_p$ (lbs)	-3183	-225
$\delta W_{to} / \delta (L/D)$ (lbs)	-64.4	-4.55
$\delta W_{to} / \delta V$ (lb/kt)	15.0	1.07
$\delta W_{to} / \delta R$ (lb/nm)	.21	.30
$\delta W_{to} / \delta E$ (lb/hr)	.02	53.1

Figure 4.2 : CONDOR Take-off/Empty Weight Sizing

With a mission fuel fraction of 0.65 The CONDOR was placed on the curve for light civil aircraft. As a conservative initial estimate, the take-off weight of CONDOR was determined to be 12500 lbs. This corresponded to an empty weight of 8125 lbs., from Figure 4.2 The fuel fraction lines were developed using a payload weight of two-hundred pounds and a crew weight of four-hundred pounds. The CONDOR fuel fraction lines were also compared to curves for transport and fighter aircraft. However, these curves yield unrealistic weights and were henceforth neglected.

4.2 Design Point Calculation

The aircraft take-off design point was chosen on a power versus wing loading chart. During the construction of this chart, it was determined that the critical variables for the CONDOR were the constraints of cruise velocity and full weight take-off. The take-off lines were examined for several lift coefficients. Initially, a lift coefficient of 1.5 was selected, for take-off, as the highest value were a large drag penalty is not payed. The CONDOR's design point can be seen in Figure 4.3 .

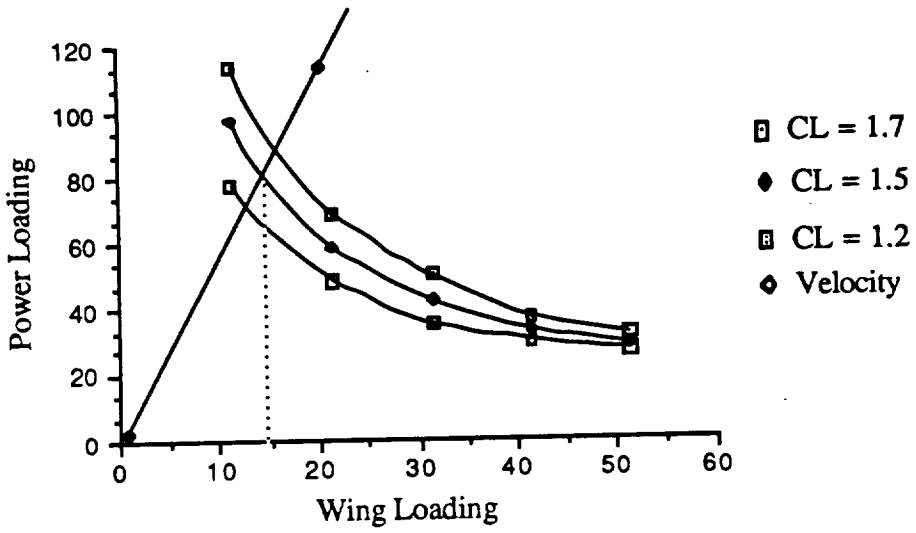

Figure 4.3 : Design Point Chart

The curves for landing, climb, and descent were calculated but were not critical for the flight conditions of the CONDOR and have been omitted from Figure 4.3 . The design point was calculated for the CONDOR at a position that allowed for a maximum power loading with a minimum wing loading. It was of major importance, structurally, that the wing loads be minimized because of the large moment arm created by the large wing span. This would minimize the bending moment at the root chord which would simplify the structure and reduce the weight of the aircraft. The wing loading of the CONDOR was selected to be 15 lbs/ft^2, this gives a power loading of 79 Hp, from figure 4.3.

4.3 Component Weight Estimate

The Aircraft was subdivided into six systems each of which contained specific aircraft components, there were a total of sixty components. The weight of each component was estimated. Several methods were used to estimate each component weight, and the average or most realistic value, relative to the CONDOR, was taken as the weight. References 39 and 49 both offer empirical equations for component weight

estimates, and these procedures are outlined in Appendix B. Table 4.1 shows a list of the data used in the empirical equations. This data represents the initial configuration and performance values.

Initial Fuselage Data
Total Length : 27.0 ft
Max. Width : 10.0 ft
Max. Height : 7.0 ft
Number of Crew : 2
Max. Perimeter : 62.3 ft

Initial Vertical Data
Vertical Tail Area : 23.38 ft.(each)
Vertical Tail Aspect Ratio : 1.55
Vertical Tail Taper Ration : 0.336
Rudder Area : 5.845 ft.
Quarter Chord Sweep : 26.0 deg.

Initial Weights
Take-off Wt. : 12500 lbs
Design Landing Wt. : 12500 lbs
Empty Wt. : 8125 lbs
Mission Fuel Wt. : 4175 lbs
Payload Wt. : 200 lbs
Engine Wt. : 375 lbs

Initial Wing Data
Wing Area : 801.0 ft
Wing Aspect Ratio : 23.43
Wing Taper Ration : 0.10
Quarter Chord Sweep : 16.5 deg.
Thickness Ratio : 0.17

Initial Performance Data
Design Cruise Speed : 150 kts
Design Dive Speed : 225 kts
Max. Level Speed : 180 kts
Ultimate Load Factor : 3.8
Landing Load Factor : 3.8

Initial Landing Gear Data
Main Gear Strut Length : 3.67 ft
Nose Gear Strut Length : 3.67 ft

Engine/Propeller Data
Number of Blades : 4
Prop. Diameter : 9.0 ft
Engine H.P. : 375

Table 4.1 : CONDOR Component Weight Estimation Input Data

Due to the unique features of the CONDOR, several components of the aircraft, such as the wing joints, required a weight estimate based on engineering judgement. This was done by examining the component weights of other aircraft, given in Reference 49, and then making an estimate to convert the value to the CONDOR. This method was used on components such as the propeller shaft, and wing joints, which weren't specifically included in any of the applicable empirical equations. The data used in the computer program is listed in table 4.2, this gives component weights and centroids. The radii of gyration have been omitted due to reduce the size of this table. It should be noted that the

wing was broken into sixteen components and the fuel system into eight components to give more accurate inertia estimates.

Component	Weight (lbs)	X-Bar	Y-Bar	Z-Bar
Fuselage	575.00	193.60	0.00	200.00
Wing (16 components)	2500.00 (total)	---	---	--- *
Control Surfaces (two)	50.00 (each)	366.00	±375.00	218.00
Verticals (two)	85.00 (each)	355.00	±440.00	230.00
Wing Joints (two)	50.00 (each)	355.00	±448.00	220.00
Main Landing Gear (two)	225.00 (each)	292.30	±191.00	208.00
Nose Landing Gear	100.00	150.00	0.00	180.00
Air In-Take	30.00	256.00	0.00	240.00
Engine	600.00	280.00	0.00	220.00
Propeller	200.00	395.00	0.00	245.00
Prop. Shaft	50.00	355.00	0.00	232.50
Transmission	150.00	315.00	0.00	220.00
Fuel Tanks (4 comp.)	700.00 (total)	---	---	--- *
Flight Computer Consul	48.00	95.00	0.00	180.00
UHF Communications	11.00	95.00	0.00	180.00
Gyro Compass	8.40	95.00	0.00	180.00
Autopilot System	168.50	232.00	0.00	200.00
Air Data Computer	14.00	95.00	0.00	180.00
Stability Augmentation	200.00	232.00	0.00	200.00
Radar Altimeter	38.20	95.00	0.00	180.00
Flight Data Recorder	15.60	95.00	0.00	180.00
Air Conditioning	150.00	232.00	0.00	200.00
Wire	150.00	220.00	0.00	190.00
Equipment Rack	150.00	232.00	0.00	200.00
Water	120.00	220.00	0.00	188.00
Food	20.00	220.00	0.00	188.00
Seats (two)	225.00 (total)	150.00	±20.00	188.00
Oxygen	15.00	220.00	0.00	188.00
Misc.	10.00	180.00	0.00	188.00
Paint	30.00	244.00	0.00	205.00
Grease	10.00	270.00	0.00	220.00
Empty Weight, W_E	7108.70	282.83	0.00	210.48
Fuel (4 components)	3700.00 (total)	---	---	--- *
Crew (two)	200.00 (each)	140.00	±20.00	200.00
Payload	200.00	244.00	0.00	180.00
Take-Off Weight, W_{TO}	11408.70	274.83	0.00	209.02

* No centroid given because of the number of components

Table 4.2 : CONDOR Weight and Balance Statement

The quantity of fuel used during the mission was calculated directly, using the average specific fuel consumption of the engine over the mission segment. The percentage of trapped fuel has been taken as one percent, which is at the lower spectrum of acceptable

values, (Reference 39). The reason for this percentage of trapped fuel is two fold. First, the mission fuel fraction for the CONDOR is higher than typical aircraft due to the long cruise mission phase. This indicates that one percent of the fuel is a considerable amount (37.0 lbs). The second reason is that in the weight estimate for the fuel tanks, additional weight was included for a sophisticated fuel pumping and C.G. control system. It is assumed that this system will reduce the amount of trapped fuel in the bladder cells.

The amount of reserve fuel was set at the fuel required for a 2 hour loiter which meets the FAR 23 requirements. This value has been included in the fuel system weight estimate, however with the In-Flight analysis this fuel was assumed to be unused, as was the trapped fuel. The total fuel breakdown is shown in figure 4.4. Note that the abscissa is based on a logarithmic scale in order to graphically show the large differences in fuel weights.

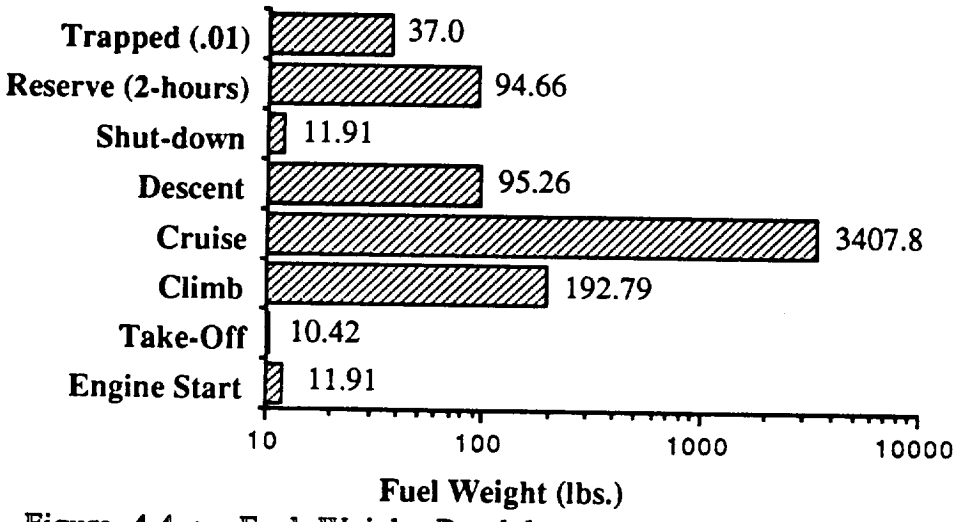

Figure 4.4 : Fuel Weight Breakdown

The computer analysis explained in Appendix B summed the component weights into their respective systems. Figure 4.5 shows the total weight distribution between the aircraft systems. It should be noted at this point that the fuel system includes the weight of the fuel bladders and pumping system.

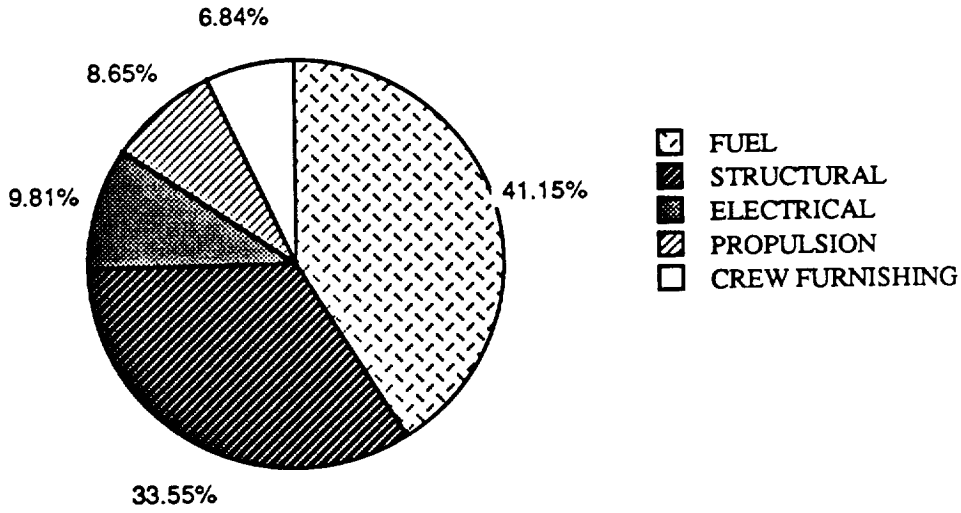

Figure 4.5 : System Weight Distribution

The final mass properties for the CONDOR along with all the system mass properties are shown in table 4.3 (generated using the computer analysis). The moments and products of inertia in this table are centered about the system centroids and aren't sum directly to get the aircraft totals.

System	Weight	X-bar	Y-bar	Z-bar	Ixx	Iyy	Izz	Ixz
Structure	3995.2	305.47	0.0	212.90	101566	4288	105584	710
Propulsion	1030.0	310.37	0.0	226.04	23	493	470	90
Fuel	4400.0	275.60	0.0	208.40	65089	914	65941	165
Electrical	1168.5	215.44	0.0	193.15	21	568	547	52
Crew	775.0	155.61	0.0	194.19	41	133	161	-16
Misc.	40.0	250.50	0.0	208.75	0	1	1	0
CONDOR	11408.7	274.83	0.0	209.02	166918	10934	177064	1771

Note: Weights = (LBS), Centroids = (IN), Inertias = ($SLUG/FT^2$)

Table 4.3 : CONDOR System Mass Properties

4.4 Transportation Section Weights

As a requirement of the RFP, the CONDOR must disassemble into sections for transport. This was accomplished by breaking the aircraft into five major sections and three sub-sections, which when arranged properly would fit into the cargo bay of a C-130 aircraft or on a tractor-trailer truck bed. For loading purposes, in is important that the weights of these sections be known. Table 4.4 lists the weights of the eight total sections created by the transportation breakdown. These weights assume that all the fuel, payload, crew and their materials have been removed.

Section	Weight (lbs)
Fuselage	2653.50
Inner Wing Sections (2)	1557.80
Outer Wing Sections (2)	377.30
Propeller	200.00
Verticals (2)	85.00
Total Transportation Weight	6893.70

Table 4.4 : Transportation Section Weight Breakdown

4.5 In-Flight Mass Properties Analysis

The mass properties given thus far are for the CONDOR at take-off. However, changes during the course of the flight are of major importance. During the mission 3700 lbs. of fuel is consumed, and this could have a profound effect on the mass properties, especially the C.G., of any aircraft. The CONDOR was balanced in an effort to limit these in-flight changes. For this analysis it was assumed that the reserve fuel remained unused. The mass properties computer program allowed for a variation of the fuel weight, giving the output data for this section.

4.5.1 In-Flight Centroid Movement

The CONDOR, because of its long endurance requirement, was balanced so that minimal changes would occur to the centroid. This was done in order to give constant handling over the mission. A nearly stationary centroid was achieved by placing the centroid of the fuel close to where the aircraft centroid was expected. An iteration process was performed until the centroid travel over the mission was less than half an inch in any of the three axis.

For stability and control reasons the C.G. travel in the X or station axis is of most importance. The graph of figure 4.6 shows the X-axis C.G. travel relative to the CONDOR's aerodynamic center, which is at station line 292.5 .

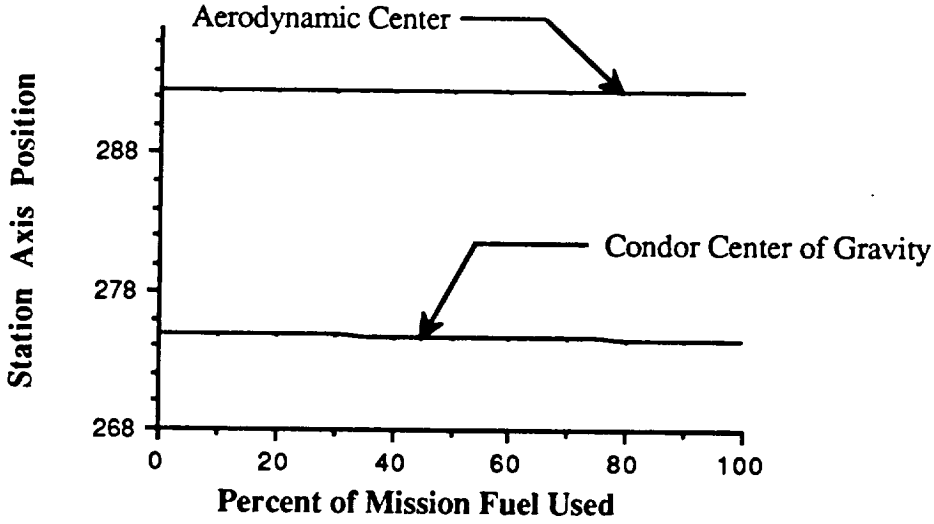

Figure 4.6 : Variation of Station Center of Gravity During Mission

It should be noted that the motion is away from the aerodynamic center, which slightly improves the pitch stability over the mission.

The C.G. motion in the Z-axis is also of minor importance in lateral stability and control. This variation during the mission is shown in the graph of figure 4.7

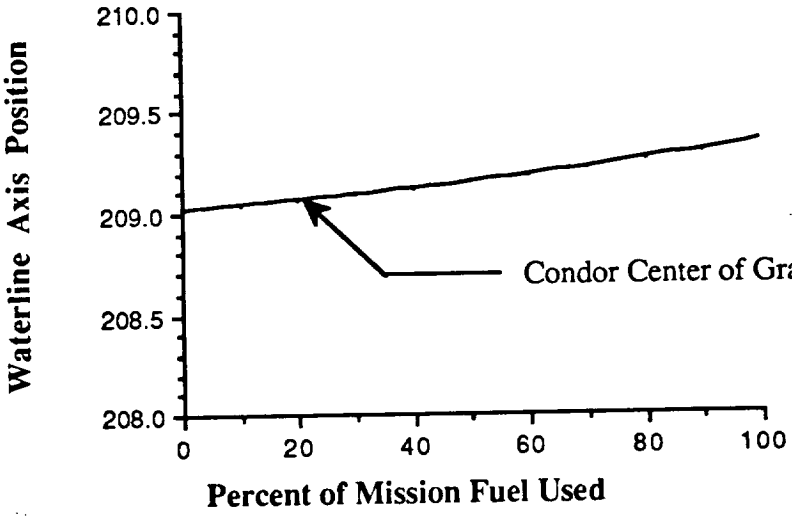

Figure 4.7 : Variation of Waterline Center of Gravity Over Mission

Note that the centroid is above the fuselage centerline, this is because of the upward wing deflections during flight.

An additional centroid excursion analysis was performed to check the changes in center of gravity when the crew and payload were removed or changed position. This data will be needed for unmanned missions, which is one of the design criteria for the CONDOR. A graph of this data is shown in figure 4.8. Note that when the crew are removed the X-axis centroid moves considerable toward the aerodynamic center.

The total centroid travel from manned take-off weight to empty weight is 8.42 inches which is 10.2% of the mean aerodynamic chord. This is well within the acceptable range (6 to 27%) for a single engine aircraft, (Reference 44). The static margin of the CONDOR for manned flight is 21% and 11% for un-manned flight.

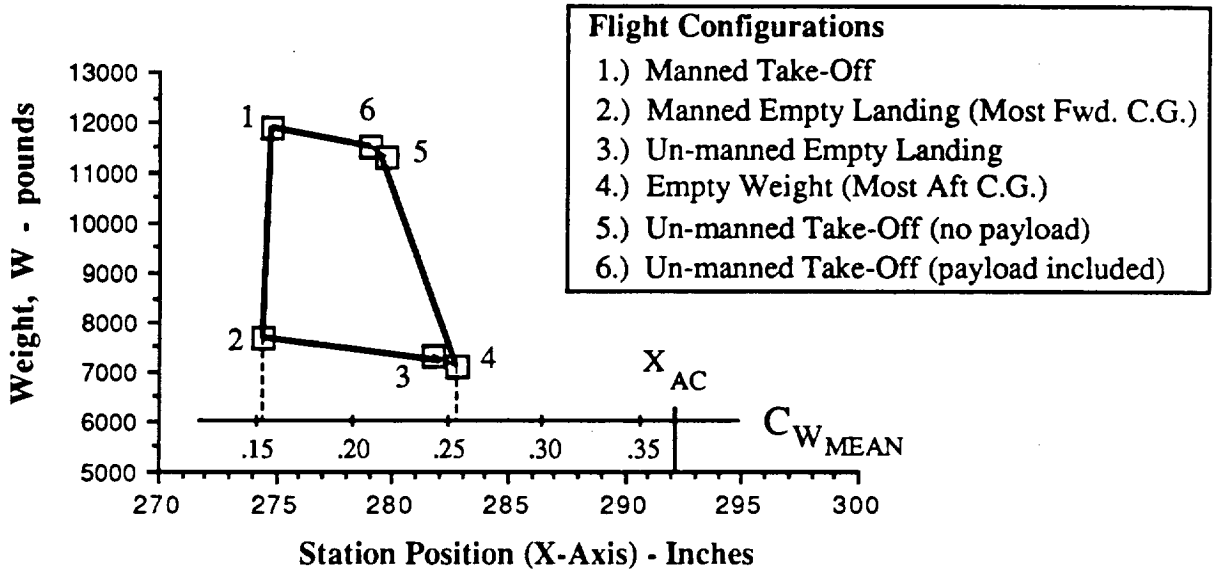

Figure 4.8 : CONDOR C.G. Excursion Diagram

4.5.2 In-Flight Moment and Product of Inertia Changes

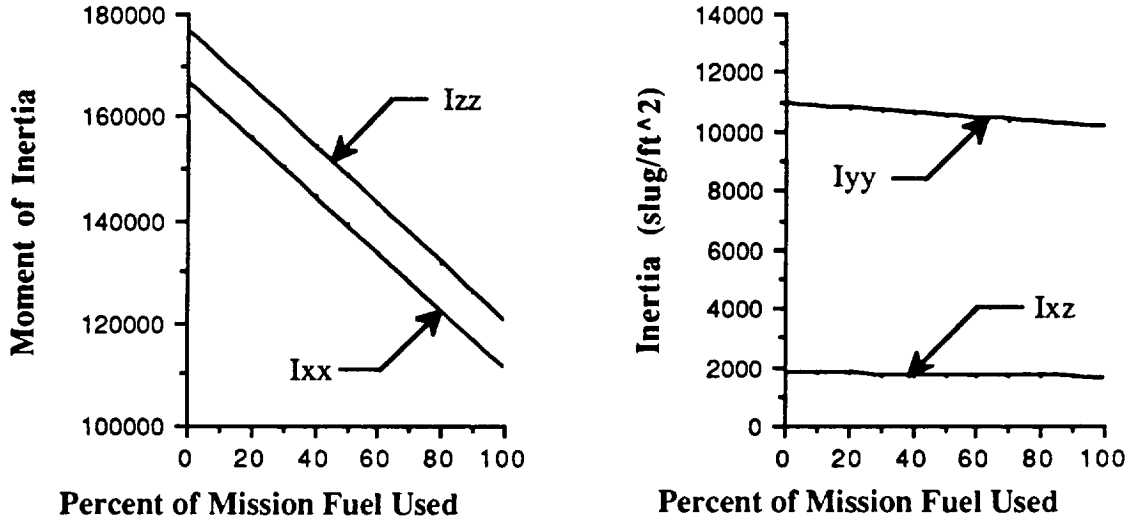

Figure 4.9: In-Flight Inertia Changes

Since the CONDOR's fuel is stored in the wings, changes in moments and products of inertia were unavoidable. However an effort was made to limit the changes by placing the fuel closer to the root of the wing. The changes in the inertias that occurred affected the dynamic stability and control of the CONDOR, and are the reason why an analysis was done on the in-flight dynamics. Figure 4.9 graphically depicts the inertia changes during the mission. The significance of these changes can be seen fully in the stability and control section (Chapter 9.0).

5.0 AERODYNAMICS

5.1 Airfoil Selection

Airfoil selection, as with any aircraft, was very crucial to the design of the CONDOR. The wing was designed with simplicity as a major goal because the wings will have to be disassembled to fit into a C-130 aircraft. It was designed to take-off and land without the use of flaps to help with this simplicity; therefore, an airfoil with a high maximum lift coefficient was necessary. Another concern in airfoil selection was the varying lift coefficient during cruise. The CONDOR's lift coefficient varies during cruise from .98 at the beginning cruise to .55 at the end; therefore, the airfoil used, must have low drag over a large range of lift coefficients. Many airfoils such as the Liebeck, Wortman, and Whitcomb were considered. The Liebeck and Wortman airfoils were not used because they are mainly designed for lower Reynolds number use ($2x10^{-6}$) than the CONDOR'S ($5x10^{5}$) which would result in higher drag. The Whitcomb GA(W)-1 was chosen because its drag is almost constant over the wide range of lift coefficients necessary, it has a maximum lift coefficient of 1.8 and it is designed to operate best at or near the CONDOR's cruise Renoylds number. The GA(W)-1 airfoil is 17% thick which will allow ample room for fuel storage. The airfoil is also a partial laminar flow airfoil with the maximum thickness occurring at 40% of the chord. This will allow (if laminar flow is assumed over 40 % of the airfoil) for approximately 20% drag reduction over non-laminar airfoils.

5.2 Planform Selection

During the planform selection of the aircraft the wing aspect ratio (AR) was maximized as much as possible to keep the wing drag-due-to-lift factor (K) as low as possible and the lift curve slope as high as possible. The root chord size was limited to 10.5 feet because of the size restraint of the C-130 transport aircraft. The tip chord of 1 foot was chosen to keep the AR high (23.4) and to reduce the lift at the outer portion of the wing; therefore, reducing the wing structural weight. The wing 1/4 chord angle of 16.5 degrees was chosen to keep the aerodynamic center aft of the center of gravity.

Winglets, which help cut down induced drag, were considered for the CONDOR, but were not used because of their limited effect with the CONDOR's small tip chord and because of the weight they would add at the wing tip.

A summary of the CONDOR planform specifications are shown in Table 3.1

5.3 Estimation of Drag

The total drag coefficient for a wing-body combination is expressed as (Reference 29),

$$C_D = (C_{D0})_{wing} + (C_{D0})_{body} + \Delta C_{D0} + C_{DL} \qquad 5.1$$

The method in the DATCOM (Reference 29) was used to calculate the zero lift drag coefficient for the wing and body of the aircraft. The flow around the wing and body of the plane was assumed to be turbulent to calculate the maximum drag. The zero lift drag for the wing and body were calculated separately based upon the wetted area of the separate components (with allowance for the appropriate reference area) and then added together. An approximate value of 5% of the wing and body zero lift drag due to the mutual interference effect was also added in the calculation of the total zero lift drag (Reference 39). The CONDOR has no base drag because it has a closed body fuselage. The drag of miscellaneous items such as the canopy, nozzle boattail, and other protuberances were also considered in the drag calculation.

The drag due to the lift is the induced drag and the viscous drag. Therefore, the drag polar equation becomes,

$$C_D = C_{D0} + K'C_L^2 + K''(C_L - C_{L\,min})^2 \qquad 5.2$$

The induced drag factor K' is given by,

$$K' = \frac{1}{\pi Ae}, \qquad 5.3$$

where the Oswald's wing efficiency factor,e, was calculated using the Weissinger wing planform efficiency factor,e', and the body diameter to wing span ratio, d/b,

$$e = e'[1 - (\frac{d}{b})^2]. \qquad 5.4$$

The corresponding e value is 0.808. The viscous drag due to the lift factor, K", is dependent upon leading edge radius and taper ratio and was found from Nicolai (Reference 39) Figure 11.6 pg.11-11. The complete form of the drag polar equation becomes,

$$C_D = C_{D0} + 0.0168\ C_L^2 + 0.027(C_L - 0.44)^2, \qquad 5.5$$

where C_{D0} for T/O, climb, and cruise is 0.00698, 0.00689, and 0.00746, respectively. The C_{D0} at cruise is larger than at the other conditions because of the change of Reynolds number at higher altitudes. During the take-off and landing phase, the landing gear adds additional drag which is 1.5 percent of the total C_{D0} value. The maximum value of L/D is 42 for T/O, landing, and climb and 37 for the cruise at the average lift coefficient. Figure 5.1 shows the drag polar for the for the CONDOR in both dirty (gear down) and clean configurations. This figure also shows a list of the component drag contributions. Figure 5.2 shows how the L/D and drag coefficient vary for different lift coefficients. It can be seen from this figure that the best lift coefficient to cruise at will be approximately .55. The CONDOR flies over a wide range of lift coefficients, and that towards the end of its cruise it flies at this optimum lift coefficient. The early cruise lift coefficients were chosen to be around 1.0 so the wing area could be kept reasonably small (801 ft^2) and the cruise velocity would be 150 Knots, as specified by the RFP.

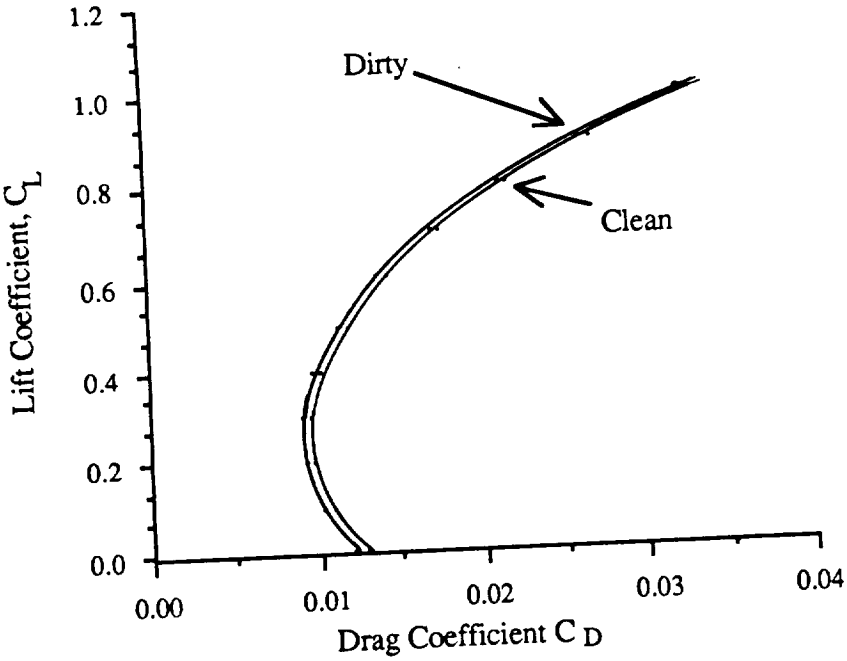

Components of Zero-lift Drag during Take-off

Wing	0.004
Fuselage	0.00114
Vertical tail	0.00034
Landing gear	0.00009
Trim	0.00071
Windshield	0.00021
Protuberence	0.00049
Total	0.00698

Figure 5.1 : Drag Polar

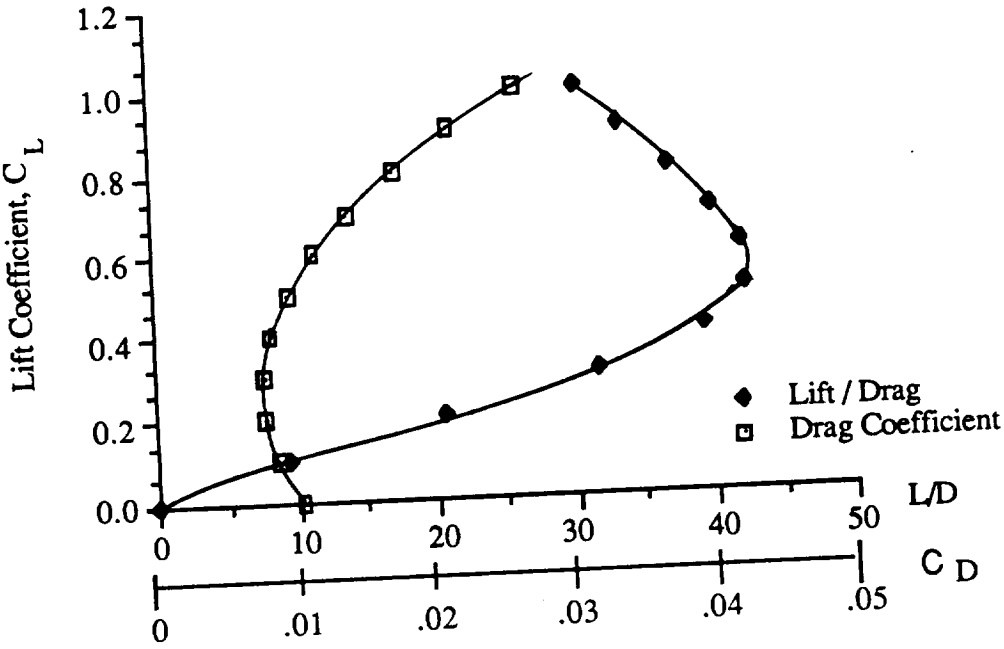

Figure 5.2 : L/D change with Drag Coefficient

6.0 PERFORMANCE

6.1 Take-off

Take-off is the distance required for an aircraft to accelerate from V = 0 to take-off speed and climb over a 50 foot obstacle. Figure 6.1 shows the take-off schematic.

The take-off analysis was completed using the method outlined in Nicolai (Reference 39) with no aircraft rotation. The analysis is broken into 3 different sections; ground roll, transition, and clearance of a 50' obstacle.

6.1.1 Ground Roll

The ground roll is the distance the plane travels from V = 0 to V = V_{TO}. The equation for the ground roll is (Reference 39):

$$S_G = \frac{1.44\,(W/S)_{TO}}{g\rho C_{Lmax}\left[\frac{T}{W} - \frac{D}{W} - \mu\left[1 - \frac{L}{W}\right]\right]} \qquad 6.1$$

It has the C_{Lmax} term in the denominator; therefore, the larger the C_{Lmax} the shorter the ground roll distance. The CONDOR will not be rotating during take-off; therefore, the C_{Lmax} value was assumed to be the maximum C_L during the ground roll. This will increase the ground roll distance as compared to a take-off with rotation. The thrust, drag, and lift terms of equation 6.1 were all determined for velocity values of $.7V_{TO}$ as outlined by Nicolai. The take-off speed, V_{TO}, is $1.2V_{Stall}$. Using a ground roll C_L = .6 (positive 2 degree ground angle of attack) and a coefficient of friction of m=.25,

S_{GR}= 3486 feet.

6.1.2 Transition

The transition distance is the distance just after take-off while the aircraft is flying at constant velocity in a constant radius arc.

$$S_T = R \sin q_{CL}, \qquad 6.2$$

where R is the arc radius and q_{CL} is defined by Figure 6.1.

Using this method,

S_T= 676 feet.

6.1.3 Clearance

The climb distance is the distance it takes the aircraft to clear a 50' object, as specified by FAR 23.

$$S_{CL}=\frac{50 - h_{TR}}{\tan q_{CL}} \qquad 6.3$$

S_{CL}= 343 feet.

The total take-off distance is 4507 feet, as shown in Figure 6.1.

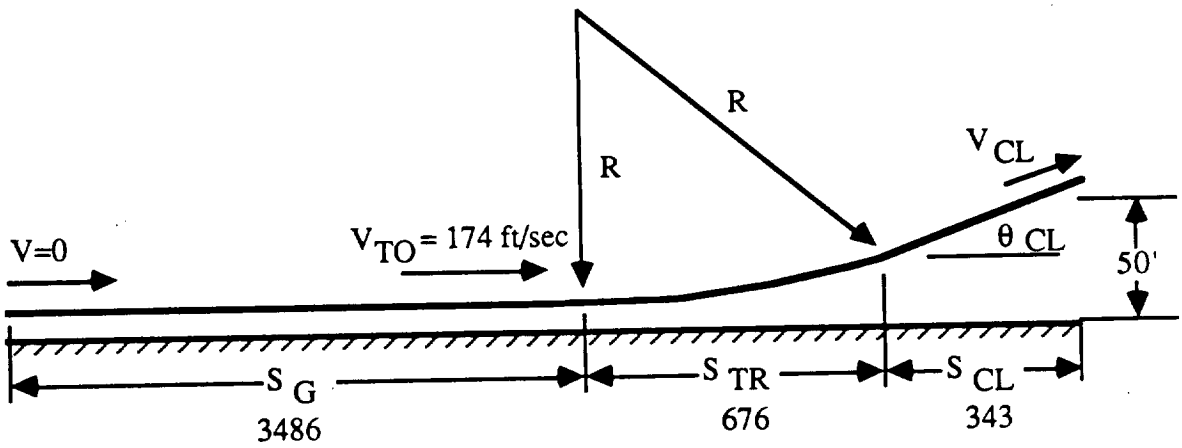

Figure 6.1 : Take-Off Schematic

6.2 Landing

The landing distance is the horizontal distance required to clear a 50 foot obstacle, land, and brake to a complete stop. The landing distance is broken into 3 parts: airborne distance, free roll, and braking distance. Figure 6.2 shows the landing schematic.

The landing distance is computed using Nicolai's (Reference 39) landing analysis. This analysis assumes the aircraft is landing with 1/2 of its fuel remaining.

6.2.1 Air Distance

The air distance is the horizontal distance required for the aircraft to travel over a 50' obstacle and touch down. This distance is given by the equation:

$$S_A = \frac{L}{D}\left[\frac{V_{50}^2 - V_{TD}^2}{2g} + 50\right] \qquad 6.4$$

with $V_{50} = 1.3\ V_{Stall}$ $V_{TD} = 1.15\ V_{Stall}$,

which are calculated using the stall velocity at landing. The drag is also calculated using this stall velocity. The drag coefficient in landing is .038, higher than it was in take-off, due to the two spoilers located on the wings that increase the drag coefficient by approximately 80%. Using this method the air distance is:

$S_A = 2021$ feet.

6.2.2 Free Roll

The free roll is the distance the plane travels after touch down and before the pilot engages the brakes. This average time is 3 seconds (Reference 39). Therefore, the free roll distance becomes:

$$S_{FR} = 3V_{TD} = 287 \text{ feet.} \qquad 6.5$$

6.2.3 Braking Distance

The braking distance is the distance it takes to stop the aircraft after the brakes have been applied. From Nicolai, the braking distance equation is:

$$S_B = \frac{W_L}{g\mu\rho S\left[\frac{C_D}{\mu} - C_{LG}\right]} \ln\left[1 + \frac{\rho S}{2W_L}\left[\frac{C_D}{\mu} - C_{LG}\right]V_{TD}^2\right] \qquad 6.6$$

with m (the breaking coefficient) =.5 (Reference 39).

Therefore, the braking distance is:

$S_B = 396$ feet.

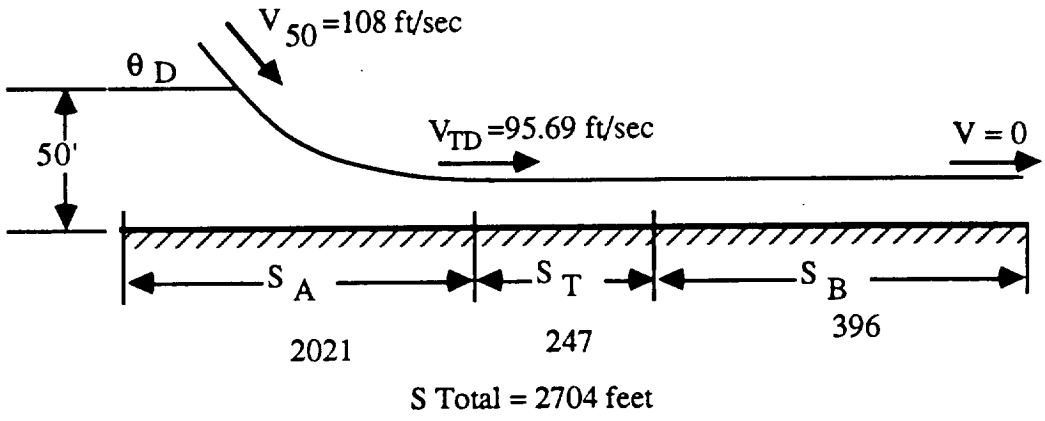

Figure 6.2 : Landing Schematic

6.2.4 Total Landing Distance

The total landing distance is the sum of the three components:

S_L= 2704 feet.

Analysis was also completed for two other cases, landing just after take-off with a full load of fuel, and landing at the ending of the mission with only reserve fuel left. These landing distances are shown in Table 6.1.

Landing Distance	Fuel 100% (V_{Stall}=145ft/sec) (C_D=.042)	Fuel 50 % Fuel (V_{Stall}=83 ft/sec) (C_D=.038)	Reserve Only (V_{Stall}=74 ft/sec) (C_D=.033)
Air	1371 ft	2021 ft	2087 ft
Free Roll	501 ft	287 ft	258 ft
Breaking	1790 ft	396 ft	314 ft
Total	3807 ft	2704 ft	2659 ft

Table 6.1 : Landing Distances

The CONDOR meets the RFP (landing distance < 5000 feet) in all cases; therefore, it can land at any time during the mission.

6.3 Rate of Climb

The rate of climb for a steady climb is given by (Reference 34):

$$\frac{dh}{dt} = \frac{P_a - P_r}{W}. \qquad 6.7$$

The turbo-charged piston engine of the CONDOR can produce constant power up to the cruising altitude of 45,000 ft. Therefore, power required for the CONDOR is calculated from (Reference 34)

$$P_r = \frac{\rho f}{2} V^3 + \frac{2(W/b)^2}{\pi \rho e} \frac{1}{V}, \qquad 6.8$$

where f is the aircraft equivalent frontal area. Figure 6.3 shows the power required and the power available for the CONDOR as the velocity increases.

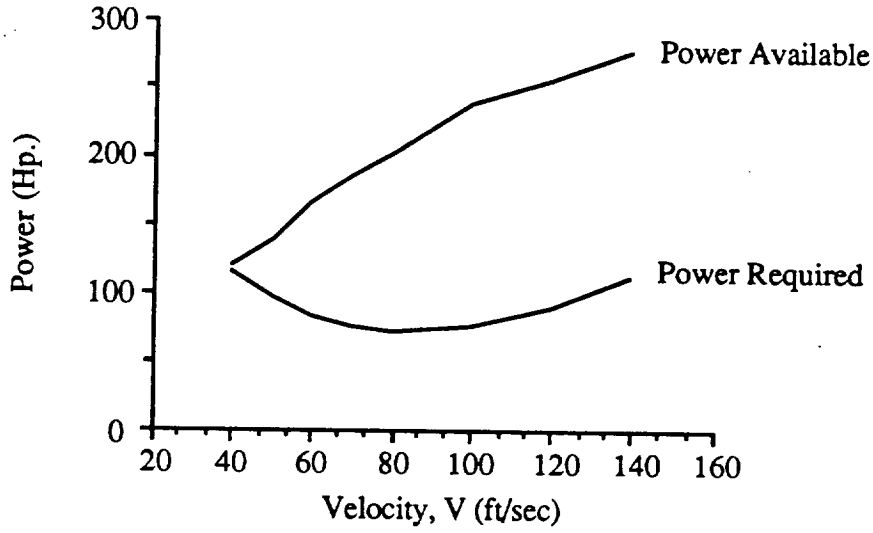

Figure 6.3 : Power Required and Power Available

The RFP states that the aircraft must climb to its cruise altitude of 45,000 feet in less than 3 hours. The climbing velocity is given by (Reference 34):

$$V_{climb} = \sqrt{\frac{2W}{\rho S}\sqrt{\frac{K}{3C_{D_0}}}}. \qquad 6.9$$

Figure 6.4 shows the rate of climb for different power settings as altitude increases, and Figure 6.5 shows the time to climb for the same power settings. FAR 23 states the aircraft

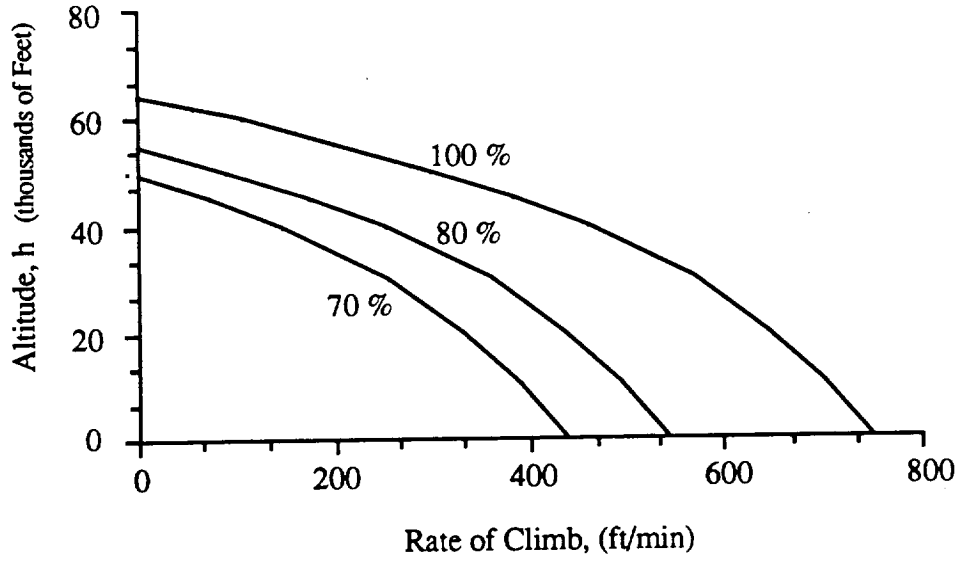

Figure 6.4 : Rate of Climb

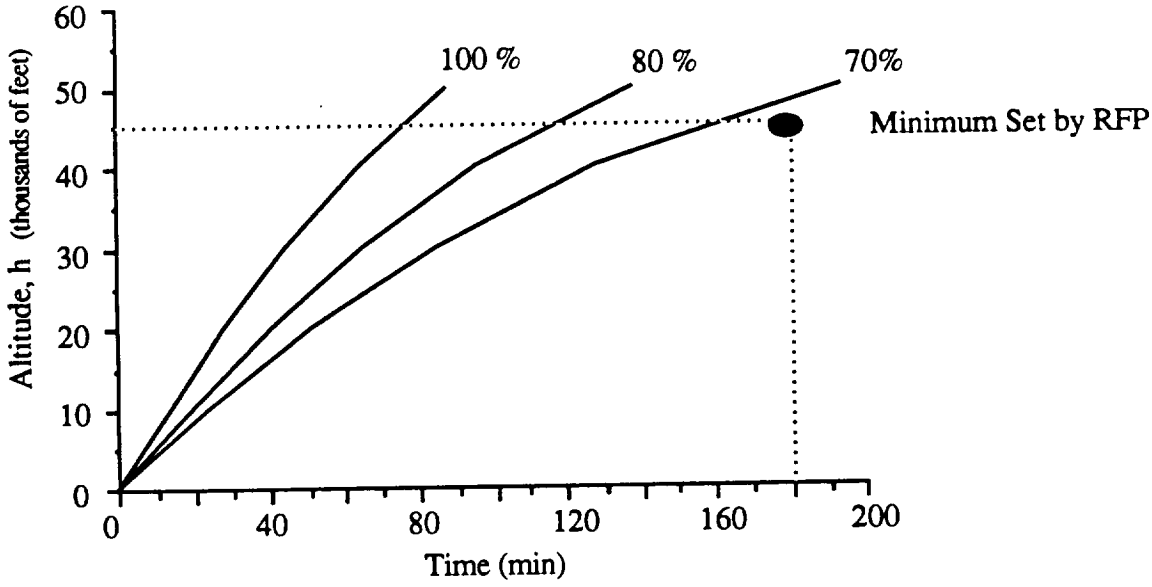

Figure 6.5 : Rate of Climb

must climb at a rate ≥ 300 ft/min; a minimum power setting of 70 % is necessary for an average climb rate of 300 ft/min to be met. Therefore, the power setting during climb will

be 70% with the average climb velocity = 238 ft/sec, and a fuel weight during climb = 192 Lbf.

The absolute ceiling and service ceiling of the CONDOR is 60,500 ft and 59,000 ft, respectively.

6.4 Endurance

The RFP requires that the endurance of the aircraft be 72 hours. The CONDOR was designed to meet this design point with a 2 hour reserve. The endurance was calculated using the following equation (Reference 34):

$$t_e = 357\left[\frac{1}{V}\right]\left[\frac{\eta}{c}\right]\left[\frac{L}{D}\right]\ln\left[\frac{W_4}{W_5}\right] \qquad 6.10$$

Using average values for the cruise, a propulsive efficiency, η, = .81, and a specific fuel consumption of .291 Lb/hp-hr; the endurance of the CONDOR is 74.57 hours, which is 2.57 hours more than the RFP requires. The extra time will be considered reserve.

7.0 PROPULSION SYSTEM DESIGN AND NOISE CONTROL

Since the RFP requires that the aircraft be able to cruise nonstop for 72 hours at high altitude (45,000 ft) an engine with extreme reliability and low fuel consumption is required. As with any other engines, low initial and operating cost, low cooling drag, high p/w ratio, and multifuel capability if possible are also desirable. The noise that is attributable to the propulsion system and method of noise reduction are other factors to consider. It is desired to have engine and propeller noise reduced to a minimum, which will decrease the acoustic insulation required for the crew cabin.

7.1 Engine Trade-Off Study

From preliminary calculations of weight, L / D, assumed propeller efficiency and power setting at cruise, an engine power of 400 hp, at sea-level, was found to be required. Various types of engines, which could yield this power rating, were studied to come up

with the best engine. Four general categories of engines were studied for comparison in this analysis, they include small Turboprops, Reciprocating, Rotary, and Diesel engines. Of all the desirable qualities of an engine, the brake specific fuel consumption (BSFC) was determined to be the most critical parameter; since a 1% deviation in BSFC could significantly alter the overall performance of the whole airplane by adding or reducing fuel weight.

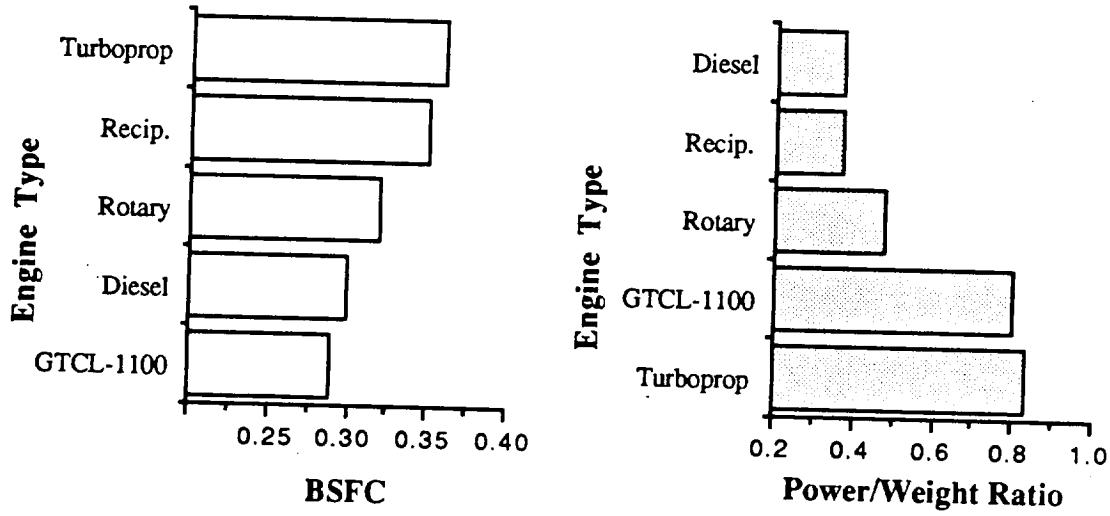

Figure 7.1 : Engine Comparison Charts

BSFC and Power/Weight ratio data, for the engines considered, is summarized in Figure 7.1. The data represents both currently available top of the line engines was well as future generation engines to be available be early 1990's. Although some of these engines do not maintain their power up to an altitude of 45,000 ft., it was assumed that some form of supercharging could be used to bring them up to altitude, without significant loss to the performance of the engine. In fact, generally supercharging the engine has favorable effect on BSFC (Reference 54). Therefore, for the comparison study, it was assumed that each engine retains its characteristics up to the altitude of 45,000 ft.

Turboprop engines are characteristically the best, of the engines examined, for operation at high altitudes. The power/weight ratio comparison in Figure 7.1, seems to put the turboprops at the top of the comparison, since it has the best ratio. However, their poor fuel consumption eliminates them from the comparison, due to the large increase in fuel weight that they would cause.

A new line of rotary engine, scheduled to be introduced to general aviation in the early 1990's by John Deere, will offer the best characteristics of rotary engines. Rotary engines in general provide better fuel consumption, and higher power/weight ratio's than reciprocating engines of the past. Additional benefits include low cooling drag, lower cost, and higher reliability relative to reciprocating engines. Due to the nature of the rotary engine, the vibration is minimal which is extremely important to avoid noise and structure fatigue.

Diesel engines offer lower BSFC values than rotary engines, as low as 0.3 lb/hp-hr in the newer engines. However, these engines do not compare favorably to the rotary engines with respect to power/weight ratio. An additional drawback of the Diesels is that they require high inlet pressures, thus necessitating a large turbo-charging system.

Reciprocating engines can be considered to be more reliable than the other engines considered. An indication of this fact is supported by the engine of the aircraft Voyager, which flew around the world nonstop. It's engine, the Voyager 200 was in operation for a majority of the 9 day flight, without a mechanical failure. The top of the line reciprocating engines are relatively new and thus there is a great potential for improvement, in terms of better efficiency and performance. For example, a reciprocating engine with a single turbocharger is rated only up to 18,000 ft. With a double turbochager and stratified charging combustion technology, it could raise the critical altitude to 45,000 ft and at the same time reducing the BSFC to 0.35 lb/hp-hr as shown in the Figure 7.1 .

An experimental engine, the GTCL-1100, uses a twin-turbocharger/supercharger system with a maximum power to a value of 375 hp. This turbocompounded engine would be flat rated to 65,000

ft., with a BSFC of a mere 0.290 lb/hp-hr at 75 % power. This gives GTCL-1100 the lowest fuel consumption of the engines investigated. The power/weight ratio for the GTCL-1100 is very close to the turboprop, as shown in Figure 7.1. These numbers were derived from a theoretical cycle analysis. It was assumed that the technology to build this engine would be in reach by the time production of the CONDOR could start. Because of this low BSFC and high power/weight ratio, this engine is more desirable than any of the previously mentioned engines.

To better illustrate the fuel consumption performance of the GTCL-1100, a carpet plot of the BSFC versus Engine Power for different RPM and manifold pressures values is shown in Figure 7.3. This plot shows that the BSFC is nearly constant for different RPM's, when the manifold pressure is kept close to the sea level value. The will be done for CONDOR's engine with the low and high pressure superchargers shown in figure 7.2 . The Turbocompounding System will give sea level manifold pressure (30 in Hg) up to an altitude of 65,000 ft. The BSFC will vary from 0.291 lb/hp-hr at the beginning of cruise to a value of 0.289 lb/hp-hr at the end of cruise. This can be seen in Figure 7.3 .

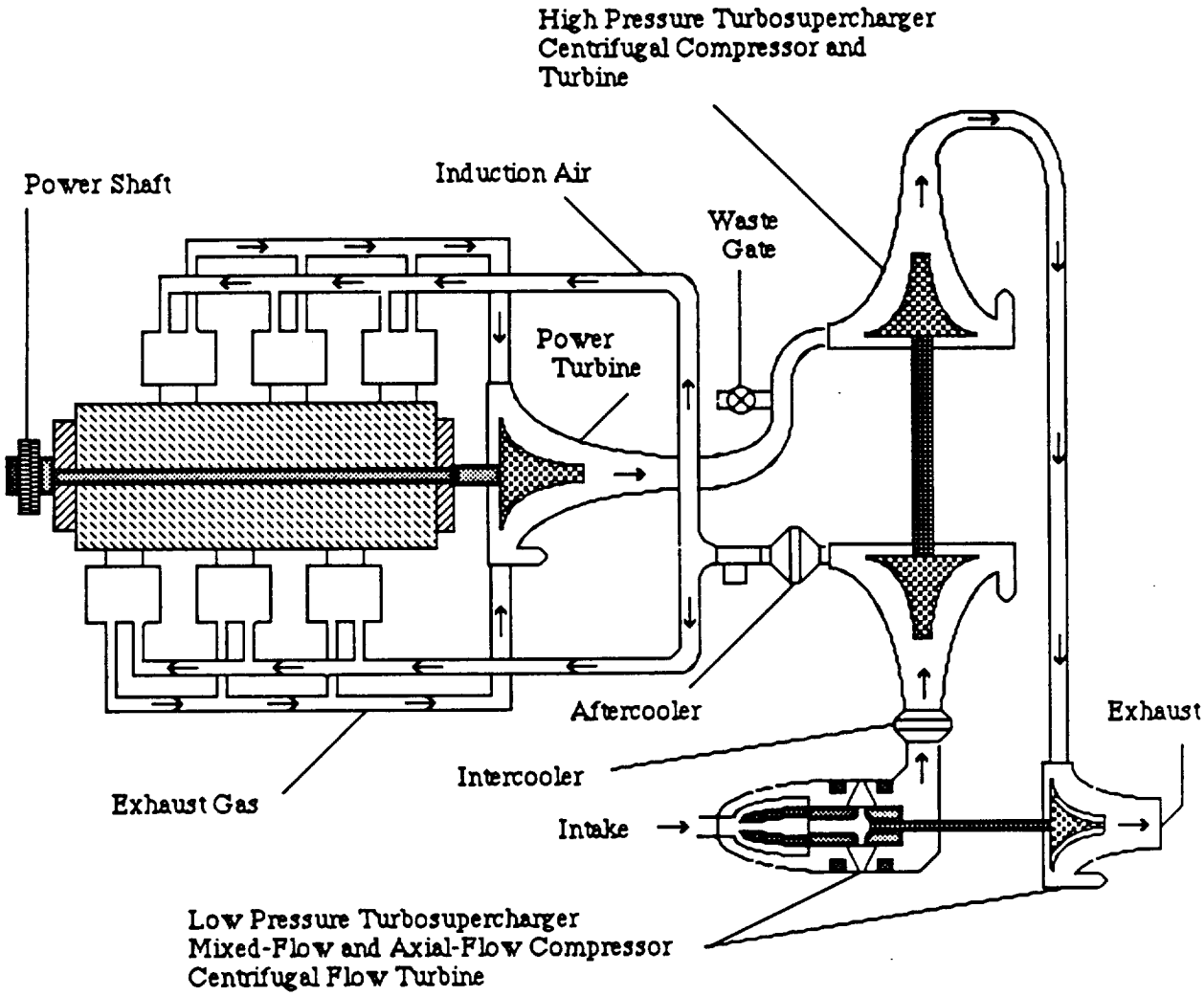

Figure 7.2 : GTCL-1100 Liquid Cooled Turbocompounded Engine Schematic

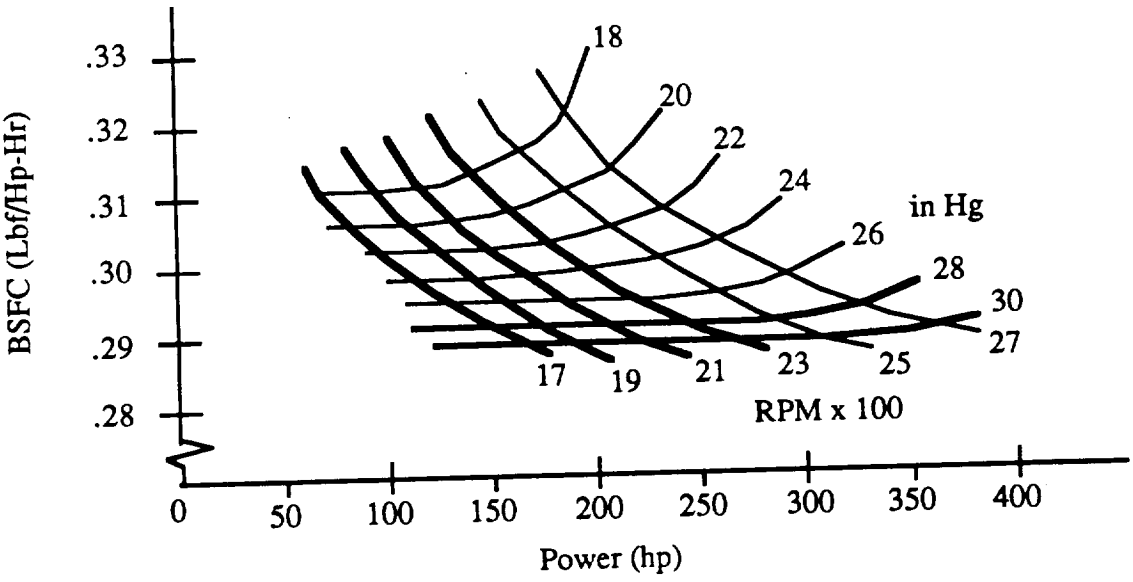

Figure 7.3 GTCL-1100 Fuel Consumption

7.2 Propeller design

The efficiency of the propeller, as with the engine, is of major importance in propeller selection. An increase in efficiency will greatly decrease the mission fuel weight of the CONDOR.. Therefore, a parametric study of 2,3,4 and 6 bladed propellers was done for varying diameters. Table 7.1 lists the factors given consideration in the propeller selection.

1) Maximum Obtainable Efficiency
2) Overall Propeller Weight
3) Convenience Factor (Storage)
4) Limit Noise Production
5) Cost of Materials and Manufacturing

Table 7.1: Propeller Selection Considerations

Propeller efficiency is increased with propeller diameter, for a given number of blades. The lower the number of blades, the better the efficiency possible. Therefore,

strictly from an efficiency point of view, a large propeller with a small number of blades is desired (Reference 22).

The maximum size of the propeller is, in effect, limited by the RFP transportation breakdown requirement. The CONDOR must breakdown into pieces which can fit into the cargo bay of a C-130 aircraft. The cargo bay has a width of 10.25 ft. and a height of 9.23 ft., placing the propeller diagonal would significantly reduce the space for other components. To give flexibility in the storage position of the propeller, a diameter of 9.00 ft. was selected. The propeller also had to clear the runway on take-off and landing; the 9 foot propeller was small enough to allow this.

The weight of a propeller increases, as one would expect, with diameter and the number of blades. This can be seen in figure 7.4 which shows propeller weight versus diameter for a various numbers of blades. The curves of this graph are based on equations form the methods of Hamilton Standard.

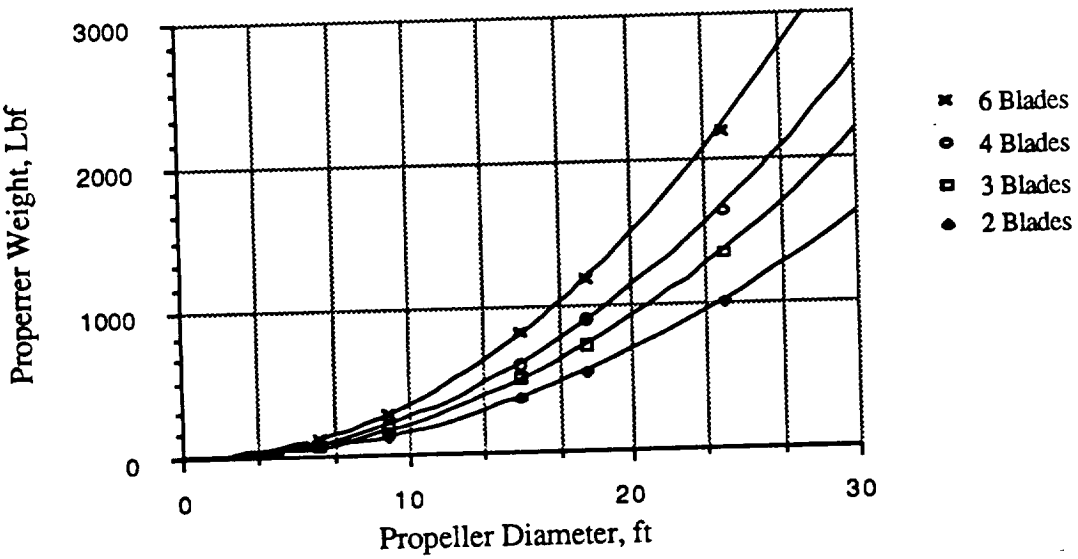

Figure 7.4 : Propeller Weight Change with Diameter

The curves in this graph are for propellers made of composite materials. Composites were chosen because they will decreased the weight and noise, relative to a metal propeller.

Noise production is also significantly decreased if the number of blades is increased. The propeller noise is usually the main component in noise productions. To increase crew comfort, the internal noise levels of the CONDOR are being limited in the design. This was the major factor for choosing a four bladed propeller for the CONDOR. The loss in propeller efficiency was deemed acceptable to reduce the noise production.

Another factor that is important, but not so obvious, is the convenience factor. This is a measure of the degree of relative ease in removing, storing and reassembling the CONDOR. The longer it takes to get ready for a flight, the more it will cost to operate. This concern has been satisfied by selecting a propeller diameter which will easily fit into either the C-130 cargo bay, or into the back of a tractor trailer.

The pertinent data on the CONDOR's Propeller is given in table 7.2.

Diameter :	9.00 ft
Number of Blades :	4.0
Propeller Efficiency :	.85
Operation RPM :	1850
Advance Ratio :	1.1
Activity Factor :	80.0
Average C_L :	.71

Table 7.2 : Propeller Data

7.3 Aircraft Noise

Continuous exposure to high intensity noise can induce mental and physical fatigue to the members of an aircraft crew. Although the noise levels produced will not permanently damage the ears of the crew, it will certainly cut down their eagerness to strap

into the cockpit. This will ultimately affect their performance in flight, which could endanger the successful completion of the mission. Therefore, to provide the crew with a decent working environment and to secure mission reliability, the noise inside the cabin must be reduced to a level as far under 80 dB as reasonably possible.

The ground noise was not considered important because the CONDOR operates almost always at 45,000 feet.

7.3.1 Propulsion System Noise Sources

For the CONDOR there are three primary sources from the Propulsion System that contribute to interior noise. They are :

1) Airborne propeller noise
2) Airborne fuselage noise
3) Engine vibration

This neglects any noise from the cockpit instruments, the fuel pumping system, the air conditioning system, or other minor sources.

7.3.2 Methods of Noise Reduction

One of the three sources of noise mentioned, the propeller noise, predominates over the other two especially for a tractor type configuration. With that in mind, a pusher propeller configuration was adopted. An additional advantage of a pusher propeller configuration is the unobstructed forward and downward fields of view for the crew.

Having a pusher configuration completely eliminates acoustic impingement on parts of the aircraft. However, due to the location of the propeller, it has to operate partially in the fuselage's wake which will induce vibration on the propeller. The tail boom was raised and stretched to minimize this problem, with a small weight penalty being payed. Also, having a longer tail boom attenuates the vibrational transmission. To further reduce the noise and weight, a simple belt driven gear reduction was utilized. Maintenance on this type of gear system will be less than a standard transmission because of the simplicity of the

belts. Engine vibration can be reduced by use of hydraulic damper mountings. Furthermore, since the engine has three turbines, the noise coming out from the exhaust is muffled, thus the use of a separate muffler is not required.

To achieve a quieter environment within the crew cabin, the fuselage walls are lined with leaded vinyl, an acoustical insulation. This insulation is placed between the inner and outer surfaces of the fuselage.

With these methods of noise reduction it is expect that the CONDOR's cabin will have noise levels averaging 72 db. The internal noise level of the CONDOR is compared to that of other vehicles in figure 7.5 .

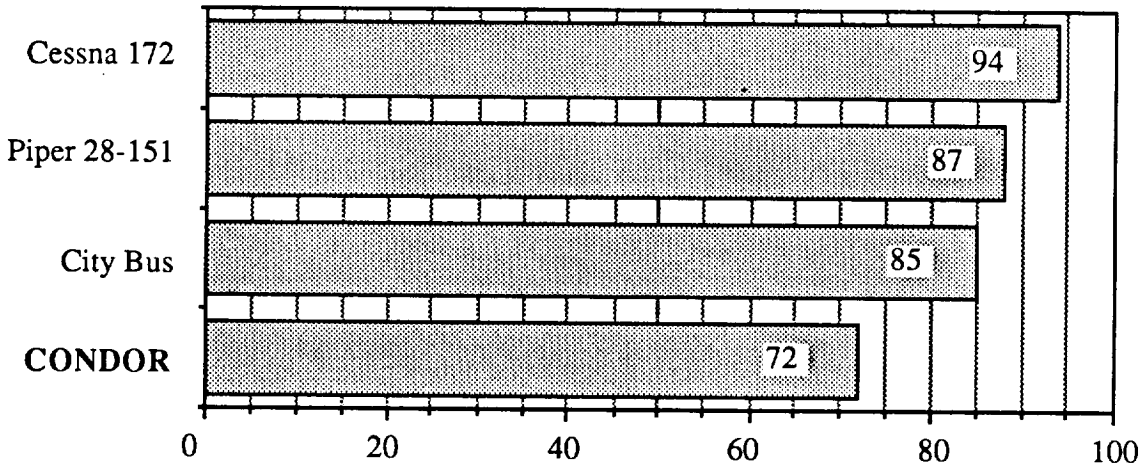

Figure 7.5 : Noise Level Comparison

7.4 Fuel system

The CONDOR will run on standard aviation gasoline, which is compatible with the GTCL-1100 engine. The fuel is stored completely, in four separate bladdered tanks, within the wing of the CONDOR. Each tank holding approximately 550 lbs or 96 gals. of fuel and separated by rib structure. The tanks begin at the fuselage/wing interface and extend spanwise, between the wing spars located at ten and fifty percent chord. This

positioning puts the centroid of the fuel system on the centroid of the manned aircraft, which eliminates almost all of the C.G. manned mission travel. Placing the tanks on the inner span, limited the interia variations over the mission, this position also has the greatest volume potential in the wing. Structural considerations were also satisfied by this placement which decreased the fuel weight moment arm.

The fuel, if unheated, will freeze at 45,000 ft. with standard day conditions. The freezing temperature of aviation gasoline is -60° F, and the temperature at 45,000 ft is -70° F. Therefore, a means of heating the fuel is required. The fuel will be used to cool the engine, and the engine will in return heat the fuel. By running the fuel (from the tanks) through a heat exchanger, the temperature of the fuel can be maintained well above the freezing temperature. Since some heat is picked up by the fuel, less outside air is needed to cool the engine, thus reducing the cooling drag. The on board computer will monitor the temperatures of the engine and will adjust them when necessary.

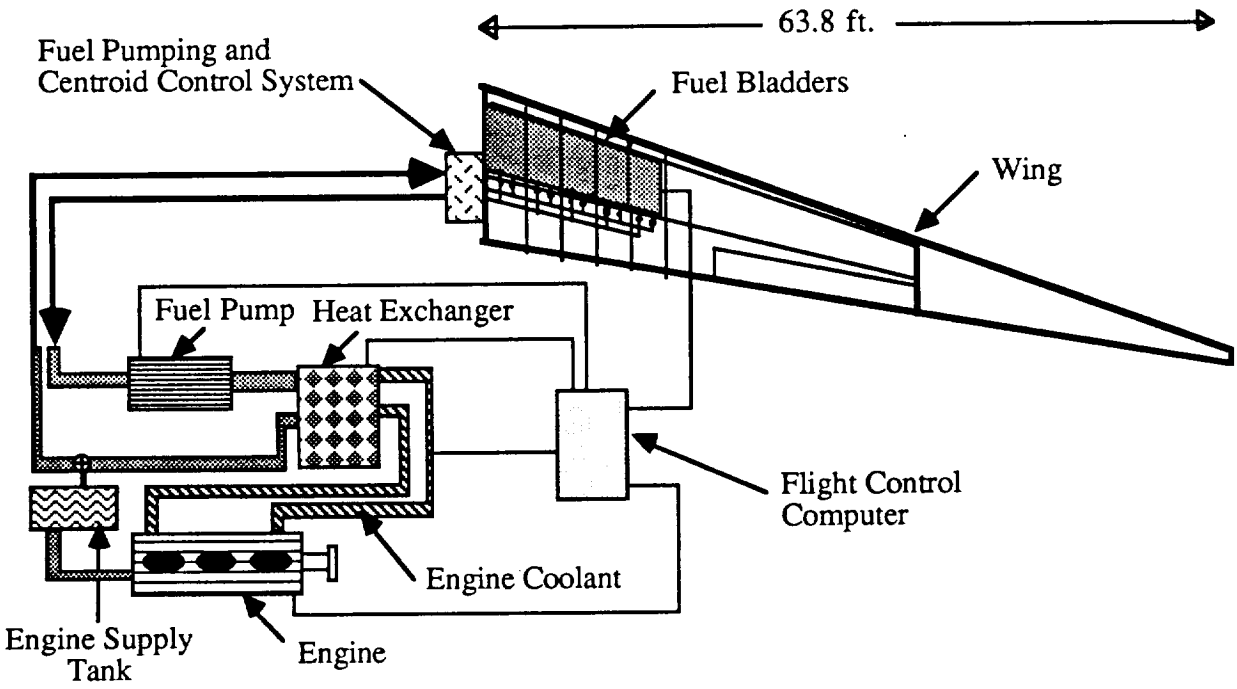

Figure 7.6 : Fuel System Schematic

8.0 STRUCTURAL ANALYSIS

8.1 Wing Structure

The flying wing configuration chosen presents some difficult structural problems. Approximately 70% of the take-off weight is carried in the wings (fuel and wing weight). Furthermore, the wing must be disassembled to fit into a C-130 aircraft or onto the back of a tractor trailer.

The wing structure must carry all of the fuel (3700 Lbf), landing gear, and the control surfaces, which makes the total wing weight during take-off 5720 Lbf. Figure 8.1 shows the wing in detail. The wing was designed with simplicity and minimal maintenance in mind because the RFP states "... high reliability along with reduced and minimal maintenance is required. Ease of inspection, component accessibility, loading, and selection of materials must be considered." To comply with this portion of the RFP the material used for most of the aircraft has to be highly durable, easily checked for any structural fatigue, and easily fixable if there is any structural fatigue. For these reasons aluminum was chosen over any composite material for the wing because it is easily inspected and repaired, and access panels can be easily installed in aluminum with out it damaging the integrity of the structure (this will allow for easy component accessibility). Aluminum is also a very tough material that will be able to withstand the inevitable rough treatment that will occur in transportation. The cost saving of aluminum, which is approximately 90 % over graphite-epoxy composite (Reference 6), is another reason aluminum was chosen over a composite. All of these qualities outweigh the weight savings that a composite would provide.

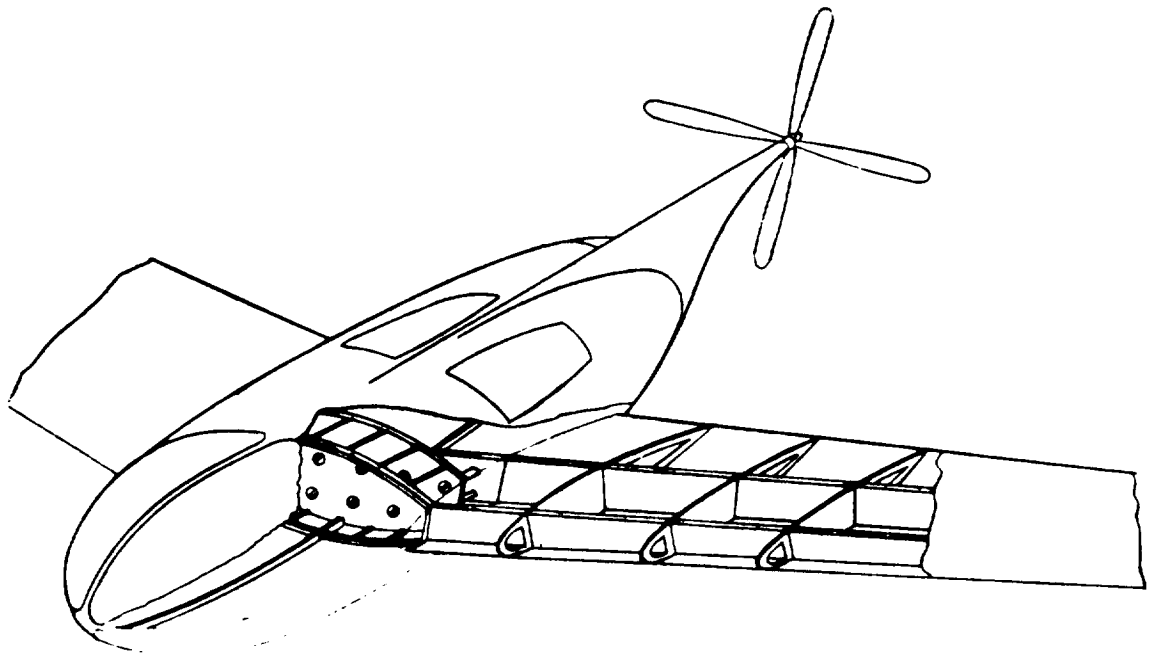

Figure 8.1 : Wing Structure

A main spar located at 50 % of the wing chord was chosen to support most of the structural loads along with a smaller front spar located at 10 % of the chord. This spar location will allow for all of the fuel to be located in the wing between the two spars. The front spar will also greatly reduce the twist of the wing caused by the fuel weight. The two spars are the major connection between the fuselage and the wings, aluminum 2024-T4 was chosen as the wing material because it can easily carry the loads specified by the design and FAR 23.

Figure 8.1 also shows the rib location and shape. The spacing and the thickness of the ribs was determined by the equivalent normal pressure that tends to force the top and bottom surfaces of the wing together (Reference 27). The purpose of these ribs, placed every three feet apart (Reference 46), is to stabilize the wing structure by providing torsional stiffness to the spar. The ribs are bonded to the inner skin of the wing instead of riveting to decrease structure weight (Reference 5), increase smoothness of external surfaces, and increase the fatigue strength by 40 percent (Reference 5). The ribs will be made from 2024-T3 aluminum sheet.

8.2 V-n Diagram

The V-n diagram for the aircraft must be constructed before the structure of the aircraft can be completed. This diagram was completed using the method outlined in FAR 23, and is shown in Figure 8.2.

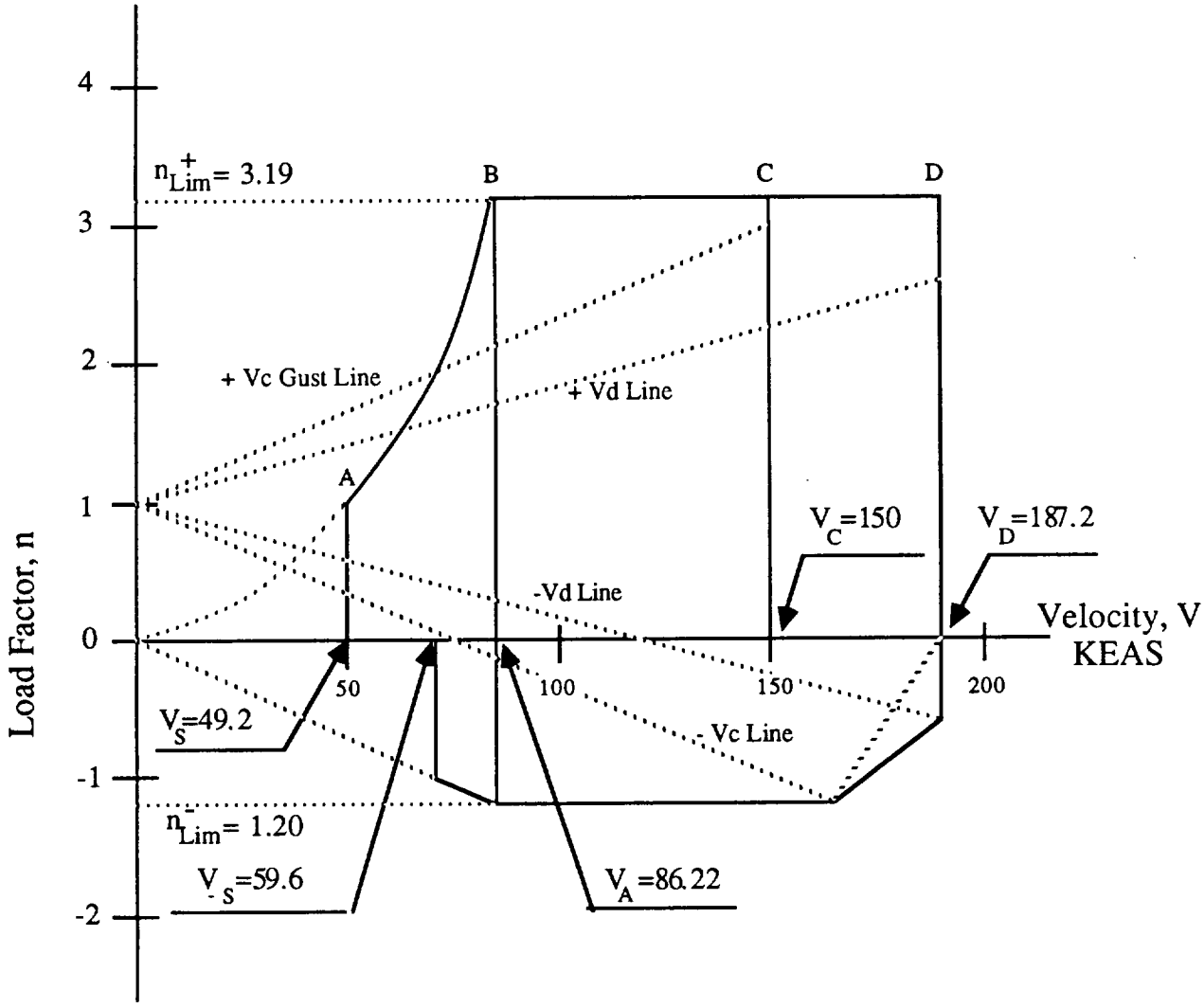

Figure 8.2 : V-n Diagram

On this V-n diagram the letters correspond to the following.

A Stall speed at 1-g.
B Minimum maneuvering speed during cruise.
C Design cruise speed
D Maximum diving speed

Under FAR 23 there must be a 1.5 factor of safety added to the limit load factor, this will make up the ultimate load factor. As shown on Figure 8.2, the limit load factor is 3.19; therefore, the ultimate load factor is 4.7. The structure was designed to withstand this ultimate load factor.

Elliptic loading was used to examine the loads of the aircraft and to calculate the maximum bending moment, shear force, and deflection in the wing. These were calculated using the following equations (Reference 27).

$$V = \int_{C_R}^{C_t} \text{Load}\, dx \qquad 8.1$$

$$M_B = \int_{C_R}^{C_t} V\, dx \qquad 8.2$$

$$D_S = \int_{C_R}^{C_t} \frac{M_B}{EI}\, dx \qquad 8.3$$

$$D = \int_{C_R}^{C_t} S_D\, dx \qquad 8.4$$

Table 8.1 is a summary of the maximum loads, moments, and deflections on the wing.

Condition	Moment (Lb-Ft)	Shear (Lb.)	Tip Deflection (Ft.)	Tip Twist (Deg.)
Cruise (n=1)	194,000	6,210	1.01	3.16
Limit load (n=3.19)	625,000	19,900	3.27	6.66
Ultimate load (n=4.7)	920,000	229,300	4.81	9.81

Table 8.1 : Aircraft Loads at Different Flight Conditions

To accommodate the above loads, the wing structure will be made with the following.

Skin: thickness=0.04 in. of aluminum

Front Spar (loc. 10% chord) thickness=.00234 % chord

Main Spar (loc. 50 % chord) thickness=.00312 % chord

Total Wing Structure Weight 2500 Lbf.

8.3 Fuselage Structure

The fuselage must be able to carry the payload, instruments, propulsion system, and two crew members. The fuselage must either be pressurized or the crew members must wear pressure suits. The mission profile states that the crew must stay in the air for 3 days. For this long mission it is impossible to require the crew to work in pressure suits, especially if these pilots are to fly the aircraft on a regular basis. Therefore, the fuselage will have to be pressurized which will require a highly reenforced structure.

The fuselage structure is shown in Figure 8.3 and 8.4. It will be constructed out of aluminum alloy base beam and two main bulkheads. The base beam will be placed at the center line of the fuselage to support the engine, the pilots, and the flight instruments. The base beam will also act as a stiffener in the connections of the two bulkheads. The base beam will extend to the nose of the aircraft to help distribute the loads in the windshield of the fuselage and to add safety in the event of a crash. The front bulkhead will be constructed of aluminum 2024-T4 to give support to the front wing spar located at 10% of the chord. The rear bulkhead will be constructed of an aluminum alloy honeycomb sandwich to support the main spar of the wing located at 50% of the chord. The main spar will slide into the spar slit to support the large bending moment which is transmitted by the wing. Since the bending moment is carried into the rear bulkhead by the main spar, the rear bulkhead will be connected to the front bulkhead with the stiffeners forming a torque box in a fuselage to assist in the support of the bending moment.

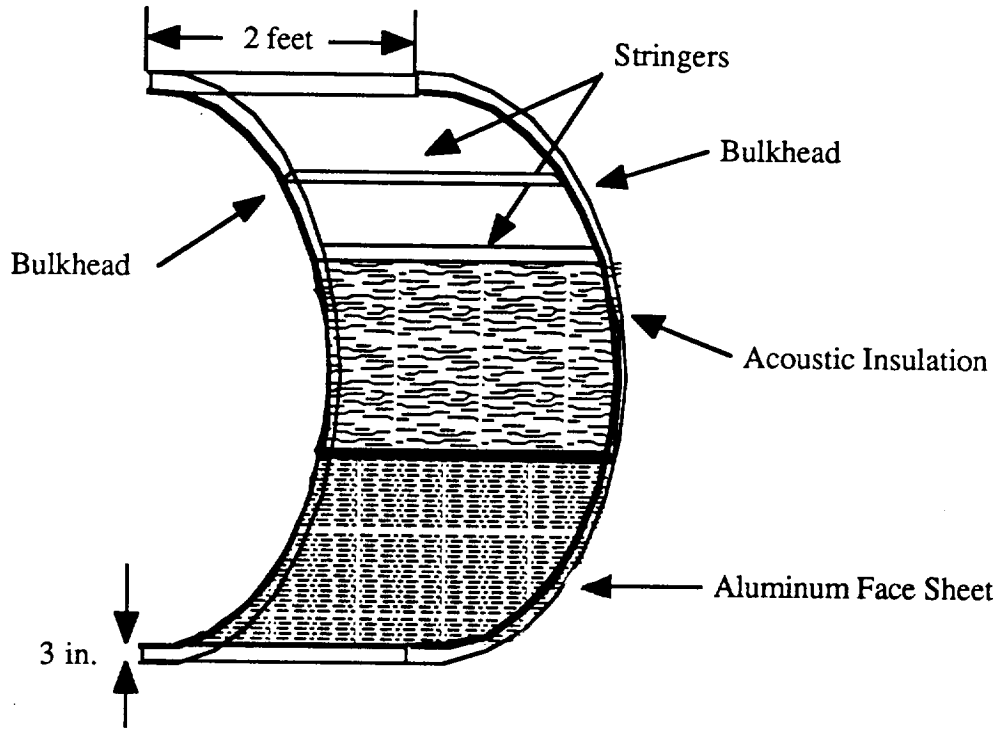

Figure 8.3 : Fuselage Cut-out

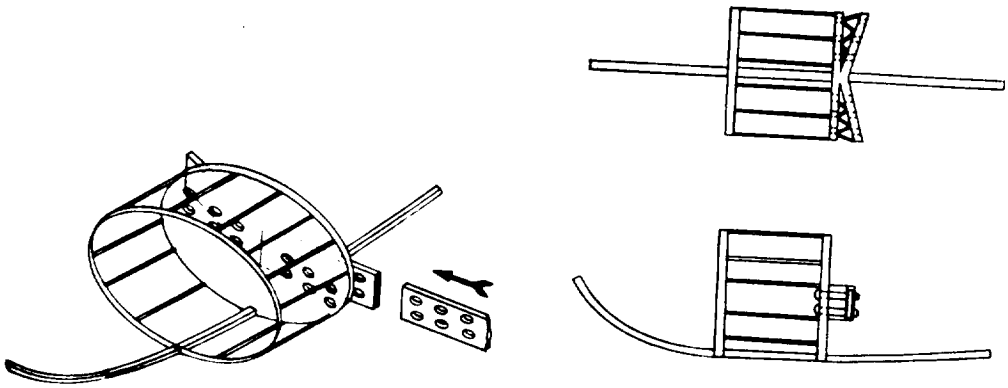

Figure 8.4 : Fuselage Bulkheads

The fuselage will also have to withstand non-aerodynamic forces on the ground during the assembly and disassembly phases and in the loading into the C-130 aircraft. For this reason and the multiple and prolonged pressurizations the aircraft will go through, aluminum was chosen for the fuselage skin. Figure 8.3 shows the fuselage side panel; it will consist of longitudinal stiffeners, made out of aluminum 2024-T4, to resist axial and

bending moments; transverse frames placed two feet apart, also made out of aluminum 2024-T4; and two aluminum panels separated with 3 inches of acoustical insulation. The longitudinal stiffeners and bulkheads will be bonded to the skin to provide a smooth surface and to counteract the radial and tangential stresses in the pressurized cockpit. The method outlined in Reference 41 was used to calculate the stresses the fuselage walls will have to handle. These stresses are shown in Table 8.2.

Inside Radius (in)	Outside Radius (in)	Wall Thickness (in)	σ_t(psi)
66.0	66.5	0.5	1330
66.0	66.25	0.25	2660
66.0	66.1	0.1	6652
66.0	66.05	0.05	13304
66.0	66.04	0.04	1663.03

Table 8.2 : Fuselage Stresses

The endurance level for aluminum 2024-T4 is 18,000 psi. It can be seen from the above table that a wall thickness of .04 in is necessary to keep the stresses below the allowable limits. The inside wall of the fuselage will be .1 in thick to allow a suitable factor of safety (2.7), and the outside wall thickness will be .04 in thick. In the case of inner wall rupture, the outside wall thickness will be sufficient to allow the aircraft to remain pressurized.

The RFP states "... the long-endurance aircraft is to use human powers of observation, the pilot's forward and downward fields of views must not be obstructed to any significant degree." For this reason a very large windshield will be used to allow for pilot vision. The material chosen for the cockpit windshield is Lexan; this material is not strong enough to withstand the cabin pressures at 45,000 alone; therefore, a web structure will be used to help distribute some of the stresses in the fuselage.

8.4 Propeller Shaft Housing and Vertical Stabilizers

The propeller shaft housing and the vertical tails will be made with aluminum for the same reasons as the wings and fuselage. The shaft housing will be made out of the same basic construction as the fuselage, but the thickness of the walls will be .1 in for both walls, and the bulkhead spacing will be .5 feet. This extra structural strength is necessary to counteract the vibration that will be created by the propeller shaft.

8.5 Aircraft breakdown and Transportation

8.5.1 Component Disassembly

The RFP requires the airplane must fit into C-130 transport and into the back of a tractor trailer. This requirement was met by the disassembly of the Condor into five major sections and three sub-sections. Figure 8.5 shows the detail cut down of the aircraft. The wings will be disassembled at the root chord and 40 feet from the root chord. The outer wings will be placed at the top of the transport. The fuselage will be placed into center of the transport. The inner wing sections will be placed vertically on both left and right wall of the cargo bay. Finally, the propeller will be positioned behind the fuselage. The final packed aircraft is shown in Figure 8.6. Packing into a tractor trailer is not shown because it is similar to that of the C-130.

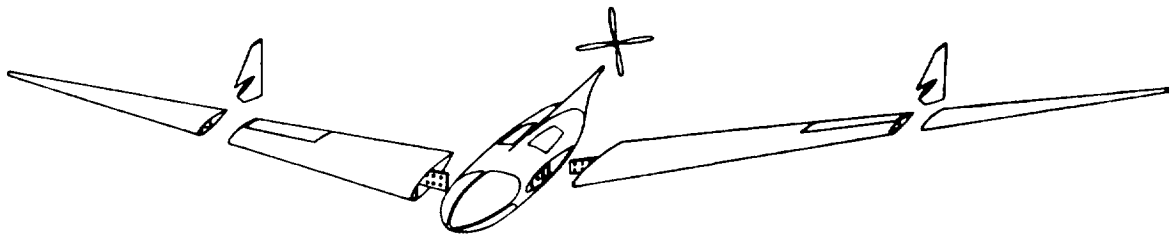

Figure 8.5 : Aircraft Breakdown

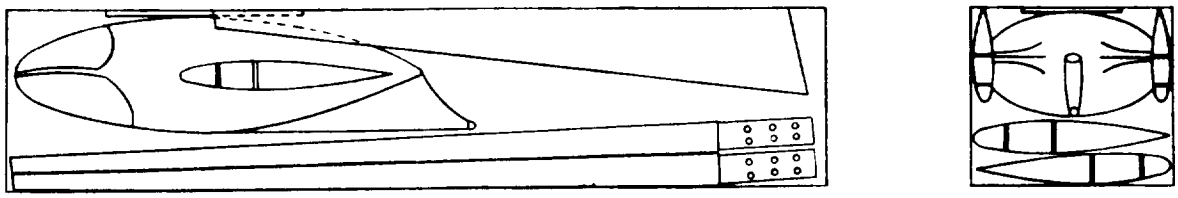

Figure 8.6 : Aircraft Transportation

8.5.2 Joint Assembly

Assembly joints must be constructed to allow for the disassembly as mentioned in the above section. Figure 8.1 and 8.7 shows the joints at the root chord and the wing, respectively. The main spar will be inserted into the fuselage rear bulkhead, and pins will be inserted from the cockpit to lock the main spar to the fuselage. A hook is used for the initial connection of the main wing sections, this hook is used to hold the wing in place while the pins are inserted into the wing joint. The bottom plate of the spar will have additional plates for connection.

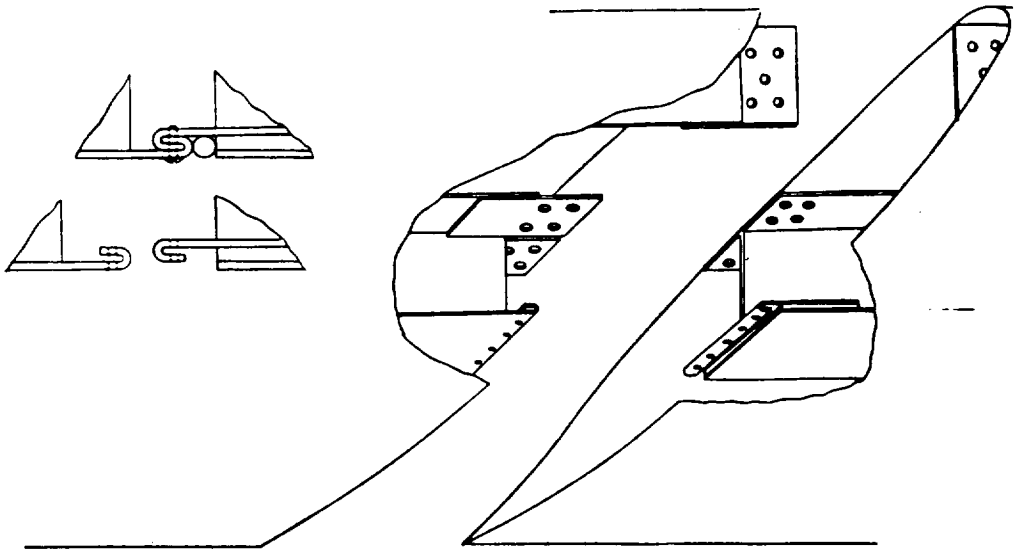

Figure 8.7 : Wing Joint

8.6 Landing Gear

Three operational characteristics were considered in the design of the CONDOR's landing gear. These were suitable damping of landing oscillations, stability during runway taxi, and satisfactory front and rear to wing characteristics.

8.6.1 Possible Landing Gear Configurations

Two types of landing gear designs were initially considered for the flying wing. These are the tricycle landing gear design, and bicycle landing gear with outriggers. Due to the wingspan of the CONDOR, it was determined that outriggers would be necessary for both designs; with the bicycle design they would be primary outriggers while the tricycle would use secondary outriggers. Since the aircraft has such a long wing span, the landing gear has to have a wide enough track in order to provide the necessary lateral stability during runway taxi. If the track is too short then the aircraft will tip over in the event of a hard turn. Both of the above mentioned landing gear designs provide the necessary track for the aircraft to be laterally stable. However, longitudinal stability must also be considered. Since the aircraft is very short lengthwise the bicycle landing gear design does not provide enough wheelbase length for the aircraft to be stable longitudinally. The tricycle landing gear design gives a larger wheelbase, because the nose landing gear can be placed further forward than with the bicycle gear, and thus the required increase in longitudinal stability is obtained. The outriggers in the tricycle landing gear design serve the purpose of protecting the wing tips from touching the runway in the event of a hard landing. The tricycle landing gear with outriggers was chosen for the CONDOR because of the above mentioned reasons.

8.6.2 Landing Gear Configuration and Specifications

The CONDOR's landing gear is a tricycle arrangement, with the main gear positioned out on the wings, and the nose gear at the front center of the fuselage. The layout of the landing gear can be seen in Figure 8.8.

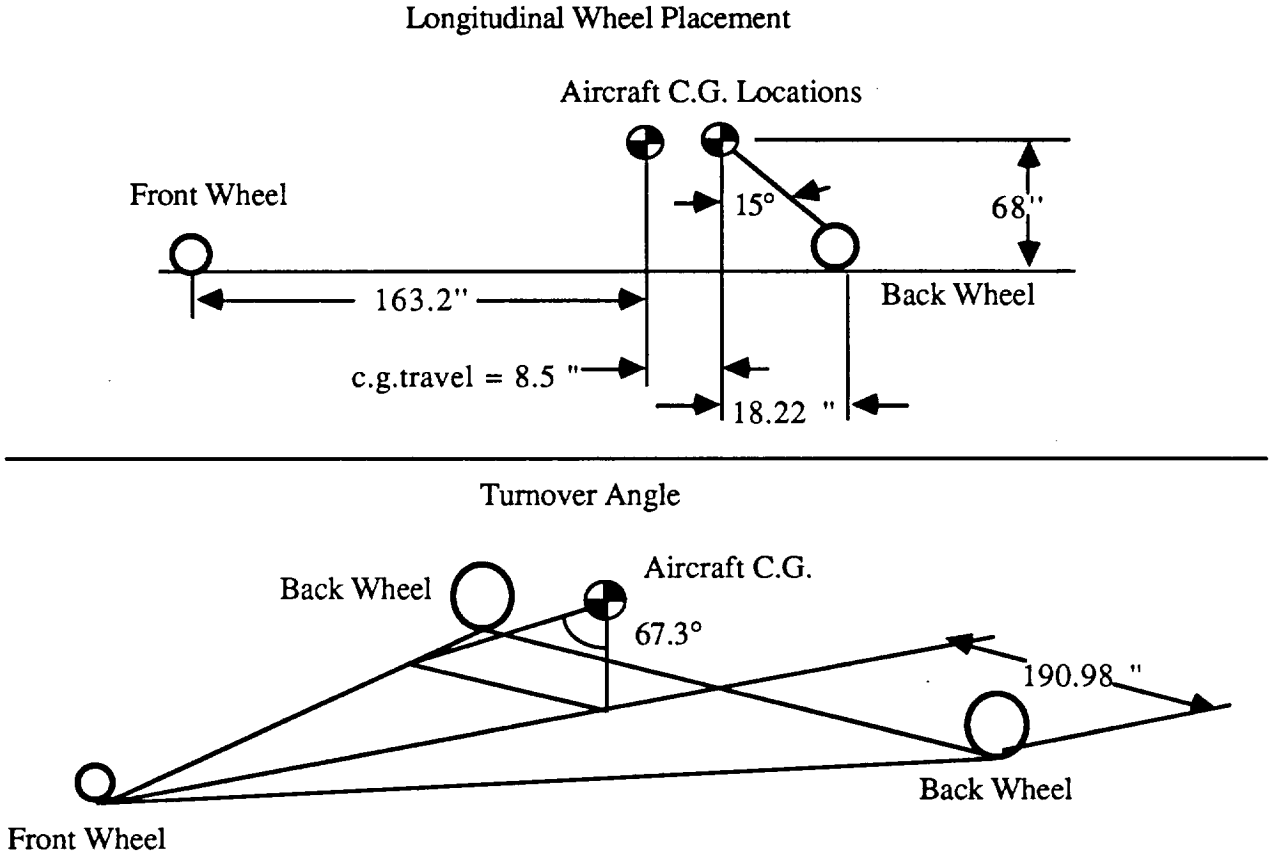

Figure 8.8 : Landing Gear Placement

The landing gear system uses oleopneumatic technology for oscillation dampening. The two main landing gear struts are placed on the wing and they retract sideways into the wing (Figure 8.9). Since the wing is relatively thick (1.7765 feet at the root) there is no problem with the placement of the landing gear in the wing. The main landing gear struts have one tire per strut, with the tire size of 22x5.75-12. These tires are high pressure tires (220 psi),

which have a weight advantage over lower pressure tires. The length of the main landing gear struts is 68 inches.

The nose landing gear strut has one wheel. The type VII nose tire has a size of 18x5.5, with a pressure of 140 psi. The weight savings, for a higher pressure tire was rejected in favor of the smoother ride since the nose gear is on the fuselage.

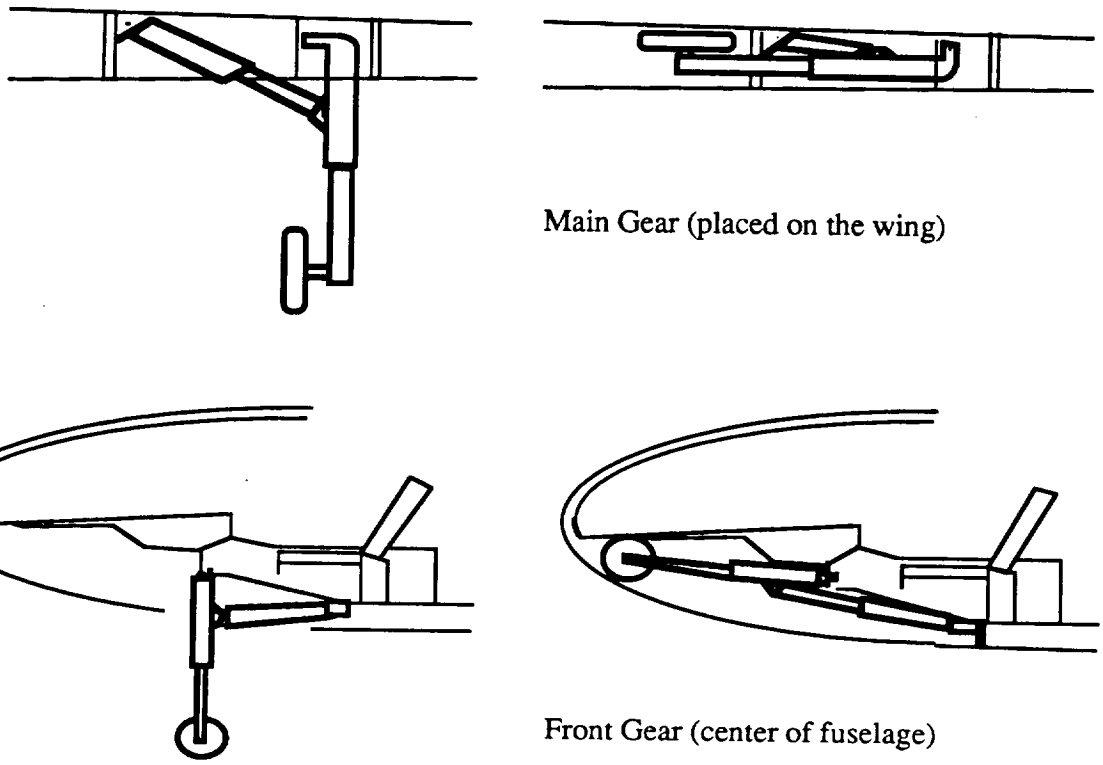

Figure 8.9 : Landing Gear Design and Retraction

8.6.3 Landing Gear Design Methods

The method used to design the landing gear involves both the static and dynamic (braking) aspects of the aircraft and is straight forward. The dynamic aspect is especially important for the nose strut and wheel; as the aircraft brakes, the nose wheel will suffer the biggest impact. The position of the landing gear is determined as a function of the aircraft

center of gravity location. Once the center of gravity location and travel are known, then the main landing gear is attached at an angle of 15 degrees from the vertical c.g. location (Figure 8.8). The furthest rearward position of the aircraft C.G. was used for this calculation. This is necessary to insure that the aircraft will not tip over when it is being towed from the rear and the brakes are suddenly applied.

8.6.4 Landing Gear Loads

The static load limits, on the nose gear, should be within 8% to 15% of the weight of the aircraft to allow for tracking of the aircraft. The nose gear of the CONDOR has a load of 15% with the c.g. forward. The nose gear dynamic load was calculated for a 10 ft/sec^2 deceleration. The landing gear static load and the nose gear dynamic load are calculated using formulas from Reference 23. Table 8.3 lists the values for the landing gear loads.

Max. Static Main Gear Load (per strut)	= 5450.5 lbs
Max. Static Nose Gear Load	= 1882.46 lbs
Min. Static Nose Gear Load	= 1648.96 lbs
Max. Braking Nose Gear Load	= 3793.70 lbs

Table no. 8.3 : Landing Gear Loads

8.6.5 Landing Gear Dynamic Response

The dynamic response of the landing gear was modeled using a simple model of a point mass, supported by a spring and a damper. A free-body-diagram of the system is shown in figure 8.10.

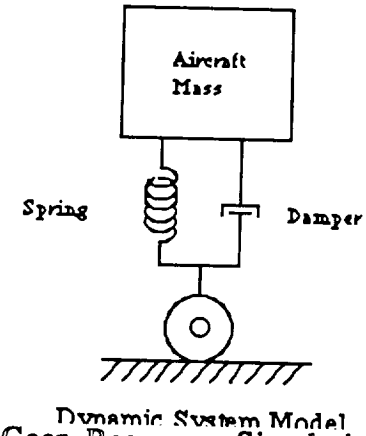

Figure 8.10 : Landing Gear Response Simulation Model

For the purpose of crew comfort it was decided that the dynamic oscillation due to landing should be dampened within 3.0 seconds after touch down. The total displacement during landing was also limited to less then 1.00 ft. Using these requirements the spring constant and the damping coefficient were set.

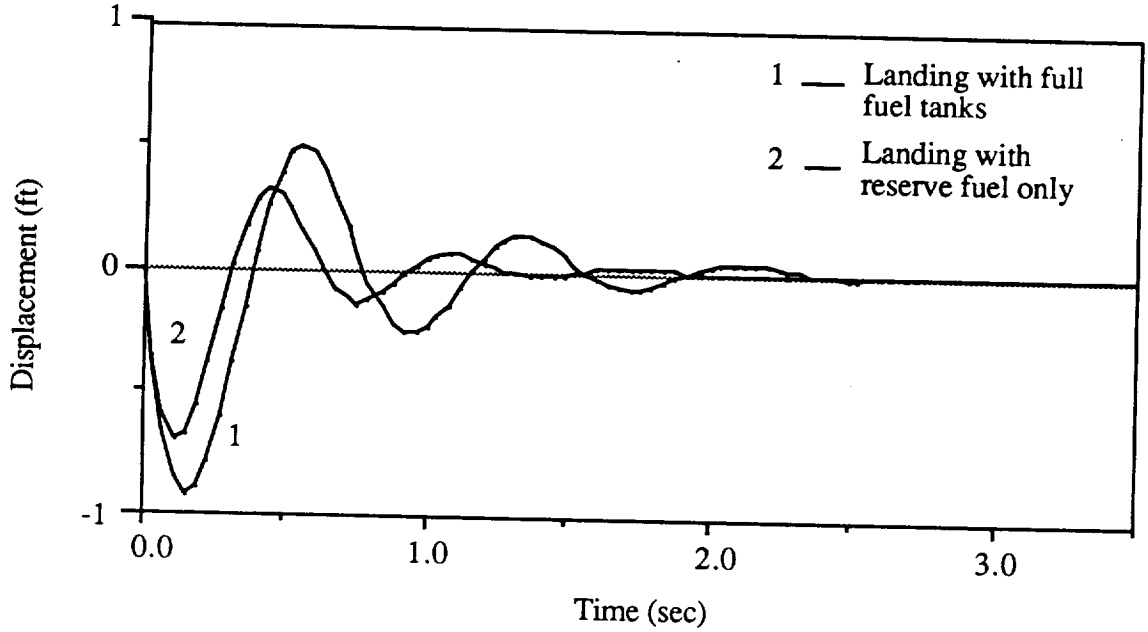

Figure 8.11 : Landing Gear Time Response

The following values were used for the CONDOR.

Total Spring Constant = 25000 lb/ft
Total Damping Coefficient = 1200 lb/ft-sec

Using these values the time response for the landing of the CONDOR was determined. The oscillatory response is shown in Figure 8.11 . The simulation was done for two landing cases : (1) Landing with full fuel tanks, (2) Landing with reserve fuel only.

9.0 AIRPLANE STABILITY AND CONTROL

The CONDOR was designed to be certified under FAR-23 requirements. Since the CONDOR may also be used by the military it was decided to include the MIL-F-8785B requirements for airworthiness. These requirements, and those of FAR-23, were satisfied by the CONDOR.

9.1 Control System Selection

A digital Fly-By-Wire (FBW) system was chosen over a mechanical one for the CONDOR's primary flight controls. This was done only after a comparison of the two systems. The advantages of the FBW are:

1) Lighter Weight
2) Ease of Maintenance
3) Easier integration of an stability augmentation system (SAS) and autopilot,
4) Fewer moving parts, thus a simpler and more reliable system
5) Ease of assembly and disassembly of the aircraft

It is felt that with adequate testing and redundancy of critical electrical components, the FAA will certify a FBW system in a FAR 23 aircraft.

A Stability Augmentation System (SAS) was chosen for the CONDOR for two reasons: 1) use of a FBW system 2) the flying wing configuration will be unstable if pushed to large angle of attacks. This SAS will be used to trim the aircraft, damp out any pilot induced oscillations, automatically integrate the controls on the CONDOR, and control aircraft dynamics under unstable flight conditions. The SAS will give the CONDOR level one handling qualities in all situations. The use of the SAS permitted a smaller static margin, relative to an un-augmented flying wing, and a reduced trim drag for the CONDOR.

The CONDOR's backup safety system will offer redundancy of all critical control system components. A redundant flight computer will be placed within the flight control system along with internal redundancy for the components of the SAS. Each control surface will be equipped with an additional controller and actuator. The CONDOR was designed so that if the flight computers fail they can be shut off and the aircraft can be flown without any artificial augmentation at a handling quality of level 2. The CONDOR will be able to fly with only one elevon and one rudder in operation, but the response rates will be cut in half. The worst case situation would be a power failure; if that should happen a stand alone power generator would come on line, driven a rechargeable battery. The battery would receive continuous charging, while in flight, from the power tapped off of the engine. This power unit would operate long enough for the pilots to make a safe landing.

9.2 Static Stability Derivatives

The CONDOR stability and control derivatives were estimated using the formulations presented by Roskam (References 42 and 43). These equations are functions of aircraft geometry and operating conditions. Table 9.1 lists the variables and values used.

Variable	Value
Wing Surface Area	801 ft^2
Wing Span	137 ft
Wing Quarter Chord Sweep Angle	16.5 deg.
Vertical Tail Surface Area	23.38 ft2
Vertical Tail Span	5.375 ft
Cruise Mach Number	.314
Wing Efficiency	.976
Vertical Tail Half Chord Sweep Angle	16.0 deg.
Vertical Tail Quarter Chord Sweep Angle	26.0 deg.
Fuselage Diameter	10.0 ft
Lift Coefficient (beginning cruise)	.69
Oswalds Efficiency Factor	.95
Wing Dihedral	0.00 deg.
Wing Twist	0.00 deg.
Drag Coefficient (beginning cruise)	.025
Angle of Attack (beginning cruise)	1.40 deg.
Ratio of Actual Wing Section Lift Curve Slope to 2Π	.976
Rudder Flap Chord	$.30C_v$

Table 9.1 : CONDOR Stability Derivative Input Variables

With the exception of the small fuselage, The CONDOR is a flying wing. Therefore, the analysis was done assuming that the aircraft is a pure flying wing with small rudders.

To simplify the design process, computer programs were developed to calculate the stability derivatives of the CONDOR, along with its dynamic response. The longitudinal derivatives were determined in the program STABWING and the lateral/directional derivatives in LAT-ANALYSIS. STABWING also was written to calculate the dimensional derivatives as well as the dynamic response of the CONDOR. These programs were written, by group members, using the methods previously mentioned from References 42 and 43.

The geometry and operating conditions used in the programs are listed in Table 9.1.

Variable	Climb	Begin-Cruise	Mid-Cruise	End-Cruise	Approach
Weight (lbs.)	11908.7	11698.7	9808.7	7918.7	7708.7
X-bar Centroid (in.)	274.83	274.82	274.67	274.44	274.41
Z-bar Centroid (in.)	209.02	209.03	209.15	209.32	209.35
Ixx (slug/ft^2)	166900	164100	139000	113900	111100
Iyy (slug/ft^2)	10934	10895	10542	10189	10150
Izz (slug/ft^2)	177100	174250	144800	123350	120500
Ixz (slug/ft^2)	1778	1771	1707	1640	1630
Lift Coefficient	1.4	.69	.57	.463	.4
Velocity (ft/sec)	254	254	254	254	254
Drag Coefficient	.03	.025	.0225	.02	.009
Angle of Attack (deg.)	6.0	1.4	.5	-.2	-.4

Table 9.2 : Stability and Control Flight Conditions

The computer analysis allowed easy, quick changes in aircraft configuration and operating conditions. It also allowed testing at a number of flight conditions. Both the longitudinal and lateral/directional stability derivatives were calculated for five flight conditions as defined in table 9.2 .

9.2.1 Static Longitudinal Stability

The main stability problem with the flying wing configuration is that it is very sensitive in pitch due to a small moment of inertia about its lateral axis. Sweep was added to keep the aerodynamic center behind the center of gravity and thus increase the static margin. The longitudinal stability derivatives were calculated for five power-off flight conditions, as defined in Table 9.3 . The derivatives were determined using the computer program previously mentioned. The aircraft geometry was simplified to a pure wing with no twist. 16.5 degrees of sweep at the quarter cord was chosen after it was decided that a static margin of 20 would give adequate handling qualities. Although high, relative to typical aircraft, the CONDOR's static margin is necessary for the flying wing configuration. The calculated power off longitudinal stability derivatives appear in Table 9.3. Numerically they all fall within acceptable ranges, as specified in Reference 42.

Derivative	Climb	Beg-Cruise	Mid-Cruise	End-Cruise	Approach
C_{D_α}	0.1969	0.1132	0.0936	0.0760	0.1969
C_{L_α}	5.7356	5.7356	5.7356	5.7356	5.7356
$C_{m_{\alpha(rad)}}$	-1.2329	-1.2329	-1.2383	-1.2490	-1.2329
C_{D_u}	0.0000	0.0000	0.0000	0.0000	0.0000
C_{L_u}	0.1313	0.0755	0.0624	0.0507	0.1313
C_{m_u}	0.0000	0.0000	0.0000	0.0000	0.0000
C_{D_q}	0.0000	0.0000	0.0000	0.0000	0.0000
C_{L_q}	6.7203	6.7203	6.7367	6.7695	6.7203
$C_{m_{q(rad)}}$	-11.2969	-11.2969	-11.3098	-11.3359	-11.2969
C_{D_α}	0.0000	0.0000	0.0000	0.0000	0.0000
$C_{L\alpha}$	0.2958	0.2958	0.2958	0.2958	0.2958
C_{m_α}	0.0000	0.0000	0.0000	0.0000	0.0000

Table 9.3 : Longitudinal Stability Derivatives

9.2.2 Lateral Stabiltiy and Control

The lateral/directional stability derivatives were calculated for the five flight conditions, (Climb, Begin-Cruise, Mid-Cruise, End-Cruise, Descent), of Table 9.2, using the computer program that was previously mentioned. The vertical control surfaces give the CONDOR control in yaw and the wing elevons are used to control the rolling motion. Their effectiveness is shown in the control derivatives at the end of table 9.4, and in the dynamic analysis section. All of the values for the lateral/directional derivatives are listed in the Table 9.4 .

Derivative	Climb	Beg-Cruise	Mid-Cruise	End-Cruise	Approach
C_{Y_β}	-.12159	-.12160	-.12160	-.12160	-.12159
C_{l_β}	-.13400	-.10240	-.09495	-.08829	-.08432
C_{N_β}	3.19E-04	1.70E-04	1.36E-04	1.09E-04	1.15E-04
C_{Y_P}	-.00328	-.00417	-.00434	-.00447	-.00444
C_{l_P}	-.30207	-.30207	-.30207	-.30207	-.30207
C_{N_P}	.16934	.09724	.08028	.06516	.05626
C_{Y_R}	.01127	.01097	.01090	.01084	.01086
C_{l_R}	.27743	.15965	.13193	.10722	.09266
C_{N_R}	-.06144	-.02584	-.01967	-.01493	-.00927
$C_{Y_{dA}}$	0.0000	0.0000	0.0000	0.0000	0.0000
$C_{l_{dA}}$	.01371	.01371	.01371	.01371	.01371
$C_{N_{dA}}$	-8.22E-04	-4.73E-04	-3.91E-04	-3.17E-04	-2.74E-04
$C_{Y_{dR}}$	.02068	.02068	.02068	.02068	.02068
$C_{l_{dR}}$	3.43E-04	4.37E-04	4.55E-04	4.69E-04	4.66E-04
$C_{N_{dR}}$	-.00118	-.00115	-.00114	-.00114	-.00114

Table 9.4 : Lateral/Directional Stability Derivatives

9.3 Trim Diagrams

The trim analysis was based on the CONDOR's lift curve as determined in the aerodynamics section. The trim diagrams were constructed using the methods presented by Reference 42. It was assumed that elevon deflections would be limited to ± 20°. Figure 9.1 shows the variation of wing lift coefficient with angle of attack for for different elevon deflections.

Initially a trim analysis was done on the standard GAW-1 airfoil. However the CONDORS trim conditions with this non-reflexed wing were unacceptable. It was necessary to add reflex to the airfoil. Reflex of negative three degrees was added to the standard GAW-1 airfoil. An iterative process involving these trim diagrams was used to size the elevons on the wing. The trim conditions for both the non-reflexed and reflexed wing are shown in Figure 9.1.

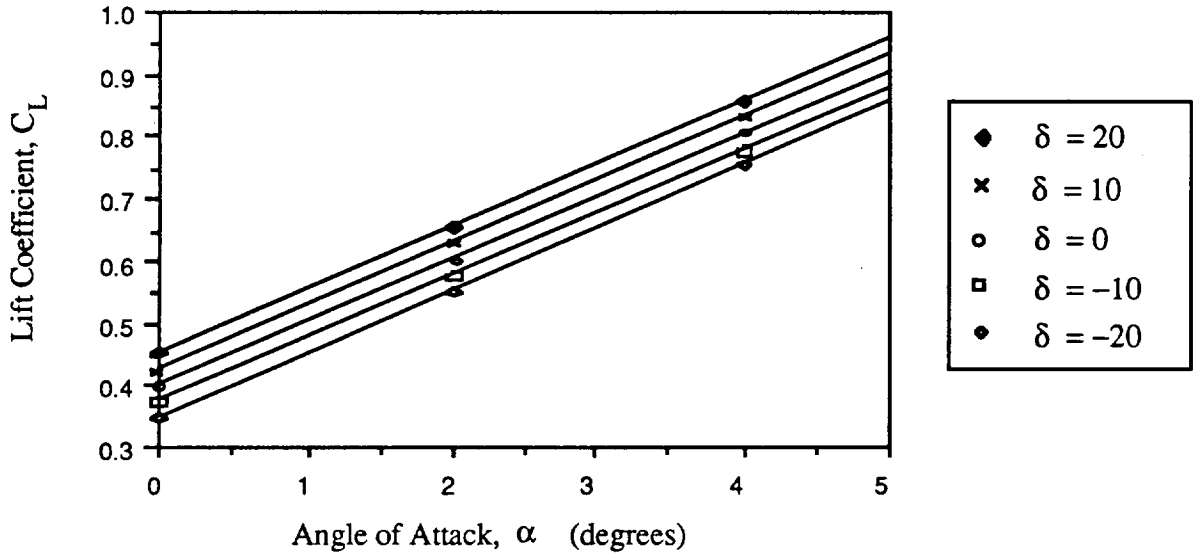

Figure 9.1: Lift Curve Variation with Elevon Deflection

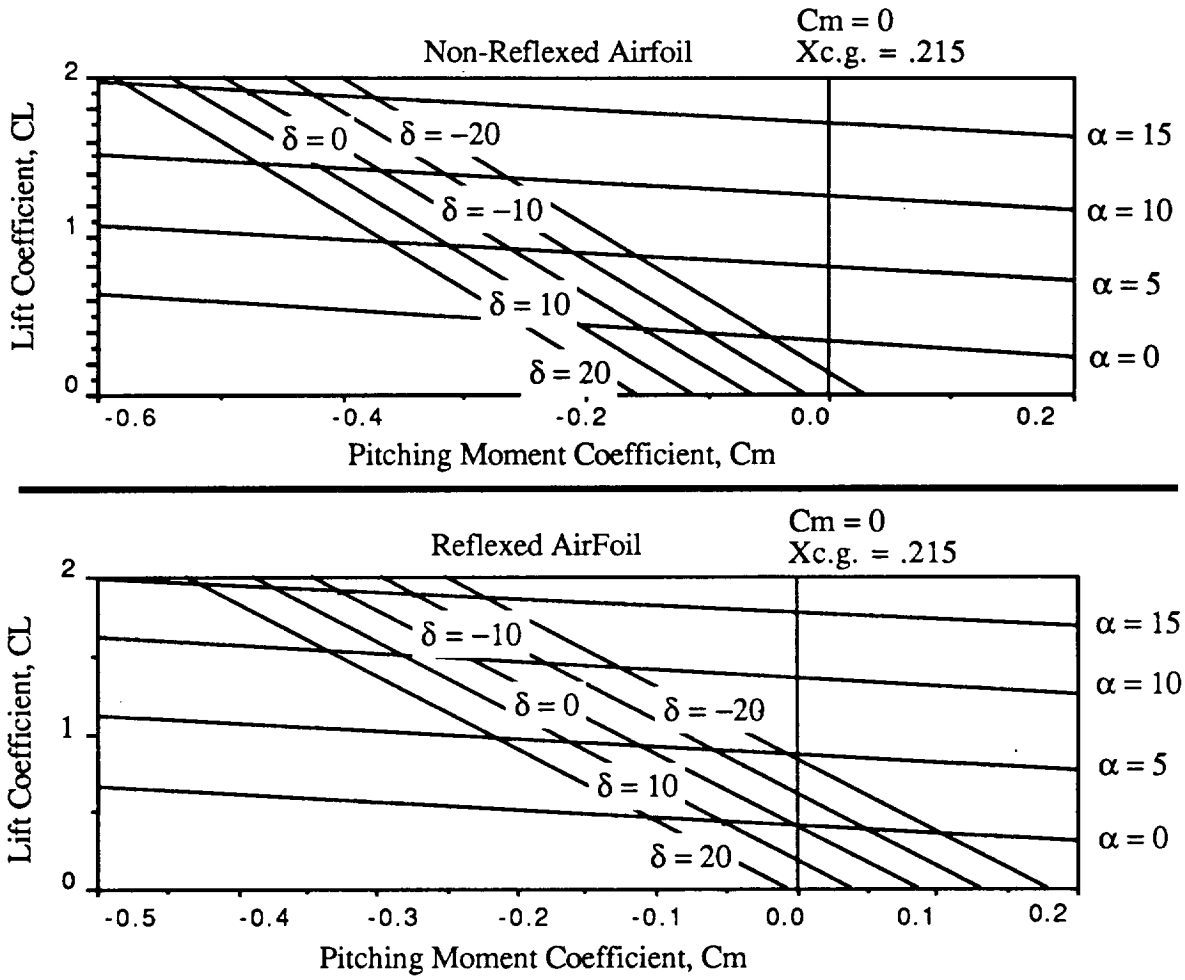

Figure 9.2 : Trim Conditions for the CONDOR

With the reflexed wing at an average cruise angle of attack the CONDOR trims with less than one degree negative elevon deflection. With one degree of elevon deflection, the trim drag will be kept small. Without reflex, elevon deflections in the region of negative thirty degrees would be necessary. Therefore, reflexing the wing of the CONDOR greatly decreases trim drag.

Calculation of the change in C_{Do} was completed and the reflex only adds approximately .0001 to the CONDOR's C_{Do}.

9.4 Dynamic Stability and Control Analysis

This section will look at the changes in the dynamic stability and control, over the mission, and compare them to the requirements of the MIL-F-8785B. The in-flight analysis is warranted because of the large changes in the CONDOR'S moments and products of inertia during the mission. These changes are documented in the mass properties section (Chapter 4) of this report. The methods used to estimate the dynamics of the aircraft are outlined by Roskam (Reference 42). The dynamic variables are estimated as simple equations of the stability derivatives. These equations assume an independence between the aircraft modes of motion. The In-flight analysis was done for five flight conditions (Climb, Begin-Cruise, Mid-Cruise, End-Cruise, Approach). The stability derivatives were calculated for each of these five cases, they are listed in Figures 9.3 and 9.4. Each graph done for this analysis shows these five flight conditions and the requirements of the military specification.

Previous Flying-Wing configurations have been criticized for pitch instability. Therefore, the CONDOR'S Short Period dynamic response was examined first. Figure 9.3 shows the short period variation for the five flight conditions. The Military Specification MIL-F-8785B rates aircraft flying qualities on a scale of one to three, level 1 being best. The CONDOR meets level 1 for short period damping ratio in each of the five conditions.

Short period natural frequency is also level 1 quality for the five flight conditions.

In the Phugoid flight mode, the MIL-F-8785B only restricts the damping ratio. This ratio is shown in figure 9.5, which shows that the CONDOR only meets the requirements of flight level 2. Therefore the SAS will be used to bring this damping ratio up to level 1 quality.

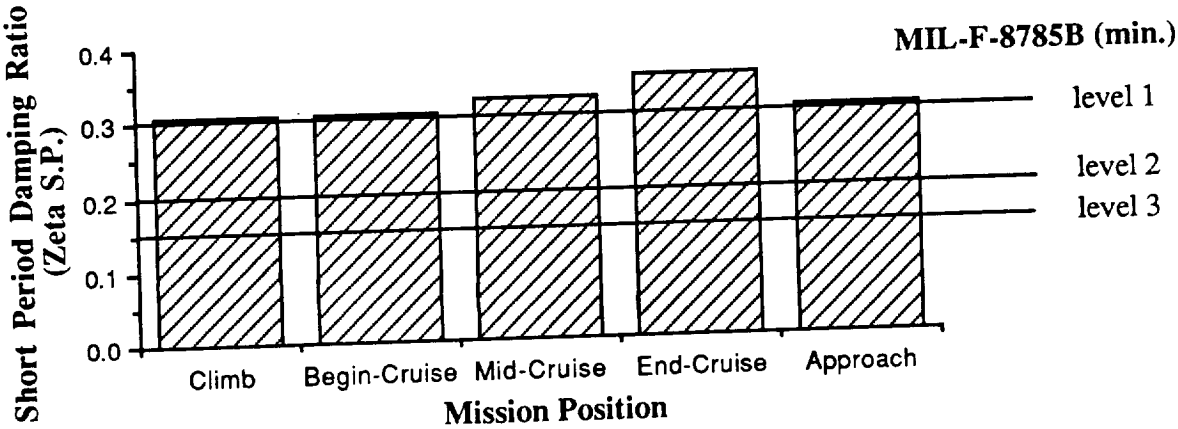

Figure 9.3 : Short Period Damping Ratio

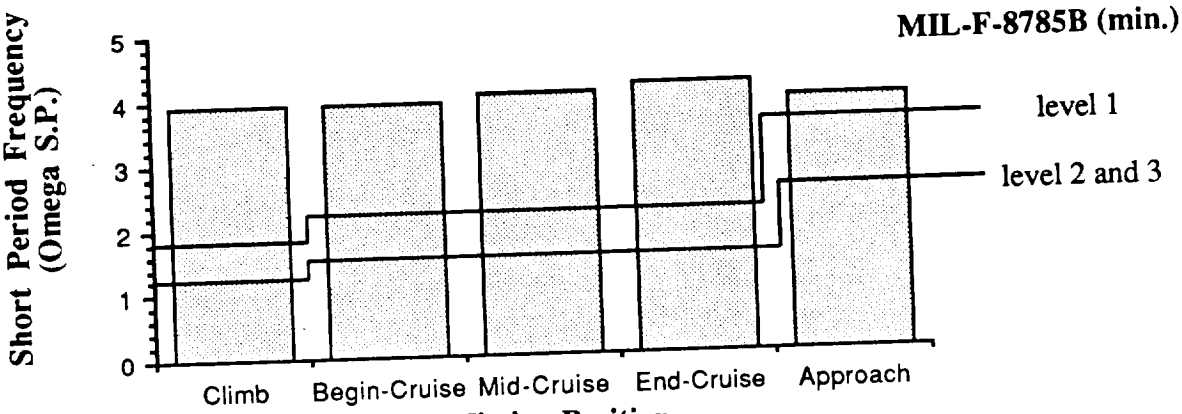

Figure 9.4 : Short Period Natural Frequency

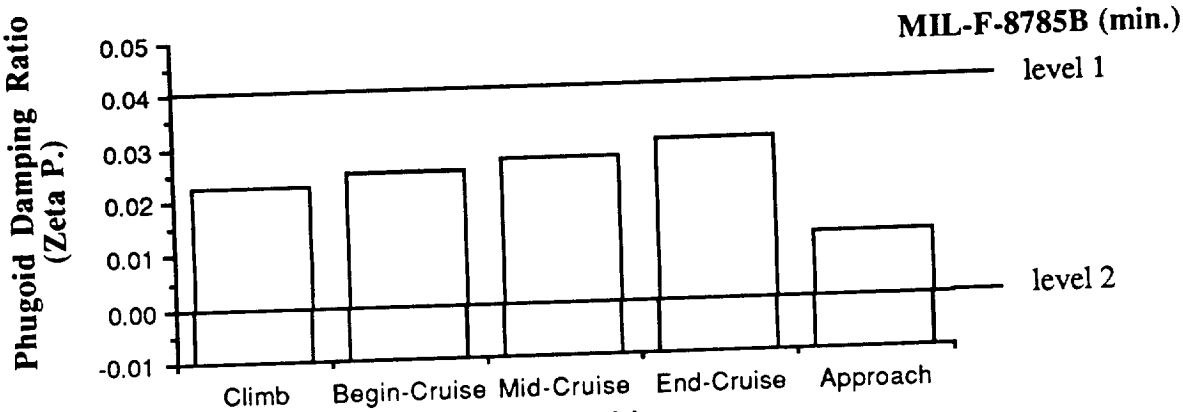

Figure 9.5 : Phugoid Damping Ratio

The roll-mode time constant is graphed in Figure 9.6 for the CONDOR. The values are all below level 1 requirements, and will be augmented by the SAS.

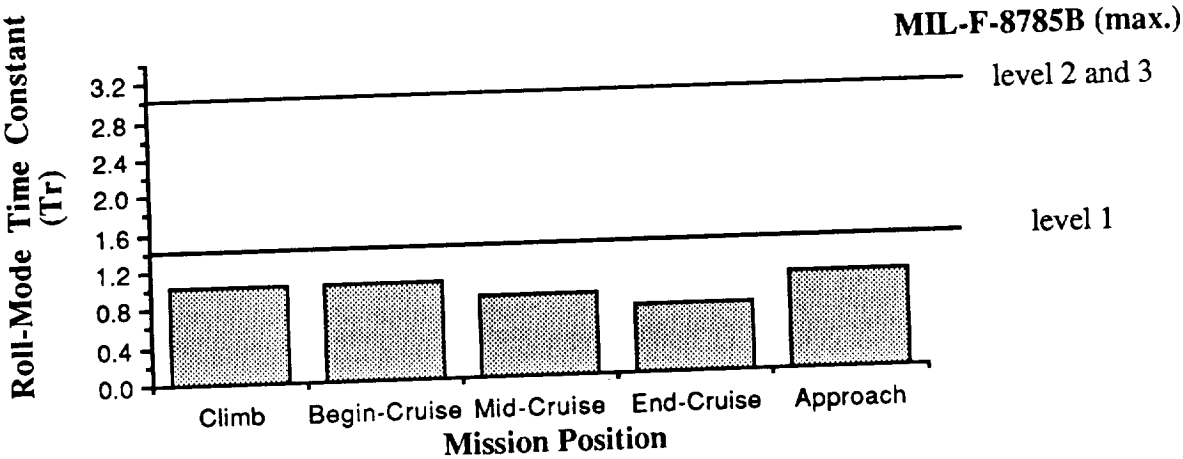

Figure 9.6 : Roll-Mode Time Constant

The Spiral-Mode requirements are based on the time to double amplitude value for the aircraft. The CONDOR is shown to have level 2 characteristics for this flight mode, except in the approach flight condition, were it is level 1. Once again, augmentation will be used to up-grade this flying quality. These results are shown in Figure 9.7

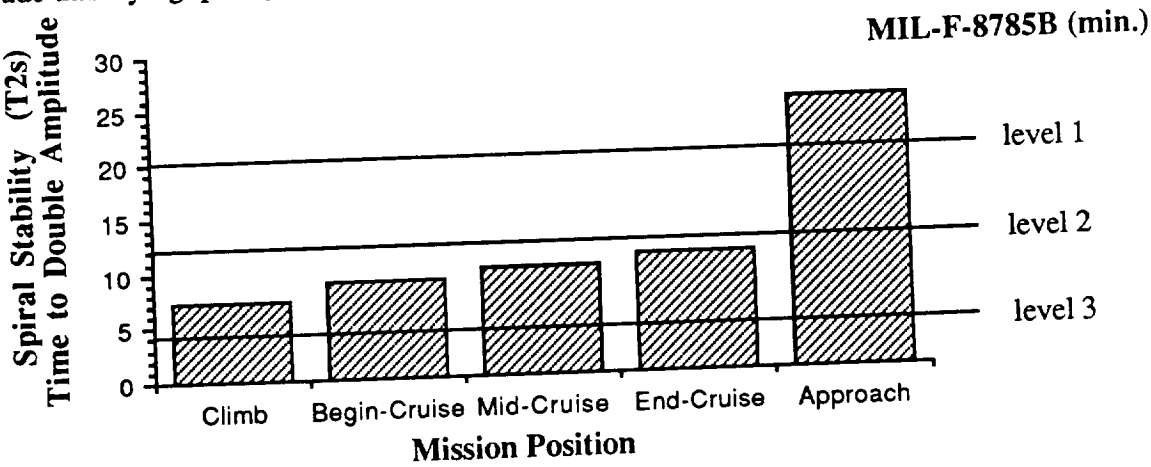

Figure 9.7 : Spiral Stabiltiy - Time to Double Amplitude

The dutch roll flight mode is also governed by the MIL-F-8785B. The CONDOR characteristics are level 2 for all the flight conditions except climb where it is level 1. The other modes will be augmented to level 1.

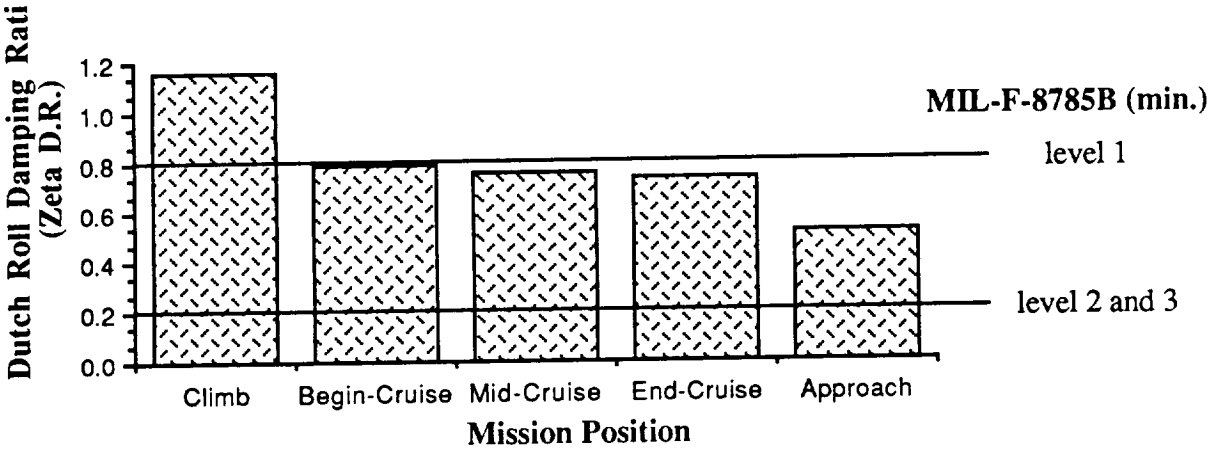

Figure 9.8 : Dutch Roll Damping Ratio

The climb and approach dutch roll natural frequency is only level 2 as shown in Figure 9.9, but is level 1 in all other flight conditions.

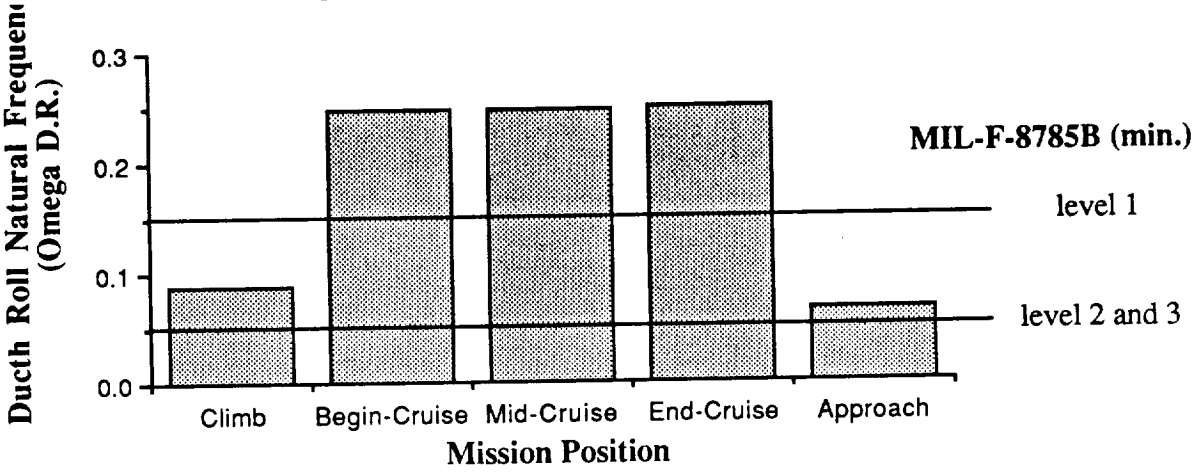

Figure 9.9 : Dutch Roll Natural Frequency

In General, the CONDOR exhibited level 2 flight characteristics according to the requirements of MIL-F-8785B. A Stabiltiy Augmentation System (SAS) will be used to

bring all of the CONDOR's flight dynamics up to level 1, which satisfy the FAR-23 requirements. However, in the case of a SAS failure the CONDOR is still flyable with acceptable flight dynamics with a minimum of level 2.

9.3 CONDOR's Control System

The CONDOR's flight control system consists of a main Flight Computer, controllers, Electro Hydrostatic Actuators (EHA), and three rate gyro sensors. The flight computer will take inputs from the the pilot, the autopilot/rate gyro sensors, and the EHA from each control surface. It will process the incoming data and output commands to the control surfaces. This will enable the flight computer to make decisions concerning the CONDOR's stability. Figure 9.10 shows the schematic of the CONDOR's Fly-By-Wire system, with a list of advantages.

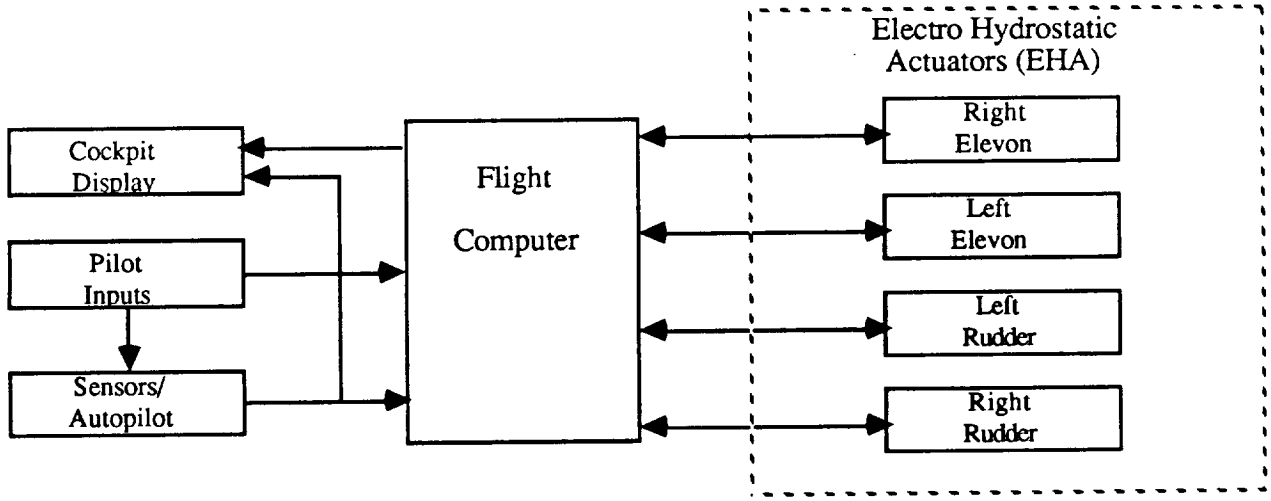

ADVANTAGES

- System Loss Probability < 10 -7 per Hr.
- Quadruplex Computers
- Quadruplex Primary Input Sensors
- Fault Tolerent Computers

Figure 9.10 : Fly-By-Wire Layout Schematic

Note that the main flight computer contains four self-sufficient computer systems which operate by majority decision, this results in a highly redundant system with low loss probability.

The System was laid out as shown in Figure 9.11. The wiring that runs within the wing is placed directly behind the second spar, which is located at fifty-percent chord. The system equipment that is stored in the fuselage is placed in a rack at the back of the crew compartment, to give easy access for the crew and ground repair.

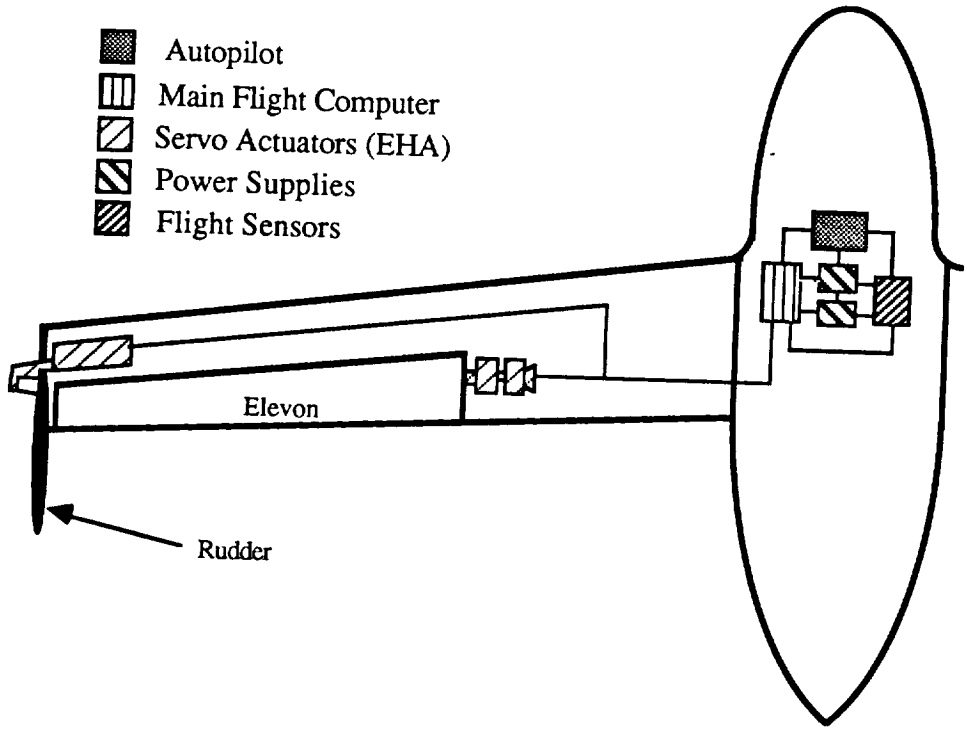

Figure 9.11 : Stability Augmentation Control System

The Servo Actuators in the wing also have easy access with removeable panels on the wing. The actuators self-contained electro-hydraulic system, which gives independent operations, allows for easy replacement if failure occurs. At each of the four control surfaces, redundant actuators and servos are present.

10.0 CREW AND PAYLOAD ACCOMMODATIONS

The CONDOR must support 2 crew members and 200 Lbf of payload during a 72 hour mission. Special attention was paid to these two design criteria.

10.1 Crew Accommodations

The crew must be supported as comfortably as possible during the 72 hour mission. Their field of vision must be unobstructed so they can use their powers of observation throughout the mission (Reference 1). For these reasons the crew compartment was made as large as possible with transparent materials (Lexan) used in much of the forward fuselage. Figure 10.1 shows the inboard profile of the CONDOR. This figure shows that there is a maximum vertical height of 5'7". A height of 6'0" would have been preferred, but this would have produced a fuselage too large to fit into the C-130 aircraft or tractor trailer. It is believed that the 5'7" maximum headroom will provide ample room for the pilots to stretch and remain comfortable.

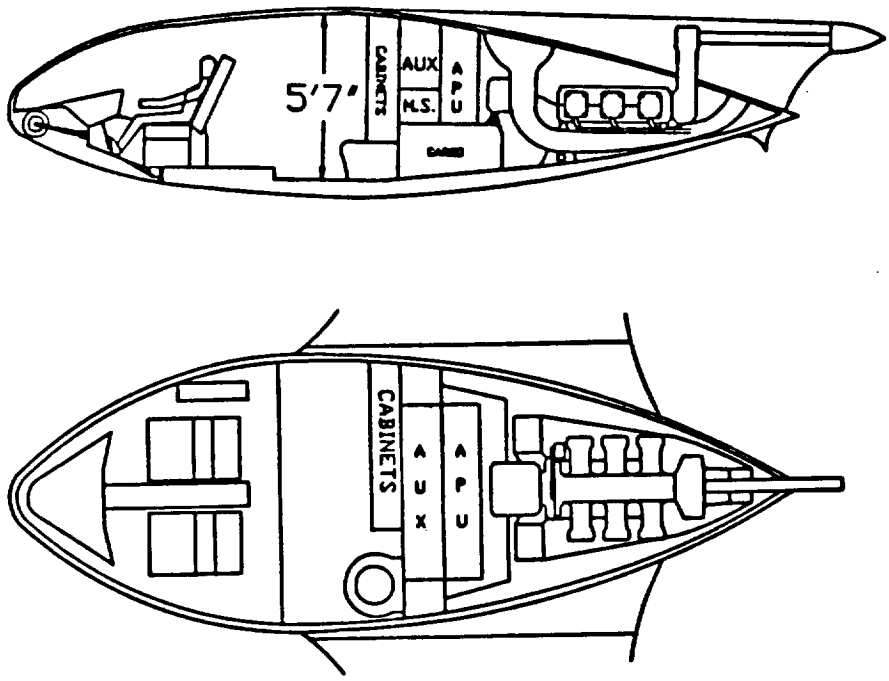

Figure 10.1 : Inboard Profile

10.1.1 Seating Arrangements and Cockpit Displays

There is a pilot and co-pilot seat located next to one another. The aircraft can be flown from either seat, but the best view of all cockpit displays is seen from the pilots seat. The CONDOR was designed for one crew member to sleep while the other monitors the flight (with the autopilot flying the aircraft most of the time). The co-pilot seat converts into the bed, with the seat sliding rearward and collapsing to the floor to keep his feet out of the pilots way.

The instrument panel is shown in Figure 10.2. The pilot is seated on the left side of the aircraft; therefore, the main instruments are placed on the left side of the instrument panel. The right side is reserved for controls that will activate and operate the large number of different instruments and experiments which will be part of the airplane cargo. The Condor will be equipped with a full array of instruments including the instruments necessary for full IFR conditions.

10.1.2 Pilot Vision

The crews vision should not be obstructed to any significant degree, as stated by the RFP. Figure 10.3 shows the pilots field of vision. It is shown in this figure that the crew can see in any direction except backward with 260° side to side, and 275° up and down vision. With all of this transparent material heating and exposure to the radiation of the sun was found to be a problem. To counter this problem, the Lexan will be treated with a radiation blocking material and the upper parts of the cockpit have an extendable "visor" to block much of the heat provided by the sun.

10.1.3 Essentials for Life

Food and water will be supplied for the crew. It will be located in the cabinets, as shown in Figure 10.1. 5.6 gallons of water is supplied for each crew member, and 10 Lbs of food. A dry toilet (emptied after each flight) is located behind the pilots seat , and will have a small curtain for privacy.

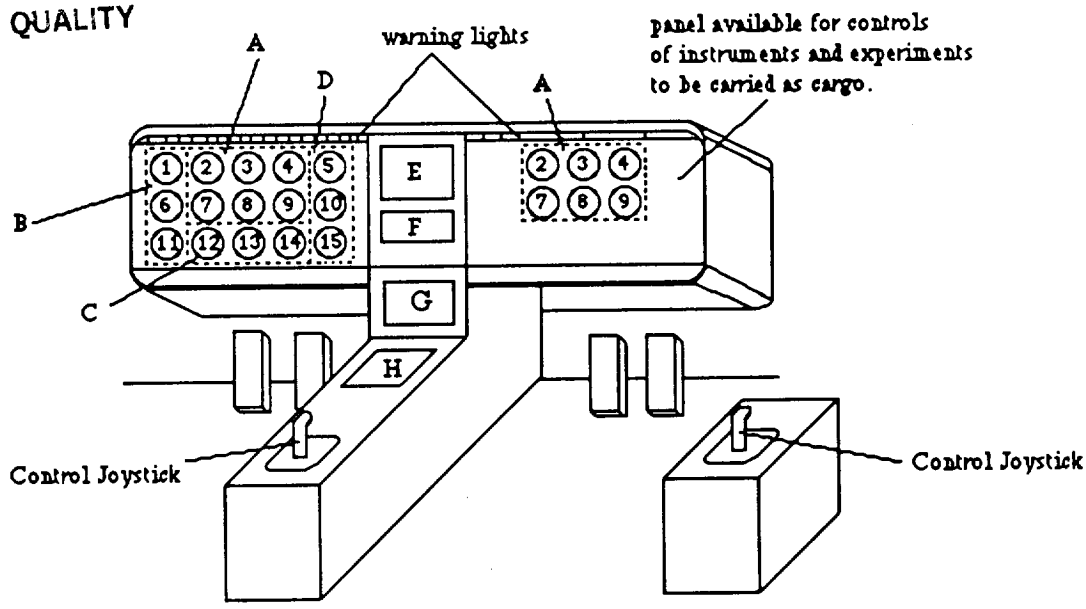

Instruments:

1. Aux.
2. Altimeter
3. Vertical Airspeed Indicator
4. Airspeed Indicator
5. Engine Water Temperature
6. Aux.
7. Directional Gyro
8. Artificial Horizon
9. Turn Coordinator
10. Oil Temperature
11. Aux.
12. Fuel Flow Gage
13. Left Fuel Tank Quantity
14. Right Fuel Tank Quantity
15. Oil Pressure

Instrument Groups:

A. Flight Instruments
B. Optional Instruments
C. Fuel Management
D. Engine Monitoring
E. Auto Pilot
F. Navigation / Com.
G. Weather Radar
H. Alphanumeric Keyboard

Figure 10.2 : Instrument Panel

10.2 Payload Bay

The payload bay must at least have a volume of 4 ft^3 and be able to carry 200 Lbf, as required by the RFP. The CONDOR's payload bay is shown in Figure 10.4, and has a volume of 4.6 ft^3. Careful attention was paid to the payload bay so that it will be able to support many types of equipment. The bay is located below the main spar as shown in Figures 10.1 and 10.4. It is made of the same material as the fuselage windshield so that video cameras can be used. Any controls needed to control the payload will be hooked up to the cockpit display and monitored by the crew. The power supplied to the payload bay is 2000 watts, as required by the RFP.

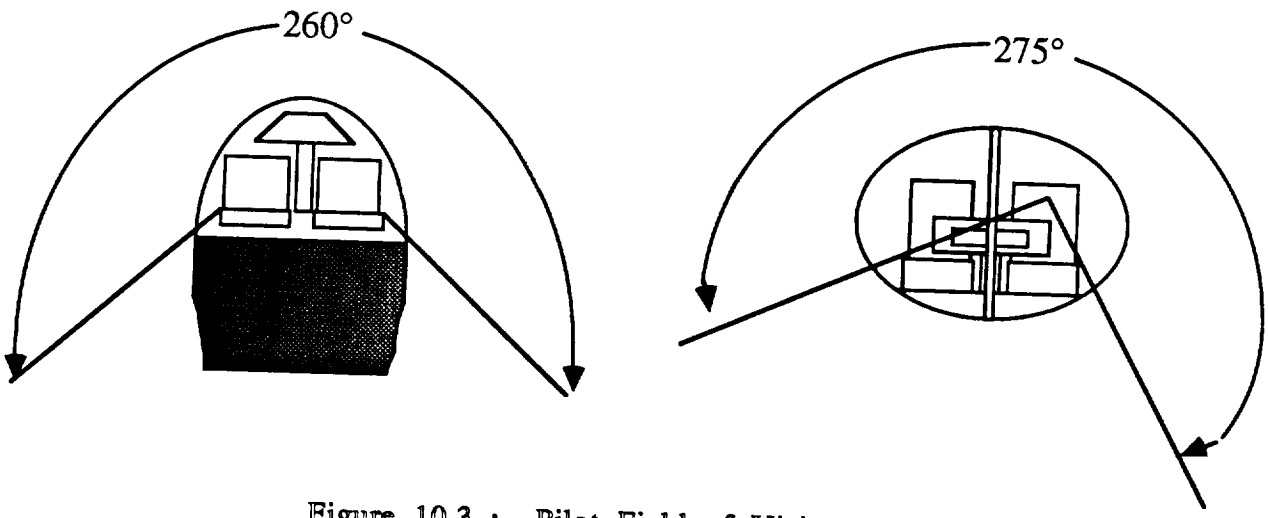

Figure 10.3 : Pilot Field of Vision

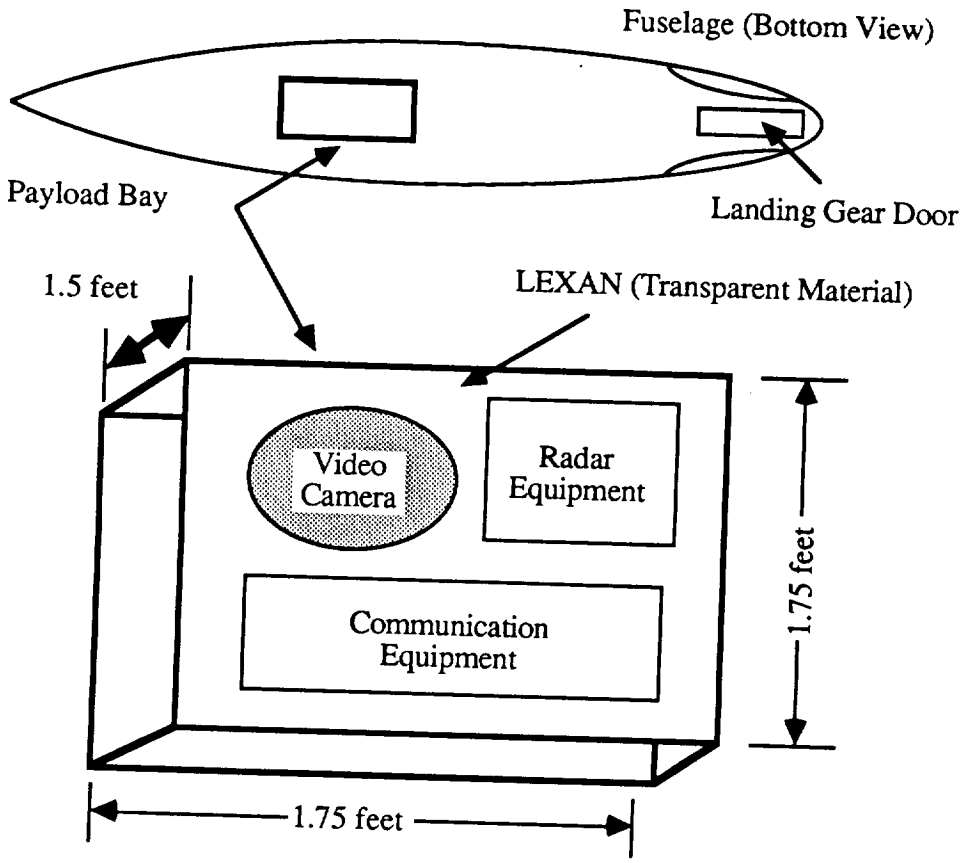

Figure 13.4 : Payload Bay

11.0 MANUFACTURING, TESTING, AND CERTIFICATION

11.1 Manufacturing

The CONDOR long endurance aircraft is being designed to be disassembled and transported inside of a C-130 aircraft or tractor trailer. This disassembly will mean that each section can be manufactured as a separate part. Figure 11.1 shows the separate peaces of the CONDOR. From these separate parts that the manufacture plan was completed.

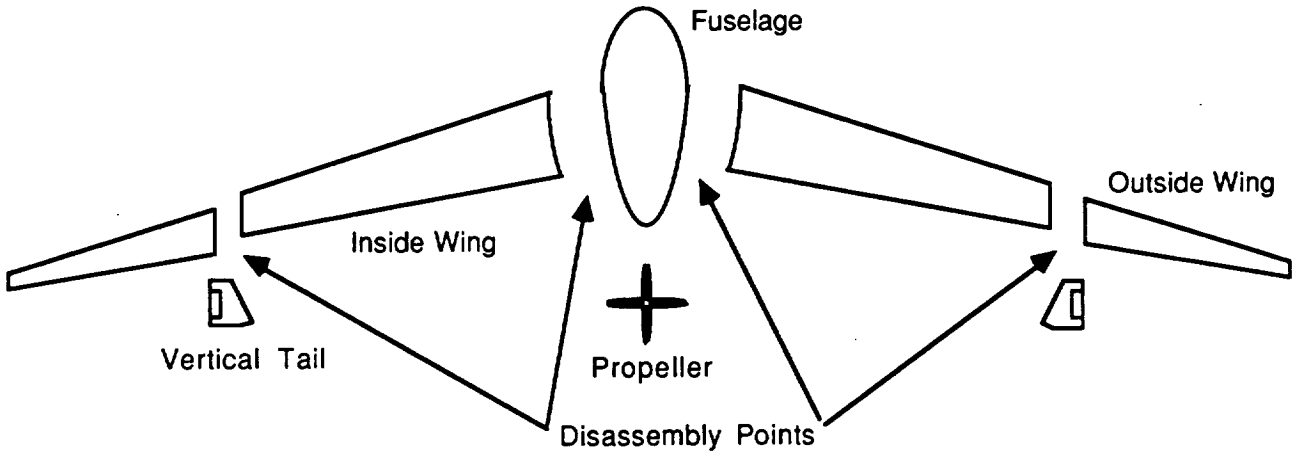

FIGURE 11.1 : Aircraft Disassembly Points

1

A six phase testing and assembly sequence will be utilized and is illustrated in Figure 11.2. The testing portion of this program is an important part of the overall quality control. The testing and assembly sequence is outlined below:

Phase 1 - Raw materials and subcontracted items are received for the assembly process. These materials are then inspected by quality control with approximately 5% of the materials not meeting the standards; therefore, being scrapped.

Phase 2 - Subsystem testing is performed for the systems that were certified in Phase 1. The following component assembly is started.

1) Wing Sections

2)Vertical Tail Sections
3) Fuselage
4) Landing Gear
5) Stability Augmentation System Integrated into Wing
6) Fuel system

Phase 3 - Exhaustive testing is performed on the components of the previous level, and prepared for final assembly. The following components are then assembled in the plant.

1) Main Landing Gear is Attached to Wing
2) Front Landing Gear Attached to Fuselage
3) Control Surfaces are Attached to Wing and Vertical Tails
4) Engine Installed in Fuselage
5) Final Systems Installed

The aircraft is then moved outside for final assembly of structure as follows:

1) Inner Wing Sections are Attached to Fuselage
2) Outer Wing Sections are Attached to Inner Wing Sections
3) Vertical Tails are Attached to Wings
4) Propeller is attached to Propeller Shaft

Phase 4 - Testing is performed on total structure. The detailed interior work is completed.

Phase 5 - Flight testing and certification is completed (see Section 11.2).

Phase 6 - Delivery of aircraft to customer.

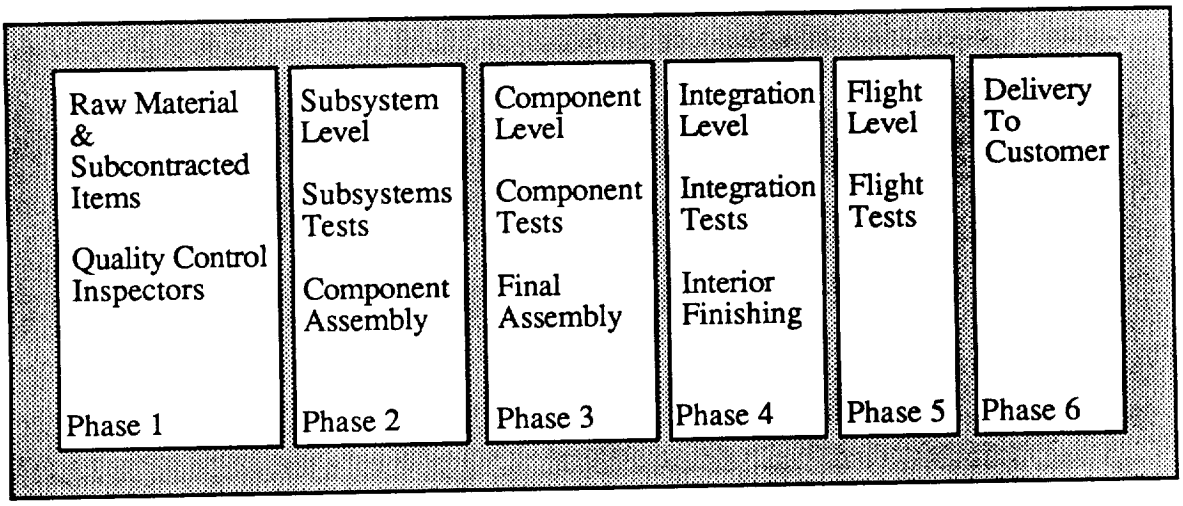

Figure 11.2 : Manufacturing Phases

11.1.2 Assembly

The CONDOR will be produced in small numbers; therefore, automatic assembly is not profitable. For this reason, jigs will be used for the construction. These jigs will be constructed with simplicity of manufacture in mind. The CONDOR's wing structure is relatively simple and is broken into four parts, therefore the jigs can be kept relatively small and inexpensive.

11.1.3 Production Facility

Figure 11.3 shows the factory floor plan necessary to build the CONDOR. This floor plan is for the minimum space required to manufacture five planes each month, or 60 each year. Final assembly of the aircraft will take place outside because of the large wing span.

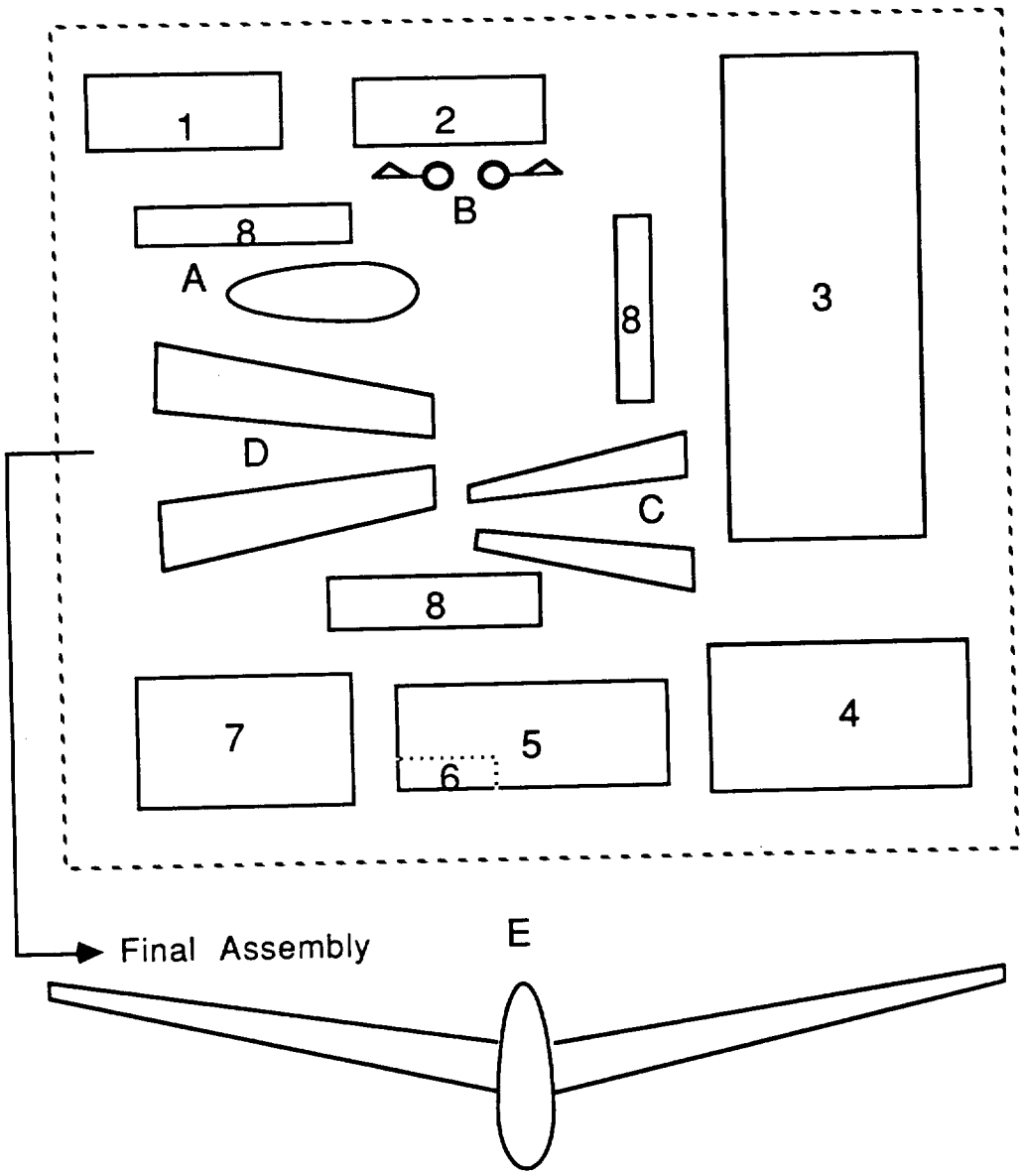

1. Receiving, Fuselage Structure Stamping Machines and Assembly
2. Landing Gear Assembly and Storage.
3. Wing and Vertical Tail Stamping and Assembly.
4. Autoclave
5. Systems Shop
6. Engine Storage
7. Interior Shop
8. Tools Storing Area

A. Fuselage Assembly, Avionics Assembly and Propulsion Integration
B. Landing Gear Assembly
C. Outside Wing Assembly
D. Inside Wing Assembly
E. Final Assembly, Fuselage Systems Assembly, Final Checkout

Figure 11.3 : Assembly Layout

11.2 Testing and Certification

Testing and certification of any aircraft plays a very important roll in the success of the aircraft. For this reason, there was strict compliance to the Federal Aircraft Regulation (FAR) part 23 during the design phase. Testing will be continuous during the manufacturing, assembly, and flight testing phases of the CONDOR to make sure the aircraft does meet the mandatory requirements set by FAR 23.

11.3 Other Regulation Compliance

The RFP states that this aircraft also will have possible military applications. For this reason, the CONDOR was designed to comply not only with FAR 23, but also with the MIL-SPECS. This will allow the aircraft to be certified with the military and enhance the number of possible costumers.

12.0 ECONOMIC ANALYSIS

The purpose of the economic analysis is to investigate the cost of the Condor aircraft program from the prototype costs to the production costs for different number of aircraft produced.

12.1 Cost Estimate Methods

The development cost of the Condor is based on statistical relationships between airplane design, performance parameters, and airplane price. The method used in the cost estimation is from DAPCA -Development and Procurement Cost for Aircraft- (a cost estimating computer program). Some assumptions were made in calculating the cost. These assumptions are.

* three prototype aircraft built and used for flight testing
* avionics cost is 50% of engine cost
* the number of aircraft produced per month is 5
* the profit is 10% of the final cost

The following are major inputs to the DAPCA method:

AMPR weight = 4218 lbs
max. speed = 187 knots
no. of engines per aircraft = 1
engine and avionics cost = 100000 $

no. of test airplanes = 3
engineering hourly rate = 37.75 $
manufacturing hourly rate = 21.60 $
tooling hourly rate = 27.20 $

12.2 Prototype and Development Cost

The prototype and flight test costs for the CONDOR are shown in Table 12.1, and the developmental costs are shown in Table 12.2

Airframes	Hours	Cost
Development Support		1,139,000
Flight-test		224,000
Engineering	426,000	16,087,000
Tooling	184,000	5,002,000
Manufacturing	164,000	3,540,000
Quality Control	21,000	460,000
Material		867,000
Engines and Avionics		
Mqt Development		33,216,000
Recurring Development		3,305,000
Production		269,000
Total without fee		64,110,000
Fee		6,411,000
Total		70,521,000

Table 12.1 : Prototype and Flight Test Costs

Airframes	Hours	Cost
Development Support		979,000
Flight-test		224,000
Engineering	242,000	9,151,000
Tooling	515,000	14,020,000
Manufacturing	575,000	12,411,000
Quality Control	75,000	1,613,000
Material		2,087,000
Engines and Avionics		
Mqt Development		33,216,000
Recurring Development		3,305,000
Production		269,000
Total without fee		77,275,000
Fee		7,727,000
Total		85,002,000

Table 12.2 : Developmental Costs

12.3 Production Costs

The production costs were determined for different numbers of aircraft and program lengths. The results are shown in Table 12.3

Airplanes Produced	Number Per Month	Production Program Length
50	5	10 months
100	5	20 months
150	5	30 months
200	5	40 months
250	5	50 months

Table 12.3 : Production Program Length

The estimated number of aircraft to be sold is 100 because the mission profile for the CONDOR is very specific. The Condor cost breakdown is presented in Table 12.4. As the number of planes built increases the price for each individual plane goes down, as

shown in Figure 12.1. For a production run of 100 planes this table shows that the final cost of each aircraft is $987,000.

Component	Cost				
No. of units	50	100	150	200	250
A.Engineering	54,000	83,000	64,000	53,000	15,000
B.Tooling	88,000	152,000	116,000	95,000	24,000
C.Manufacturing	556,000	668,000	567,000	503,000	263,000
D.Quality Control	72,000	87,000	74,000	65,000	34,000
E.Material	304,000	323,000	299,000	284,000	219,000
F.Engines and Avionics	133,000	94,000	79,000	71,000	65,000
G.Fee	121,000	90,000	76,000	68,000	62,000
Total	1,328,000	987,000	836,000	745,000	683,000

Table 12.4 : CONDOR Unit Production Cost

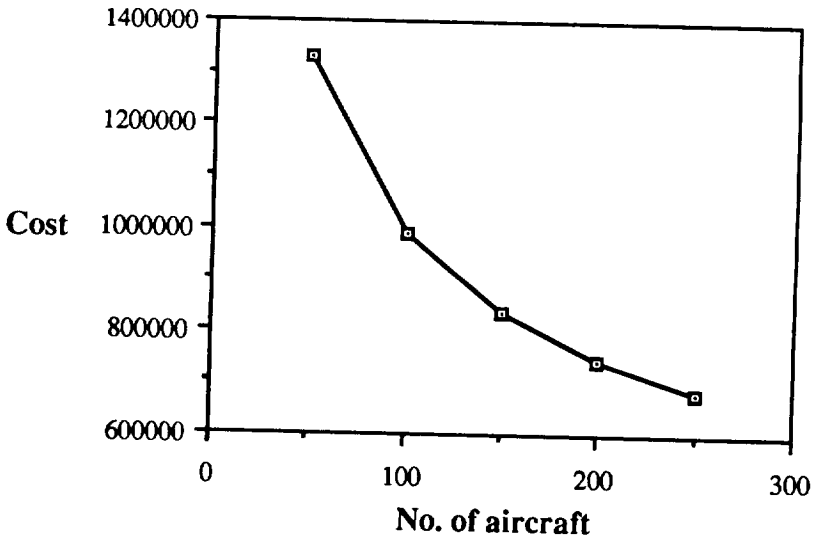

Figure 12.1 : Airplane Cost for Different Number of Aircraft

13.0 RFP COMPLIANCE

Strict attention, as mentioned throughout the text, was paid to the RFP to make sure the CONDOR meets its requirements in every way. Table 13.1 is a list of the major RFP points and how the CONDOR meets them.

RFP	CONDOR
• 72 Hour Cruise at 45,000 feet	met with 2 hours of reserve
• Cruise Speed ≥ 150 Knots	V_c = 150 Knots
• Payload of 2000 pounds	met with easy accessibility
• Time to Climb ≤ 3 hours	T_c = 2.75 hours
• Take-Off and Land ≤ 5000 feet	take-off = 4505 ft - landing = 2704 ft
• 2 Comfortable Crew Members	met, 5'7" headroom - comfortable sleeping arrangements
• Breakdown to Fit into C-130 or Tractor Trailer	meets both
•High Pilot Visibility	met with 260° side to side - 275° up - down
• High reliability	reciprocating engine long time between overhauls redundant flight control system simplicity of design
• Comply with FAR part 23	complies with both FAR 23 and MIL-Spec.

Table 13.1 : RFP Compliance

14.0 CONCLUSIONS

The CONDOR has proven itself a feasible design in that it meets all performance, stability and crew comfort requirements set forth while retaining a relatively low price.

The CONDOR employs new technologies such as future generation engines, quiet propeller, active noise reduction, and a SAS/Fly-by-Wire system, yet is conventional in construction for ease in manufacturing, and easy disassembly for transportation on the ground. The CONDOR utilizes a flying wing configuration for light weight design and low drag flight. The all aluminum construction of the CONDOR offers durability with low manufacturing and repair costs. However, the most attractive feature of the CONDOR is its spacious crew accommodations.

Conclusions concerning specific design objectives are noted below:

EFFICIENCY:

- The use of a reflexed GAW-1 airfoil and a large span flying wing configuration yield high aerodynamic efficiency; (L/D = 37)
- The GTCL-1100 reciprocating engine gives lower fuel consumption, 0.290 lb/bhp/hr in cruise, than the other engines considered.
- The large diameter, four bladed propeller will offer efficiency of .85

NOISE:

- The pusher propeller configuration will place the major source of noise downstream of the crew cabin.
- Acoustic insulation reduces the cabin noise to protect the flight crew from excessive noise during the long duration flight.
- An active noise reduction system will further reduce the noise within the crew cabin to 72 db.

COST:

- For a production program of 100 units over 2 years, the CONDOR can sell for less than a million dollars each (1988 base) and yield a total return on investment of ten percent (10%).
- The CONDOR fuel system is designed to use aviation gasoline which will provide ease of purchase and significant savings in operation costs.
- The all aluminum structure provides low cost and manufacturing simplicity along with a durable construction.

CREW COMFORT:

- The reclining flight seats provides for spacious sleeping quarters.

- The 5'7" vertical cabin clearance gives ample room to stretch and mobility during flight operations.
- A pressurized, climate controlled crew cabin provides a tee-shirt working environment.
- Consistent handling qualities offers easy aircraft control throughout the mission.

The combination of new technology, high performance, reasonable cost, crew comfort, and conventional construction makes the CONDOR an attractive resource for both military and civilian operators. Taken from the current stage of development, the CONDOR could be certified and manufactured with initial delivers made in the early 1990's. The critical element in the CONDOR's production is the development of the new generation engine, the GTCL-1100. Once produced, the CONDOR will easily fulfill the missions specified with the RFP.

REFERENCES

1. AIAA/GENERAL Dynamics Corporation, Team Aircraft Design Competion, "Request for Proposal for a High Altitude Long Endurance Aircraft," 1988

2. Akkerman, J. "High Altitude Aerodynamic Planform Concept Evaluation and Prototype Engine Testing," NASA TM-58256, Jan. 1984

3. Allen, D. Introduction to Aerospace Structural Analysis, John Wiley & sons, USA 1985

4. Anon., "Aerodynamics and Acoustics of Propellers," AGARD-CP-366, October 1984

5. Anon., "Bonded Aircraft Structures," CIBA Limited, Duxford, Cambridge 1957

6. Anon., "Economic Analysis for Composites"

7. Anon., "Prediction Procedures for Near-Fetid and Far Field Propeller Noise," Aerospace Information Report 1407, May 1977

8. Araves, E., "The Feasibility of a High-Altitude Aircraft Planform with Consideration of Technological and Societal Constraints," NASA TM-84508, June, 1982

9. Areiner, W., R. Mount, "High Performance, Stratified Charge Rotary Engines for General Aviation," AIAA-86-1553

10. Ashmead, G., Aircraft Production Methods, Chilton Company, Inc., 1956

11. Azar, J., and D. Peery, Aircraft Structures, McGraw-Hill Book Company, San Francisco, 1982

12. Badgley, P., and D. Myers, "Stratified Charge Rotary Aircraft Engine Technology Abatement Program," NASA CR-174812, Jan 31 1985

13. Badgley, P., M. Berkowitz, D. Ellis,J. Hernbrey, A. Higgins, C. Jones, D. Myers, E. Norwood, and W. Pratt, "Advanced Strafied Charge Rotary Aircraft Engine Design Study by Curtis-Wright Corporation, Cessna Aircraft Corporation," NASA CR-165398, Jan. 29, 1982

14. Bantel, J., W. Hardy, and R. Mount, "Advanced Liquid-Cooled, Turbocharged and Intercooled Stratified Charge Rotary Engines for Aircraft," SAE Technical Paper Series 871039, April 28-30 1987

15. Bavuso, S., "Reliability and Maintainability Assessment Factors for Reliable Fault-Tolerant Systems," NASA Conference Publication 2296, October 1983

16. Block, P., and M. Takallu, "Prediction of Added Noise Due to the Effect of Unsteady Flow on Pusher Propellers," AIAA 87-0255, Jan. 12-15, 1987

17. Boggess, H., and D. Brimm, Aircraft Maintenance, 4th edition, Pitman Publishing Corporation, 1962

18. Bott, H., and H. Doonsch, "Porsche Aircraft Engine pfm 3200," SAE Technical Paper Series 850895, April 16-19 1985

19. Bruhn, E., Analysis and Design of Airplane Structure, Tri-State Offset Co., Cincinnati, Ohio 1949

20. Collins, R., Flying Safely, Declacorte Press, 1977

21. Corning, G., Supersonic and Subsonic Airplane Design, Braun Brumfield, Inc., Ann Arbor, Michigan 1960

22. Crigler, J., and R. Jaquis, "Propeller-Efficiency Charts for Light Airplanes," NASA TN-1338, July 1247

23. Currey, N., Landing Gear Design Handbook, McGraw-Hill, Inc., New York 1982

24. Dwiggins, D., The Complete Book of Cockpits, Tab Books, Inc., 1982

25. Goldschmied, F., "Aerodynamic Design of Low-Speed Aircraft with a NASA Fuselage/Wake-Propeller Configuration," AIAA-86-2693, Oct 20-22, 1986

26. Hamilton Standard Propeller Charts, "Generalized Method of Propeller Performance Estimation," June 1963

27. Higdon, A., Mechanics of Materials 4th ed., John Wiley & Sons, New York 1979

28. Hill, A., "Digital Fly-by-Wire-Experience," AGARD-LS-143, October 1985

29. Hoak, D.E., et al, USAF Datcom, Air Force Flight Dynamics Laboratory, WPAFB, Ohio.

30. Horne, D., Aircraft Production Technology, Cambridge University Press, 1986

31. Kaufman, J., "Terrestrial Environmental (Climatic) Criteria Guidelines for Use in Aerospace Vehicle Development," NASA TM-78118, Nov. 1977

32. Koenig, W., "Performance of High-Altitude, Long Endurance, Turboprop Airplane Using Conventional or Cryogenic Fuels," NASA TM-84534, Jan. 1983

33. McCarthy, R., "Manufacture of Composite Propeller Blades for Commuter Aircraft," SAE Technical Paper Series 850875, April 19 1985

34. McCormick, B., Aerodynamics, Aeronautics, and Flight Mechanics, John Wiley & Sons, 1979

35. Megson, T., Aircraft Structures for Engineering Students, Edward Arnold, Bedford Square, London 1972

36. Metzgen, F., "Strategies for Aircraft Interior Noise Reduction in Existing and Future Propeller Aircraft," SAE Technical Paper Series 810560, April 7-10 1981

37. Miley, S., and D. Ward, "Pratical Flight Test Method for Determining Reciprocating Engine Cooling Requirements," Journal of Aircraft Vol. 21 No. 12, Dec. 1984

38. NASA, "NASA Conference Publication 2321," United States National Aeronautics and Space Administration Scientific and Technical Information Branch, 1984

39. Nicolai, L., Fundamentals of Aircraft Design, Mets, Inc. : 6520 Kingsland Court San Jose, California 95120 , 1984

40. Pallett, E., Aircraft Instruments 2nd ed., Pitman Publishing. Inc., Mass. 1981

41. Peery, D., Aircraft Structures, McGraw-Hill, New York, N.Y. 1982

42. Roskam, J, Airplane Flight Dynamics and Automatic Flight Control, Roskam Aviation and Engineering Corp. , Rt 4, Box 274, Ottawa KS 66067; 1983

43. Roskam, J, Methods for Estimating Stability and Control Derivatives of Conventional Subsonic Airplanes, Published by the author : 519 Boulder, Lawrence Kansas, 66044; Fourth Printing, 1983

44. Roskam, J., Airplane Design, Part I: Component Weight Estimation, Roskam Aviation and Engineering Corp.,Rt. 4, Box 274, Ottawa, KS 66067, 1985

45. Roskam, J., Airplane Design, Part II: Component Weight Estimation, Roskam Aviation and Engineering Corp.,Rt. 4, Box 274, Ottawa, KS 66067, 1985

46. Roskam, J., Airplane Design, Part III: Component Weight Estimation, Roskam Aviation and Engineering Corp.,Rt. 4, Box 274, Ottawa, KS 66067, 1985

47. Roskam, J., Airplane Design, Part IV: Component Weight Estimation, Roskam Aviation and Engineering Corp.,Rt. 4, Box 274, Ottawa, KS 66067, 1985

48. Roskam, J., Airplane Design, Part V: Component Weight Estimation, Roskam Aviation and Engineering Corp.,Rt. 4, Box 274, Ottawa, KS 66067, 1985

49. Shannon, R., Engineering Management, John Wiley & Sons, 1980

50. Shanley, F., Weight-Strength Analysis of Aircraft Structure, Dover Publications, Inc., New York, N.Y. 1960

51. Shevell, R., Fundamentals of Flight, Prentice-Hall, Inc., 1983

52. Siberry, M., Instruments of Flight Control, Crane, Russak & Co., Inc., New York, N.Y. 1974

53. Taylor, J.W.R., Jane's All the World's Aircraft, Published annually by: Jane's Publishing Co., London, England.

54. Teledyne, "GTCL-1100 Liquid Cooled Turbocompound High Altitude Long Endurance Propulsion System Preliminary Specification," Oct. 26, 1987

55. Torenbek, E., Synthesis of Subsonic Airplane Design, Delft University Press, Delft, Holland, 1982

56. Wilby, J., "Interior Noise of General Aviation Aircraft," SAE Technical Paper Series, August 16-19 1982

57. Wilkinson, R., "Design and Development of the Voyager 200/300 Liquid Cooled Aircraft Engine," SAE Technical Paper Series 871042, April 28-30, 1987

58. Wood, K., Airplane Design, Boulder, Colorado 1954

APPENDIX A: Request For Proposal

Design Objectives and Requirements

Request for Proposal for a Long-Endurance Aircraft

I. OPPORTUNITY DESCRIPTION

New lightweight propulsion and structural concepts make possible the design and operation of manned aircraft with sufficient endurance to continuously monitor activities during either natural or man-caused events. Such vehicles would, in some cases, provide limited alternatives to satellites. These vehicles flying at high altitudes could be positioned over selected positions on Earth for several days at a time and would have reuse capability.

Current manned aircraft such as the TR-1 and U-2 can provide a number of hours of continuous operation, and unmanned prototype vehicles have been built with similar capabilities. A manned experimental aircraft recently stayed aloft just over 9 days and traveled 25,012 statute miles. Satellites peform high-altitude Earth surveillance, but the flexibility and resolution provided by their sensors are less than that offered by aircraft. The long-endurance aircraft could complement the use of satellites for those applications that require continuous or more frequent data sampling than available with satellites.

The list of potential applications for a manned long-endurance aircraft is lengthy. The applications fall within three broad areas—military, scientific, and civil. Proposed military applications include command and control, communications relay, surveillance, intelligence, and over-the-horizon targeting. Scientific applications include astronautical observations, atmospheric, and oceanographic research. Numerous civil applications exist, including border patrol surveillance, 200-mile fishery limit enforcement, water pollution monitoring, atmospheric pollution monitoring, resource management, emergency response communications, monitoring natural and man-made diasters, and search and rescue. Agriculture, in particular, has an established need for low-cost frequent crop monitoring of disease or insect infestation and moisture content to guide in the use of herbicides or insecticides and to optimize the use of water resources in irrigation.

Aircraft meeting the proposed requirements generally resemble very high aspect ratio winged motor gilders or ultralight aircraft. The aircraft is required to maintain continuous altitude at or above 45,000 feet for at least a 3-day duration. Although an unmanned aircraft could perform many of the potential missions, a manned vehicle has much greater mission effectiveness. The crew and accommodations could be replaced by a remote control system for those missions that are best performed unmanned. The aircraft should be designed to break down for transport by C-130 aircraft and by tractor-trailer on the highway. It is envisioned that takeoff and landing would be from conventional general-aviation length runways. An aircraft with such capabilities has a large military and commerical market potential due to the great variety of potential missions.

II. PROJECT OBJECTIVES

The objective is the design of a new class of manned long-endurance aircraft that has the versatility to perform a number of commercial, civil, scientific, and military missions. Although a manned mission much longer than that proposed has recently been accomplished, it should be considered a special case that demonstrated the feasibility of such aircraft. Pilots that will somewhat routinely fly 3-day missions can hardly be expected to endure the hardships of the Voyager crew. Providing acceptable accommodations for a crew of two and a 3-day mission presents a most challenging project. Numerous design studies and a fairly comprehensive data base exist for unmanned missions of high-altitude long-endurance aircraft, which include a spectrum of propulsion types and aircraft configurations. The inclusion of manned aircraft presents a special challenge, but it also greatly adds to the overall usefulness of such aircraft. An unmanned system is yet to be developed that can supplement the powers of human intelligence and observation. However, some missions, such as routine mapping missions, do not require a manned presence, and the overall usefulness of the proposed vehicle would be enhanced by the consideration of dual-role vehicles in which the crew could be replaced by a remotely piloted capability.

In general, long endurance is accomplished at relatively low flight speeds. Low flight speed entails several special considerations. One of the most obvious considerations is the effect that wind speed will have on such a vehicle. The general shape of wind profiles across the United States can be found in NASA TM 78118, which can be used as a guide in the design criteria for long-endurance low-speed aircraft. Long endurance entails long time between required maintenance calls and high reliability of the total system, including on-board mission equipment.

The potential limits of endurance for chemically fueled airplanes is based largely on the fuel carried and the efficiency of the engines. Chemically fueled engines typically suffer significant reductions in power and efficiency with increases in altitude. Although thrust requirements are generally small, the propellers must operate in a low-density atmosphere, requiring either high rotational speeds or large diameters. Reynolds numbers at these altitudes will be low. To design the propellers to operate relatively efficiently at these flight conditions may require them to operate inefficiently at off-design conditions, that is, takeoff and climb. Low Reynolds numbers, on the

other hand, offer the potential to achieve significant laminar flow, which may be important to achieving the low-drag levels needed for a long-endurance mission. Recently developed low-Reynolds-number, high-lift-to-drag-ratio airfoils should be considered for the wings and propellers. Very large, lightweight, structural designs tend to have a high degree of flexibility, which must be considered in the design of the control surfaces. The structural design must provide acceptable flutter characteristics or flutter suppression techniques.

III. REQUIREMENTS AND CONSTRAINTS

The aircraft must meet standards, rules, and regulations pertinent to aircraft certification and established by the Federal Aviation Administration. The aircraft design should comply with Federal Aviation Regulation Part 23—Airplane Airworthiness.

1) *Performance:* The aircraft should have the following operational characteristics:

a) Maintain continuous altitude at or above 45,000 feet for at least a 3-day duration.

b) Crew accommodations to support a two-man crew comfortably during this period.

c) Accommodate a payload of 200 lb with the minimum dimensions of 4 ft^3 and a power requirement of 2000 watts. (Does not include crew and crew accommodations).

d) Takeoff and landing distances should be consistent with that generally found at large general-aviation fields—5000 feet (sea level, standard day).

e) Time to reach cruising altitude should not exceed 3 hours and should not be counted as part of the 72-hour endurance (assume standard day).

f) Nominal cruise true airspeed must exceed 150 knots.

g) Aircraft structure should be designed to an ultimate load factor of at least 3.8.

h) Internal dimensions for C-130 transport shall be:

Length, ft	41.42
Length with ramp, ft	51.71
Width, ft	10.25
Height, ft	9.23
Floor area, excluding ramp, ft^2	425
Volume, including ramp, ft^3	4300

2) *Maintenance Features:* The aircraft will be operating from remote fields, so high reliability along with reduced and minimal maintenance is required. Ease of inspection, component accessibility, loading, and selection of materials must be considered.

3) *Cockpit Design:* Since the object of having a man in the long-endurance aircraft is to use human powers of observation, the pilot's forward and downward fields of view must not be obstructed to any significant degree.

IV. DATA REQUIREMENTS

The final proposal, based on the previously stated objectives, requirements, and constraints, should include sections and/or data on the following:

1) Justify the final design. Describe the aircraft's performance and list its advantages as compared to other concepts considered. Also include aircraft design and sizing trade studies.

2) Include a three-view drawing of the final proposal. Drawing should include general dimensions, payload location, fuel location, crew and crew accommodations, control systems, and any other unique or unusual characteristics.

3) Indicate structural materials, structural design methods, and provide weight and balance data. Indicate center-of-gravity envelope.

4) Describe the various techniques used to determine aircraft performance, stability, control, and handling qualities, and indicate the results of these techniques. Show compliance with Federal Aviation Regulations.

Some suggested factors include:
a) Indicate propulsion system sizing and criteria.
b) Aircraft aerodynamics and methods used to estimate.
c) Describe horizontal control surface (or device) sizing showing acceptable center-of-gravity limits.
d) Vertical control surface (or device) sizing with a statement of critical factors in its sizing. Factors could be crosswind capability, directional stability, etc.
e) Roll control surface (or device) sizing with an indication of factors sizing the roll devices and critical conditions expected. Factors could be roll rate, roll acceleration capability, and crosswind controllability.
f) Takeoff and landing performance.

5) Summary of design trade-offs. Describe why the particular configuration was selected. Also describe the anticipated effect of a change of parameters (e.g., engine scale factor, aspect ratio, wing area, wing thickness, etc.) on the selected configuration's gross weight and/or performance.

6) Estimate acquisition and direct operating costs. Briefly describe proposed manufacturing methods, management organization, scheduling, and manufacturing capability proposed to produce the aircraft.

V. ENGINE DATA

A proposed set of engine and propeller data that can be used will be sent upon request by contacting:

Norman Ng
Director of Student Programs
AIAA Headquarters
1633 Broadway
New York, NY 10019
(212) 408-9726

The designers may use other propulsion data that they determine to be appropriate.

CALIFORNIA STATE POLYTECHNIC UNIVERSITY, POMONA
TEAM AIRCRAFT DESIGN

THE CONDOR:

The CONDOR is an Aircraft designed in response to a Request For Proposal (RFP), developed by AIAA and General Dynamics Corporation. As a high altitude, low speed, long endurance aircraft, the CONDOR, we believe, is the best feasible alternative. The CONDOR utilizes a flying wing configuration for light weight design and low drag flight. The all aluminum construction of the CONDOR offers durability with low manufacturing and repair costs. However, the most attractive feature of the CONDOR is its spacious crew accommodations. The reclining flight seats work as sleeping quarters and the 57" vertical cabin clearance gives ample room to stretch and move about. These spacious accommodations, are offered by the CONDOR with pressurized, air conditioned comfort.

The following table lists additional RFP requirements and how the CONDOR meets them.

RFP	CONDOR
72 Hour Cruise at 45,000 ft	Met with 2 hours of Reserve
Cruise Speed Greater Than 150 Knots	Cruise Velocity of 150 Knots
Payload of 200 Pounds	Met, with Easy Accessibility
Time to Climb Less than 3 Hours	2.75 Hours to Climb
Take-Off and Land in 5000 Ft	Take-Off = 4508 ft Landing = 1836 ft
2 Comfortable Crew Members	57" Vertical Cabin Clearance Comfortable Sleeping Arrangements
Breakdown to Fit into C-130 or Tractor Trailer	Fits into Both with Extra Room
High Pilot Visibility	Pilot has Unobstructed Downward and Upward Fields of View
High Reliability	Reciprocating Engine (few overhauls) Redundant Flight Control System Simplicity of Design All Aluminum Structure
Comply with FAR part 23	Complies with Both FAR 23 and Military Spec.

The CONDOR meets the requirements of the RFP with simplicity and reliability without sacrificing crew comfort. In addition, the CONDOR is inexpensive and easily manufactured.

CONDOR - 3-View

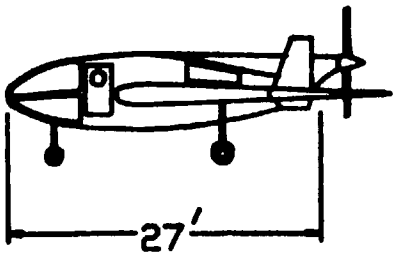

Aspect Ratio = 23.8
Wing Area = 801.5 ft
Sweep Angle @ 1/4 Chord = 16.5 °
Root Chord = 10.4 ft
Tip Chord = 1 ft
Airfoil Section is Reflexed GA(W)-1

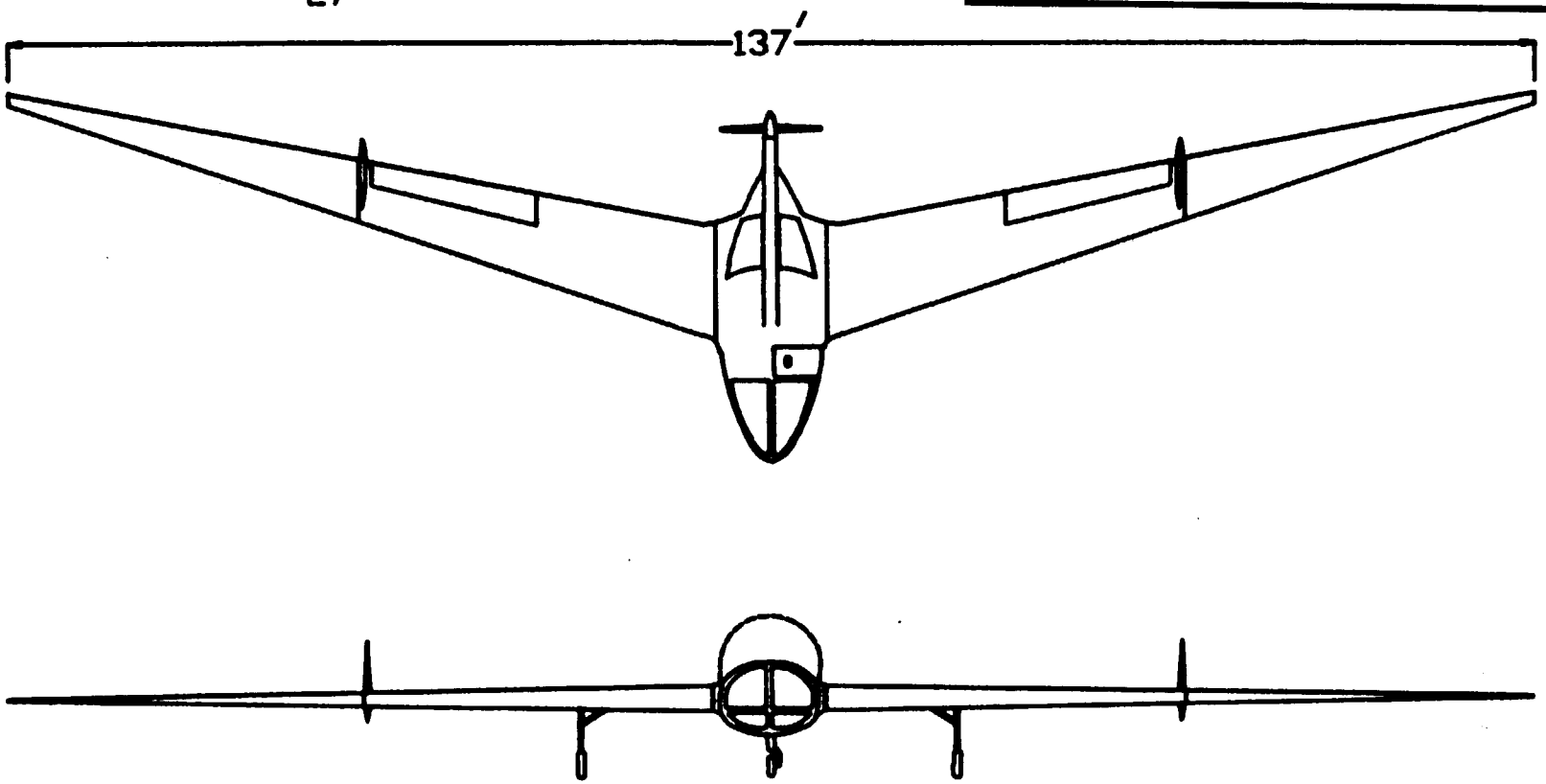

APPENDIX B: Component Mass Properties Estimates

This Appendix gives an in depth description of the methods used to estimate the mass properties of the CONDOR. To determine the total aircraft mass properties, the CONDOR was broken into fifty-seven components, each of which was placed into one of the six systems. The component weights were determined by using empirical equations, comparison to similar aircraft component weights, and in some cases specified component weights. The component moment of inertia calculation process, which includes the radius of gyration estimate, is outlined in this Appendix. The computer program developed to sum the aircraft component mass properties is also briefly described in this appendix.

Each of the aircraft components was placed within the three dimensional axis system which was developed for the CONDOR. This mass properties reference axis system can be seen in the three view of the CONDOR, Figure 3.2. References 39 and 49 develop empirical equations for the estimation of component weights. These equations are functions of the component dimensions, aircraft performance, and other aircraft specifications. The empirical equations were based on past data for specific types of aircraft. In most cases, the equations for light utility aircraft were used. However for some of the components of the CONDOR, the transport and fighter equations had to be employed. whenever possible the equations from both references were used and the average weight was used. An example equation from Nicolai (Reference 39) is shown below. This equation is for the wing of a light utility aircraft.

$$W_w = 96.948\left[\left(\frac{W_{to}\,N_{ult}}{10^5}\right)^{.65}\left(\frac{A_w}{\cos\Lambda_{1/4}}\right)^{.57}\left(\frac{S_w}{100}\right)^{.61}\left(\frac{1+\lambda_w}{2t/C_m}\right)^{.36}\left(1+\frac{V_e}{500}\right)^{.5}\right]^{.993} \qquad \text{B.1}$$

Roskam (Reference 44) offers a similar equation for the wing of a light utility aircraft, known as the Cessna Method.

$$W_w = 0.04674\,(W_{to})^{0.347}\,(S_w)^{0.360}\,(N_{ult})^{0.397}\,(A_w)^{1.712} \qquad \text{B.2}$$

The weights of some components were determined by comparison with an existing aircraft. For this purpose the Rockwell 690B (W_{to}= 10205 lbs.) was selected on the basis of aircraft type, mission, and number of crew members. The weight for the 690B component was then scaled up for the CONDOR using the relative take-off weight ratio of the two aircraft. This method was used on components that where considered to be light weight components. Therefore, error in these estimates have been limited. In a limited number of cases, the weight of a component was specified or known exactly. This was the

case with the crew members of the CONDOR, FAR23 requires that a weight of 170 lbs. be used for each crew member. Also, as a direct requirement of the aircraft RFP, two-hundred pounds must be included for the mission payload. This method was also used extensively within the electrical system, where specific weights were given, as in Nicolai (Reference 37), for electrical avionics components. Table B.1 lists the specified avionics weights taken from this reference.

Item	Weight (lbs)
UHF Communications	11.0
Gyro Compass	8.4
Autopilot System	168.5
Air Data Computer	14.0
Radar Altimeter	38.2
Flight Data Recorder	15.6

Table B.1 Avionics Equipment Weights

In addition to these exact weights the total weight for the electrical system includes additional weight as estimated by the empirical equations.

The aircraft total weight and center of gravity were then summed from the component weights and placement coordinates. The following equations were used for the center of gravity calculations, were J is the component number and N is the total number of components.

$$\bar{X} = \frac{\sum_{J=1}^{J=N} (W)_J (\bar{X})_J}{\sum_{J=1}^{J=N} (W)_J} \qquad \bar{Y} = \frac{\sum_{J=1}^{J=N} (W)_J (\bar{Y})_J}{\sum_{J=1}^{J=N} (W)_J} \qquad \bar{Z} = \frac{\sum_{J=1}^{J=N} (W)_J (\bar{Z})_J}{\sum_{J=1}^{J=N} (W)_J}$$

B.3

To facilitate the final summations of moments and products of inertia, the inertial properties of each component were calculated. This was done by first estimating the radii of gyration for each component. The radii of gyration of a component is based on it's geometric dimensions. To simplify these estimates, the components were assumed to have the simple radii of gyration formulas. For example, a section of the wing would use the equations for a trapezoidal prism. Once the radii of gyration have been estimated for each component, the moments of inertia are calculated from the following formulas.

$$I_{xx} = M R_x^2 \qquad I_{yy} = M R_y^2 \qquad I_{zz} = M R_z^2$$

B.4

The component products of inertia are zero because of the similarity of the geometric models used.

The total aircraft moments and products of inertia are then composed of the summation of these component inertias, plus the three dimensional transfer of axis inertias, for each component, as it is relocated to the aircraft center of gravity. The equation for the total roll moment of inertia and the total roll-yaw product of inertia are given in the equations below, where J is the component number and N is the total number of components.

$$I_{XX} = \sum_{J=1}^{J=N} (I_{XX})_J + \sum_{J=1}^{J=N} (M)_J [(Y_J - Y_{CG})^2 + (Z_J - Z_{CG})^2]$$

B.5

$$I_{XZ} = \sum_{J=1}^{J=N} (M)_J [(X_J - X_{CG})(Z_J - Z_{CG})]$$

B.6

A computer program, in Applesoft Basic, was developed to sum the component mass properties to the total aircraft mass properties. This program, similar to those used in industry, sums component weights, determines the aircraft center of gravity, and calculates aircraft moment and products of inertia. The component moments of inertia were calculated internally by the program with the radii of gyration as input. These inertias were then summed and relocated to the aircraft center of gravity using the equations given above. The program allows for quick calculation of the mass properties, and the ability to deal easily with configuration changes. The output includes a listing of the component properties, system mass properties, and total aircraft mass properties. In addition, an In-Flight analysis section was created which calculates the changes in mass properties during the aircraft mission.